Ancient & Historic
METALS

CONSERVATION AND SCIENTIFIC RESEARCH

Ancient & Historic
METALS

CONSERVATION AND SCIENTIFIC RESEARCH

Ancient & Historic
M E T A L S

CONSERVATION AND SCIENTIFIC RESEARCH

Proceedings of a Symposium
Organized by the J. Paul Getty Museum
and the Getty Conservation Institute
November 1991

Edited by
DAVID A. SCOTT, JERRY PODANY, BRIAN B. CONSIDINE

THE GETTY CONSERVATION INSTITUTE

Every effort has been made to contact the copyright holders of the photographs and illustrations in this book to obtain permission to publish. Any omissions will be corrected in future editions if the publisher is contacted in writing.

Cover photograph: Bronze sheathing tacks from the HMS Sirius. Courtesy of the Australian Bicentennial Authority. Photography: Pat Baker.

PICTURE CREDITS

Bassett and Chase *Considerations in the Cleaning of Ancient Chinese Bronze Vessels.* Figures 1–4: Courtesy of the Honolulu Academy of the Arts, Honolulu. Photography: J. Bassett; Figure 5: Courtesy of the Arthur M. Sackler Gallery, Smithsonian Institution, Washington, D.C.; Figures 6–8: Courtesy of the Freer Gallery of Art, Smithsonian Institution, Washington, D.C.

Bonadies *Tomography of Ancient Bronzes.* Figure 1: Courtesy of Jason Franz; Figures 2–10: Collection of the Cincinnati Art Museum. Photography: Steve Beasley.

Chapman *Techniques of Mercury Gilding.* Figures 1–3: Courtesy of Maison Mahieu, Paris; Figures 4–5: © V&A Images/Victoria and Albert Museum, London. www.vam.ac.uk

Chase *Chinese Bronzes.* Figures 1–2: Courtesy of China Institute in America, Peter Lukic, after illustration in P. Knauth, *The Metalsmiths* (New York: Time Life Books, 1974, pp. 116-117); Figure 3: Courtesy of C. S. Smith. Photography: Betty Nielson, University of Chicago; Figures 4, 9–15, 17–21. Courtesy of the Freer Gallery of Art, Smithsonian Institution, Washington, D.C.; Figures 5–6: Data from Johnston-Feller 1991; Figure 7: Courtesy of Chen Yuyan, University of Science and Technology of China, from her work with Mike Notis, Lehigh University, Bethlehem, PA. Samples made for the Freer Gallery of Art by Rob Pond, Baltimore, MD; Figure 8: Study Collection, Freer Gallery of Art, SC-B-2. Photography: E. W. Fitzhugh; Figure 16: University of-Michigan Museum of Art, Ann Arbor. Estate of Oliver J. Todd, no. 1974/1.180.

Grissom *The Conservation of Outdoor Zinc Sculpture.* Figure 2: Courtesy of the Missouri Historical Society, St.-Louis; Figure 3: Courtesy, The Winterthur Library, Printed Book and Periodical Collection. Figure 7: Courtesy of John L. Brown Photo.

Keene *Real-time Survival Rates for Treatments of Archaeological Iron.* Figures 1–3: Courtesy Museum of London. Photography: the author.

Lins and Power *The Corrosion of Bronze Monuments in Polluted Urban Sites: A Report on the Stability of Copper Mineral Species at Different pH Levels.* Photography: A. Lins.

Matero *Conservation of Architectural Metalwork.* Figures 1, 2, 3, 10, 11: Courtesy of Ohio State University Archives. Figures 2, 10, 11: Photography A. Lins.

MacLeod *Conservation of Corroded Metals.* Figures 1–3: Courtesy of the Australian Bicentennial Authority. Photography: Pat Baker; Figure 4: Courtesy of the British Museum (Natural History), London.

Marabelli *The Monument of Marcus Aurelius.* Figure 1: Courtesy of Accardo, Amodio, et al. (1989); Figure 2: Courtesy of Accardo et al. (1985); Figures 5a–b and 6: Courtesy of Accardo et al. (1983). All photos courtesy of Ministero per i Beni e le Attività Culturali, Instituto Centrale per il Restauro, Roma.

Ogden *The Technology of Medieval Jewelry.* Figure 1: Courtesy of the York Museums Trust (Yorkshire Museum); Figure 2: Courtesy of the Trustees of the British Museum. Photography: N. Whitfield and K. East; Figure 6: Courtesy of W. Duckzo; Figures 8–13, 16, 17, 19, 20: Courtesy of the Trustees of the British Museum. Photography: the author; Figures 18, 22: Courtesy Fitzwilliam Museum. Photography: the author; Figure 23: Courtesy Cambridge Centre for Precious Metal Research archive.

Oddy *Gold Foil, Strip and Wire in the Iron Age of Southern Africa.* Figures 5, 18–21, 23–25: Courtesy of the Trustees of the British Museum; Figures 2, 6, 10, 11, 13, 14, 22, 26: Courtesy of Mapungubwe Museum, University of Pretoria; Figure 16: Courtesy of Queen Victoria Museum, Harare, Zimbabwe.

Schrenk *The Royal Art of Benin.* Figures 1, 2: Gift of Joseph H. Hirshhorn to the Smithsonian Institution in 1966. Photography: Jeffrey Ploskonka, National Museum of African Art; Figures 3, 4, 6, 8: Gift of Joseph H. Hirshhorn to the Smithsonian Institution in 1966. Photography: the author; Figure 5: Purchased with funds provided by the Smithsonian Institution Collections Acquisition Program in 1982. Photography: the author; Figure 7: Gift of Joseph H. Hirshhorn to the Smithsonian Institution in 1979. Photography: the author; Figure 9: Gift of Joseph H. Hirshhorn to the Smithsonian Institution in 1977. Photography: the author.

Contents

Preface

The articles contained in this publication represent the proceedings of a three-day Symposium on Ancient and Historic Metals held at the J. Paul Getty Museum in November 1991. The conference was produced through the collaborative efforts of the Getty Museum and the Getty Conservation Institute with special funding provided by Harold Williams, chief executive officer of the Trust. The broad range of time periods, geography, and technologies discussed here reflects an important shared goal of the Getty Museum and the Getty Conservation Institute: to encourage the dissemination of knowledge that supports and furthers the conservation of cultural heritage throughout the world.

In planning the conference, the organizers sought to bring together conservators, conservation scientists, curators, and museum staff with an interest in the technology, history, structure, and corrosion of ancient and historic metalwork. They invited papers on subjects that not only spanned different time periods, but also reflected a wide range of subject matter. As the diversity of articles in this volume clearly shows, their efforts were amply rewarded. The objects studied range from Nigerian to Chinese bronzes, Zimbabwean to British gold, from the fittings of ships wrecked on the shores of Australia to pots buried for centuries beneath inland lakes, and from architectural iron to historical monuments.

To each of the authors we offer our warm gratitude for their work. We look forward to further collaborative conferences addressing topics that reflect important issues in the field of conservation. We would also like to extend our thanks to all those who made the symposium possible, particularly the staff of the J. Paul Getty Museum, who made most of the practical arrangements for the participants, designed and printed the program, and arranged for the speakers' travel and accommodations in Los Angeles.

In preparation of these proceedings for publication, we wish to thank the book's editors David A. Scott, Jerry Podany, and Brian B. Considine of the Getty Museum; as well as Irina Averkieff and Jacki Gallagher of the Getty Conservation Institute publi-

cations department; independent editorial consultants Dinah Berland and Dianne Woo; and everyone else who participated in bringing the valuable knowledge shared at the symposium to a larger audience. We hope the work presented here will serve to stimulate further investigations in the conservation of ancient and historic metals now and into the future.

Miguel Angel Corzo, Director
The Getty Conservation Institute

John Walsh, Director
The J. Paul Getty Museum

Foreword

Relatively few papers have been published in the conservation literature in recent years dealing specifically with new conservation treatments for metals. This reflects the fact that a certain degree of homeostasis has been reached on the subject. As conservators, however, we are all aware of the continuing difficulties posed by the treatment of outdoor statuary and the preservation of archaeological ironwork, areas in which continued research is still required. The Symposium on Ancient and Historic Metals, held at the J. Paul Getty Museum in November 1991, was organized for the purpose of reflecting current views on methods now in use for metals conservation, particularly in respect to ancient and historic objects.

The intention of the symposium was to focus on objects rather than archaeometallurgical aspects of smelting, extraction, or refining of metals. Conservation treatments for metal objects are subject to continued reevaluation by the profession, and the relation between treatment and technology of the metalwork is an important one. Without an appreciation of how a metal object was made and finished, it is difficult to imagine applying a conservation treatment with any justification or control.

Some of the issues concerning conservation treatments currently being reevaluated are those relating to the cleaning of patinated ancient bronzes and the corrosion of outdoor bronzes. As the sophistication of analytical and technical studies increases, it is becoming increasingly apparent that the cleaning of ancient bronze surfaces can remove evidence of association and burial context, even when careful mechanical cleaning is undertaken. These concerns are addressed in articles by Chase and Bassett. A considerable amount of work has also been published recently that discusses the etiology of basic copper sulfates and their relationship to the corrosion process of statuary exposed outdoors. Lins reassesses the evidence for the formation of some of these corrosion products based on new research reported here.

Looking at the corrosion of archaeological bronzes, Schweizer discusses the identification and investigation of patina in the classification of bronze surfaces from different land and lake environments, and Schrenk presents a detailed examination

of the bronze surfaces of sixteenth- to seventeenth-century objects from the Benin Kingdom, Nigeria. In considering marine corrosion of bronze and other metals, MacLeod describes the examination of objects recovered from shipwreck sites in Australia.

The important restoration which has been carried out on the equestrian monument of Marcus Aurelius in Rome has not been previously well described or available in English. The work of Marabelli and Fiorentino included here provides a very interesting example of a detailed conservation and restoration project. The subject of outdoor statuary is further considered in articles by Grissom and Holm, each of whom discuss the often neglected subject of the numerous historic cast-zinc sculptures in Europe and the United States that are becoming an increasing cause for concern as they deteriorate.

The corrosion of archaeological iron and the methods of treatment for more recent architectural ironwork also pose considerable difficulties for the conservators charged with their care. Keene reviews the survival rates for treatments carried out on archaeological iron from the Museum of London, while Matero examines historic American architectural ironwork finished by surface treatment. Radiography has long been accepted as very important in the examination of metals, and more recent industrial developments have led to the application of radiographic tomography. Bonadies offers an account of tomographic studies of ancient bronzes using industrial imaging systems.

Studies of gold objects tend to reveal a great deal about the technology of the society in which a given piece was produced. Oddy, Ogden, and Chapman examine decorative goldwork and manufacturing techniques in early African, medieval European, and eighteenth-century European precious metalworking, respectively.

The symposium from which this volume was compiled would not have been possible without the support of Harold Williams, chief executive officer of the J. Paul Getty Trust, as well as the encouragement of John Walsh, director of the J. Paul Getty Museum, and Miguel Angel Corzo, director of the Getty Conservation Institute. In conclusion, we wish to extend special appreciation to Frank Preusser, former associate director for programs at the Getty Conservation Institute, for supporting the idea of the conference and for guidance throughout the planning process.

David A. Scott
Jerry Podany
Brian B. Considine

The Monument of Marcus Aurelius: Research and Conservation

MAURIZIO MARABELLI

The equestrian monument of Marcus Aurelius, the most famous bronze monument of antiquity, is all that remains of the twenty-two *Equi Magni* that once adorned Late Imperial Rome. It was created according to the characteristic iconography of the so-called Type III style of the period following 161 C.E. and is thought to be connected with the celebration of a military victory of the emperor, perhaps in 173 C.E. (Fittschen 1989; Torelli 1989). The statue represents Marcus Aurelius with his right arm and hand in a relaxed pose, while his left hand is positioned as if holding the horse's reins, which are missing. The horse, of Nordic breed, is represented in the act of drawing up from a trot.

The gilt equestrian statue was probably erected in the area of the Fori and later moved to the Lateran Plaza, presumably in the eighth century following the political decline of the Imperial Fori. In the tenth century, according to the *Liber Pontificalis,* the *Caballus Constantini,* as the monument was then known, was visible in the Campus Lateranensis near the basilica of the same name and the patriarch's residence. This position corresponded to the new religious and political center of medieval Rome (De Lachenal 1989).

After the historical memory of Emperor Marcus Aurelius had been expunged, the monument first became a symbol of Constantine and papal authority. Then, in the twelfth century, according to the *Mirabilia Urbis Romae*, the statue was considered an effigy of a knight defending Rome against the barbarians. At the end of the twelfth century the statue probably underwent its first crude restoration. A further restoration certainly took place from 1466 to 1475 in at least two stages when the monument was placed on a new stone base, as shown in Filippino Lippi's fresco in the church of Santa Maria sopra Minerva (De Lachenal 1989). This restoration, carried out by the medalist Cristoforo Geremia da Mantova and the goldsmiths Corbolini and Guidocci, cost a total of 970 gold florins. About fifty years later, in January 1538, Paul III Farnese had the monument transferred to Capitoline Hill.

A new pedestal, commissioned from Michelangelo in 1539, was finally constructed in 1561 and is still visible today.

Two subsequent restorations took place, one in 1834–36 and another in 1912. The first was principally concerned with the static condition of the monument, while the second was an unscientific restoration of the surface with the addition of new dowels and the consolidation of preexistent patches and dowels (De Lachenal 1989).

In 1980 preliminary analyses of surface-corrosion products and an acoustic-emission and ultrasonics survey of the monument were carried out. The results of these tests revealed a defective structure and an extensive sulfur-dioxide attack on the surface (Marabelli 1979). In January 1981 the equestrian statue was moved to the Istituto Centrale per il Restauro (ICR) in San Michele, where it remained until the completion of the restoration in 1988. In December 1984 the results of the research were summarized in an exhibition and a catalogue (Aurelio 1984); other important results on casting and assembly techniques (Micheli 1989) and on gilding (Fiorentino 1989) were published subsequently.

The major investigations of the ICR laboratories preceding and accompanying the monument's most recent restoration included the following:

1. Static condition and structure of the monument
2. Nondestructive testing: fabrication and repair techniques
3. Analysis of the alloys
4. Thermal behavior of the monument
5. Climate and pollution: time of wetness and damage function
6. Patinas and types of corrosion
7. Process and condition of the gilding

Static Condition and Structure

Evaluation of the static condition showed that the monument rests essentially on two of the horse's legs, the left-front and the right-back, while the left-back leg acts as a balance to the oscillations of the structure caused by wind, among other disturbances. The right-front leg is raised.

Structural examination of the monument and its tensile state was carried out or coordinated by the ICR Physics Laboratory, primarily using two different techniques: finite element mathematical (FEM) model and speckle interferometry. The purpose of these measurements was to assess the limits of stability of the bronze structure under the stress of its own weight.

Initially, the weights of the horse and horseman were calculated experimentally. The distribution of thickness was measured in each case, paying particular attention to the horse and what came to be considered its critical points (bearing legs and belly). Using a steel hook equipped with a strain-gauge element, the weight of the horseman was determined with reasonable accuracy to be 620 kg ± 6 kg (Accardo et al. 1984). The same technique was used to calculate the weight of the horse at approximately 1,300 kg.

Ultrasonics were used to determine the thicknesses of the metal. For example, the average thickness of the four legs was calculated as follows: left-front, 5.9 mm; right-front, 5.4 mm; left-back, 5.8 mm; and right-back, 5.8 mm. The average thickness of the belly measured 5.5 mm and 5.6 mm. Variations in thickness (standard deviations) were found to be fairly restricted (Table 1).

In order to develop a method for structural calculation of the finished elements, the form of the horse was reproduced on a computer by transferring the coordinates of the surface from photogrammetric images. The surface of the horse was subdivided into a grid structure corresponding to 365 shell elements, 406 nodes, and 36 high-stiffness beams. The schematic structure was then simulated for conditions of stress. The movements of the horse as a rigid body were calculated at considerable loads—in particular, under the weight of the horseman. The area that showed the most stress turned out to be the juncture of the left-front leg (Accardo, Amodio, et al. 1989). Figure 1 shows the movement of the mathematical model, magnified 109 times, as the horse moves forward and to the right under the weight of the horseman.

FEM model calculations were integrated with repeated linear measurements of displacement, using linear variable differential transformers (LVDT), of the raised front leg in all three directions. Calculations were also made with the application of

TABLE 1. *Statistical elaboration of the ultrasonic measurements of thickness (mm). (For symbols, see page 6.)*

Area	X	S	$\tau1$	$\tau2$
Left-front leg	5.9	1.3	0.3	1.8
Right-front leg	5.4	1.5	2.1	4.6
Left-back leg	5.8	1.0	0.7	5.7
Right-back leg	5.8	1.5	1.1	2.5
Left side, repair	5.2	1.2	1.0	1.9
Left side, repair	6.6	1.6	−0.2	−0.2
Right side, repair	5.1	1.2	0.8	2.6
Right side, repair	7.1	1.0	1.4	−0.7
Belly, left side, V1	5.4	1.1	1.5	9.3
Belly, left side, V2	6.1	1.1	−0.1	6.3
Belly, left side, V3	6.6	1.5	−2.4	2.5
Belly, left side, V4	4.5	1.8	1.5	−0.2
Belly, left side, V5	4.9	1.2	1.1	−0.1
Belly, left side, Vt6, repair	5.3	1.6	1.0	−0.3
Belly, right side, V7	6.1	1.4	−0.05	−0.6
Belly, right side, V8	5.3	1.9	−0.05	−1.5
Belly, right side, V9	5.3	2.0	−0.1	−1.5
Belly, right side, V10	5.2	1.2	0.6	2.1
Belly, right side, Vt11, repair	6.7	2.2	−0.1	−0.1
V1 + V2 + V3 + V4 + V5 =	5.6	1.7	0.1	−0.7
V7 + V8 + V9 + V10 =	5.5	1.7	−0.2	−0.8
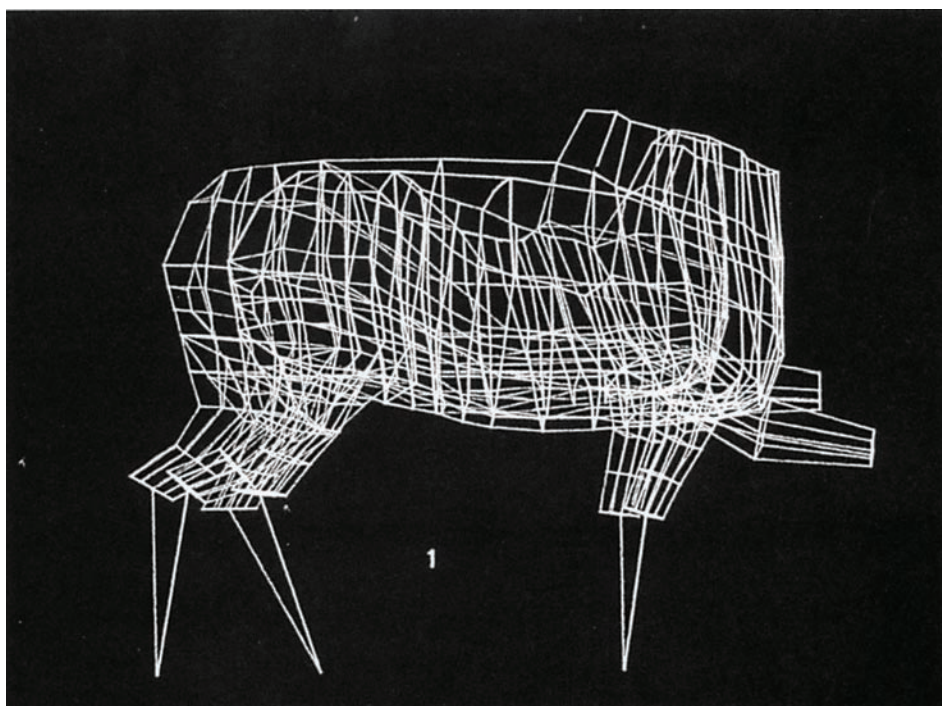
strain gauges (twenty-one groups of three elements), mostly attached to the inside of the left-front leg, and with the figure of the horseman placed on the horse in every experiment (Accardo, Bennici, et al. 1989). The greatest displacement of the left-front leg was concluded to be approximately 3 mm.

Among the possible hypotheses of attachment of the monument to its base, the one that corresponds to the minimum tension, according to the FEM model, presupposes a rigid fastening of the legs to the stone, with a forward displacement of the tip of the hoof of the left-front leg of 0.1% of the distance between this point and the corresponding back leg. This method of attachment would have been much easier to achieve than an internal framework of light, stiff metallic elements, which would have presented some difficulties in execution and maintenance (Accardo, Amodio, et al. 1989).

At the same time, the structural deformations of the horse were determined optically under a stress equal to approximately one-fourth the weight of the horseman. The structure was photographed with laser illumination (514.5 nm), first under the deformations caused by the added weight of the Marcus Aurelius, and later under normal conditions. This resulted in a kind of double exposure (Accardo et al. 1985). The photographic representation of a small area of the surface under laser illumination shows up on the film as an initial series of light and dark spots (speckles). A second series of spots corresponds to the first but is slightly displaced as a result of the deformations, producing a typical interference pattern (Young fringes).

The measurement of these displacements can be obtained by illuminating the photographic film with the same coherent light and measuring on a magnifying screen the period of the interference fringes that corresponds to the small selected area (in effect, measuring the distance between each successive fringe). From these data it is possible to determine the distance between two coupled speckles on the

FIGURE 2. *Speckle image of the neck and muzzle of the horse.*

film (d) and thereby the real displacement (L) of the structural deformation in the small area. Given the enlargement factor of the camera (M), d = ML.

Figure 2 shows the speckle image of the horse's neck and end muzzle, superimposed on the image of the surface illuminated with incoherent light; a series of segments corresponding to the displacements caused by elastic deformation of various microareas is visible. The length of the segments is proportional to the extent of the linear deformations (3 mm maximum) and their orientation to the direction of the displacements (Accardo et al. 1985).

One can deduce from these experiments that the structure of the monument, particularly that of the horse, undergoes a certain modest deformation in the elastic range when submitted to a force equal to the weight of the horseman. This is especially the case at the juncture of the left-front leg. Nevertheless the bearing legs easily withstand the weight of both statues, exhibiting a rather skillful casting under ultrasonics, showing uniform thickness reinforced with a tin-lead alloy filling.

The forces and subsequent deformations (elastic, for the most part) caused by weight, even when considered in the general context of other stresses to which the structure was submitted—such as thermal stress (discussed herein) primarily, and wind pressure (which can reach maximum values of about 57 kg/m^2) secondarily—never reach levels great enough to compromise the conservation of the monument.

Nevertheless, the numerous gaps, disjunctions, and irregularities of the structure, as well as the serious damage caused by relocations of the monument in past centuries, worried medieval conservators. These early restorers attempted, therefore, to displace some of the weight of the horseman onto two small stone columns that functioned in compression. The columns are visible in Pisanello's early fifteenth-century drawing of the left side of the monument (De Lachenal 1989). This drawing also shows a small column supporting the belly of the horse, perhaps intended to consolidate the structure at what was perceived to be the point of greatest stress.

Nondestructive Testing

Nondestructive testing played a fundamental role in the preliminary phase of study. In addition, the data obtained were essential in determining the process by which the monument was fabricated.

The ICR Chemistry Laboratory examined the major sections of the two statues at more than 10,000 measurement points using ultrasonics. Researchers divided the surface into areas of smaller dimensions, subdivided each area into a grid of 2 cm squares, then transferred each value onto a flexible acetate sheet laid out along the curvatures of the surface.

Table 1 shows the thickness values of some areas with statistical values calculated, such as the standard deviation S, the curtosis $\tau2$, and the skewness $\tau1$, or asymmetry coefficient. The horse's four legs indicate remarkable homogeneity of casting, probably achieved by rotating the clay forms containing the molten wax. The overall average value of the thicknesses (x) of the entire bronze ranges from 5 mm to 6 mm, with minimums of 3 mm and maximums of 8 mm (Canella et al. 1985).

A radiographic survey (with 300 radiograms) by Micheli, together with endoscopic examination and direct observation, permitted the identification of the constituent sections. The statue of the horseman is made up of seventeen parts, separately cast and then joined together; the individual parts (head, arms, legs, and sections of drapery) were cast by the indirect, lost-wax method.

The horse is made up of fifteen sections (muzzle and neck, body in eight parts, legs, and tail), also cast separately by the same technique and then assembled (Micheli 1989). This was the most logical and simple process for casting bronzes of large dimensions, for which a single casting would have presented unmanageable difficulties. Not only the legs of the horse but also the other self-contained parts (the head, arms, and legs of the horseman) were obtained by pouring molten wax into a negative mold and distributing it by rotating the mold.

Radiograms have shown that the original sections underwent a slow process of cooling that, on one hand, prevented large cracks and cavities and, on the other hand, contributed to the separation of lead and slag into stratified bands in a frontal direction away from the solidification of the metal (Micheli 1989). The original solderings were made by pouring the molten metal directly and often discontinuously along the edges of the sections using, where possible, preexistent mechanical junctures.

The classification of the repairs to the monument proved rather complex. The first type of treatment, contemporaneous with the fabrication, was the filling in of missing parts, pores, and spongy areas in the cast with small (a few centimeters in diameter at most) rectangular dowels. Polygonal dowels of various sizes were also used in the same situations to repair either defects in casting or imperfections in the junctures between sections. A later type of repair, difficult to date, was used to fix extensive damage or large holes in the cast. In this method, cordlike strips of metal were used to join the cast with plates made to size, slightly smaller than the lacunae. The soldering was accomplished by pouring molten metal into the interior of the lost-wax casting. The molten-metal solder covered the edges of the juncture, forming

a cordlike strip that penetrated the interconnecting spaces between the cast walls and the repair plates laid against them. The same solder also penetrated the holes made in the original bronze and in the corresponding repairs to obtain a better mechanical adherence.

It is important to point out that the discontinuous Roman solderings and the later cordlike solderings do not correspond to continuous, structural welding, as in the hard-soldering process. Ultrasonic tests have verified without a doubt that there is no structural continuity between soldering strips and joints in the metal sections (Canella et al. 1985), as denoted by the low thickness values (Fig. 3); these are joints of a mechanical kind instead.

Other assembly and repair techniques from Roman times and later have also been identified. The classification of types of dowels, plates, plugs, and cordlike strips is especially difficult because of the reuse of older elements in later repairs and the superimposition of subsequent restorations.

Particularly useful in this investigation was an instrument for the measurement of conductivity expressed in International Annealed Copper Standard (IACS) percentages (Medori 1983). The conductivity of the metallic walls was measured to a depth of a few millimeters by means of a magnetic field. If the material under examination is copper, the measured value will correspond to the maximum range (100%); for copper, tin, and lead alloys, the value will decrease from 100%, diminishing in proportion to the increase in the noncopper components.

Using this technique, about 18,000 measurements were carried out, thus allowing the clarification of doubtful cases and the partial aggregation of results of the quantitative analyses of alloys, prior to statistical analysis (Fig. 4). By the end of the experimental survey, it was possible to conclude that the original sections and the Roman repairs revealed IACS% conductivity values generally equal to or below 13%,

FIGURE 3. *Thickness measurements of soldering with cordlike strips.*

FIGURE 4. *IACS% conductivity measurements of original sections and repairs.*
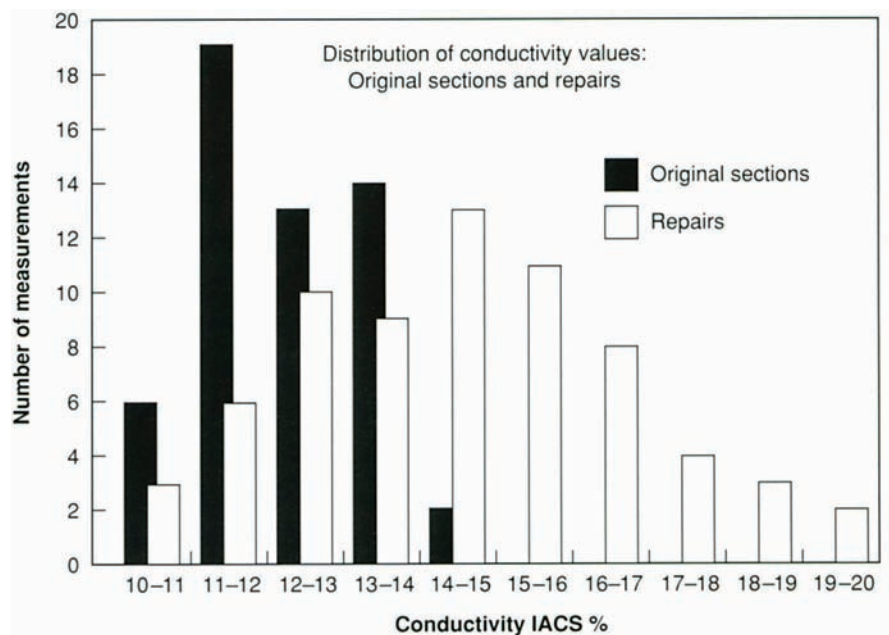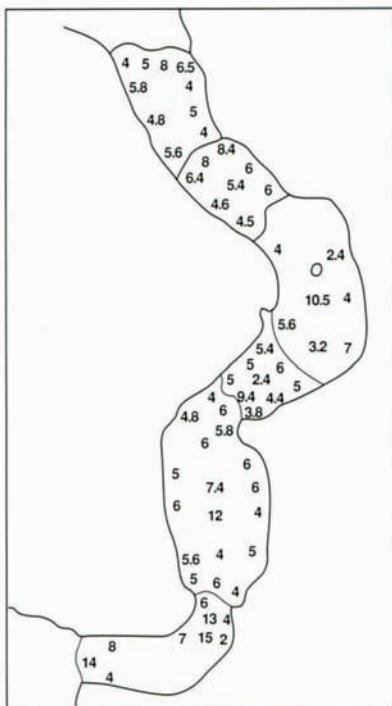
with some high points to about 15%, while the measurements of the later repair materials stayed mainly within a range of about 11–20%. The original sections of the horse and the horseman were chemically homogeneous, with rare exceptions.

Analysis of the Alloys

Quantitative analysis of the alloys was based primarily on two methods:

1. Dispersive X-ray fluorescence analysis for the principal elements (Cu, Sn, Pb)
2. Plasma spectrography for secondary trace elements (Ag, Zn, Fe, Ni, Co, As, Sb, Bi, Si)

The first technique, used largely in archaeometry, does not require particular elucidation. However, in this specific case, an original method for the preparation of the sample was developed. It consisted of dissolving about 50 to 100 mg of alloy (25–50 ml final solution), depositing 200 microliters onto a paper filter (ϕ 14 mm), and analyzing the spectrum of X-ray fluorescence obtained by the irradiation of the filter with a target of barium acetate excited by a primary X-ray source, Bα Kα = 32 KeV (Ferretti et al. 1989).

In plasma-emission spectrometry, the sample is introduced in aerosol form, into a flow of ionized argon at a range of 10,000–12,000 °C. Given the high temperature and the subsequent high level of excitation, sensitivities on the order of parts per billion or milligrams per liter are reached.

About one hundred specimens were studied in all. On initial examination the matrix of percentage values was difficult to interpret. Therefore, the values were reexamined and sequenced in light of two criteria: (1) the sources and analytical data available in the literature, and (2) the statistical elaboration of the data.

A very important passage on the description of bronze alloys used by the Romans, albeit somewhat ambiguous in part, is found in the *Natural History* of Pliny the Elder, book XXXIV, chapter 20 (1961:95–98). Pliny lists five types of bronze alloys: (1) *campana,* an alloy used for vases and utensils; (2) an alloy similar to the previous one, used for the same purposes; (3) an alloy for statues and bronze plaques; (4) *tenerrima,* an alloy for casting statues in molds; and (5) *ollaria,* an alloy for making vases.

Table 2 lists the components of these alloys according to Pliny's categories without interpretation. In the last few years, three interpretations have been given to the term *plumbum argentarium* cited by Pliny. According to Caley (1970), it is a 50/50 lead-tin alloy (Table 3). However, this interpretation seems unfounded, as Pliny refers to an alloy used for counterfeits, which "some call *argentarium*" (1961:95–98).

A second interpretation (Picon et al. 1967) identifies *plumbum argentarium* with tin (Table 4). This identification appears to be well founded because of the noticeable absence of tin in all of the alloys cited by Pliny, and because this interpretation may allow the different compositions to be typed and differentiated, as Picon et al. show rather clearly in two other publications (1966, 1969).

TABLE 2. *Alloys described by Pliny (1961).*

Alloy	aes	*a.c.	**p.a.	***p.n.	plumbum
1. *Campana,* bronze alloy for vases and utensils	90.9		9.1		
2. Alloy similar to the previous one	92.6				7.4
3. Alloy for statues and bronze plaques	68.6	22.8	8.6		
4. *Tenerrima,* alloy for casting statues in molds	87.0		4.3	8.7	
5. *Ollaria,* alloy for vases	96.2–97.1		2.9–3.8		

*a.c. = *aes collectaneum*

**p.a. = *plumbum argentarium*

***p.n. = *plumbum nigrum*

TABLE 3. *Pliny's alloys according to Caley (1970).*

Alloy	Copper	Tin	Lead
1	90.9	4.5	4.5
2	92.6	7.4	
3	86.8	6.6	6.6
	81.2–81.3	8.7–9.7	9.1–10.0
4	81.4	6.8	11.8
	72.7	7.8	19.5
5	96.2–97.1	1.4–1.9	1.4–1.9

TABLE 4. *Pliny's alloys according to Picon et al. (1967).*

Alloy	Copper	Tin	Lead
1	90.9	9.1	
2	92.6	7.4	
3	87.0–89.0	11.0–13.0	
4	86.9	4.4	8.7
5	96.2–97.1	2.9–3.8	

The third hypothesis by the *Projektgruppe Plinius* (Plinius der Ältere 1984) identifies *plumbum argentarium* with lead (Table 5). This interpretation encounters two difficulties: First, tin does not appear as an alloy component, which would require an alloy containing tin to be identified with the term *aes* in every case. Second, in the formula for statuary bronzes (alloy no. 4) lead would have to be added and named twice—as *plumbum nigrum* and as *plumbum argentarium,* respectively—without substantial difference and therefore without apparent reason.

Nevertheless this very formula of no. 4 (13% Pb) should be very close to the lead-bronze formula commonly used by the Romans for sculptural works, according to a technical tradition that dates back to the fourth century B.C.E. It is probable that the use of lead bronze was slow to be accepted because the characteristics caused by

TABLE 5. *Pliny's alloys*
according to the
Projektgruppe Plinius
(Plinius der Ältere 1985).

Alloy	Copper-bronze	Lead
1	90.9	9.1
2	92.6	7.4
3	68.6 + 22.8	8.6
4	87.0	13.0
5	96.2–97.1	2.9–3.8

the addition of lead to bronze alloys were not well known. In fact, large quantities of this metal led to the phenomenon of liquation and to the development of discolored patinas.

It is also likely that from the fourth century B.C.E. on, a technical tradition developed for the use of lead in controlled quantities in statuary, taking advantage of the metal already available on the market as a by-product of silver-working. This would explain an interesting observation concerning the statistical interpretation of the data. The results of the quantitative analysis were interpreted for various groups in order to obtain the average value, the standard deviation, the coefficients of correlation between the various elements, and the levels of statistical significance. Statistical elaboration of the data was carried out on characteristic groups of values corresponding to the types of alloys already identified by means of the preceding chemical analyses and nondestructive tests.

The logical process of the research may be summarized as follows: nondestructive testing plus visual examinations, initial identification of the alloys, sampling and chemical analysis, testing with measurements of conductivity IACS%, classification of analytical data in groups, and statistical analysis of the groups.

Several interesting conclusions can be drawn from the final results of statistical analysis, only partially shown in Table 6. First, the original sections show a negative correlation between copper and lead (-0.79), while there is no correlation between tin and either copper or lead. The standard deviation relative to the percentage concentrations of lead is relatively low. From this, one could deduce that the ancient founder was concerned about keeping the lead within a "safe" percentage by applying a formula of reference of the type:

$$100 - \text{lead} = aes + aes\ collectaneum \text{ (scrap copper and bronze)} + \text{tin}$$

The tin does not correlate with copper and lead, probably because the percentage of tin in the *aes collectaneum* varied each time without a systematic point of reference.

Second, the addition of lead confers some specific characteristics on the alloy: the fusion point of the alloy diminishes and the cast becomes more fluid, while the surface of the bronze becomes more workable and polishable with scrapers, files, and pointed tools (although the workability by hammering declines).

Third, the absence of correlations between the other alloy elements shows that the various original sections, cast separately, were made with metal from different stocks, probably also using *aes collectaneum*.

Alloy	Average %			Standard deviation %			Minimum–Maximum %		
	Cu	Sn	Pb	Cu	Sn	Pb	Cu	Sn	Pb
Roman sections	80.7	6.8	12.0	2.57	1.44	2.32	75.9 85.6	3.9 10.5	8.4 16.4
Roman soldering	74.0	6.6	19.4	1.75	2.16	1.74	71.6 77.0	3.8 10.2	16.9 23.1

Table 6 shows the statistical values for twenty-eight original Roman alloy specimens and for ten specimens of Roman soldering. For soldering, no correlation was found between copper, tin, and lead, suggesting a rather approximate mixture of principal components, the only restriction being that the cumulative percentage of tin plus lead must not drop below a certain level. In this case, the lead not only lowers the melting point and viscosity of the alloy but also acts as a true deoxidant for the soldering, forming with the tin dioxide (SnO_2) a compound (Pb_2SnO_4) that melts at 1060 °C (Steinberg 1973; Lechtman and Steinberg 1970).

The elaboration of the data for the repaired sections was still in progress in early 1992, with some difficulties of interpretation because of the great variety of alloys used for restoration (in collaboration with E. D'Arcangelo).

Thermal Behavior of the Monument

One particularly interesting area of study has been that of the environmental causes of deterioration. The exchange of thermal energy between the environment and the monument has been thoroughly investigated, revealing that the mechanical stresses suffered by the bronze in its position on Capitoline Hill have also been dependent on the daily cycles of expansion and contraction of the metal structure. A description of the thermal behavior of the material is useful for a better understanding of an important series of problems that are not only mechanical but also involve the electro-chemical and chemical corrosion of the surface.

The Piazza del Campidoglio is located about twenty meters above traffic level and is enclosed on three sides by the Palazzi Capitolini. The monument of Marcus Aurelius is placed in the center and oriented toward the northwest by 60°; that is, toward the wide ramp designed by Michelangelo. The particular placement of the monument and the geometry of the plaza allow direct sunlight to strike the metallic surface unevenly, warming different sections of the bronze at different hours of the day. In order to analyze the thermal exchange between the monument, its stone base, and the surrounding air, continuous readings of the surface temperature in ten areas were taken during the summer, along with thermovision images of the monument. At the same time, a series of acoustic-emission measurements were taken to register incidents of deformation in the horse over a 24-hour period (Accardo et al. 1983).

This last technique, in particular, operates on the principle that structural deformations and the formation or increase of cracks release microquantities of elastic
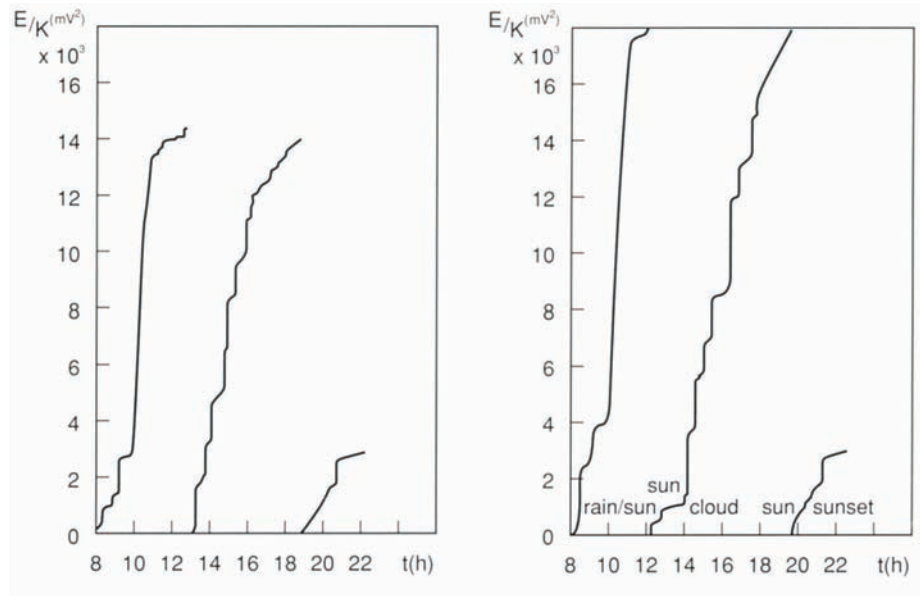
energy, causing propagation of mechanical pressure waves at a frequency greater than 10 MHz, which are picked up by a piezoelectric transducer and stored and analyzed by a sequential electronic apparatus.

Using these techniques, several important findings have emerged. First, the horse's left-front leg showed particular stress from direct solar radiation after ten o'clock in the morning. Of the two registrations in Figures 5a and 5b, the first shows the course of energy emitted on a clear day, while the second represents the phenomenon on a cloudy day with rain. It is evident that more energy is released under conditions of maximum irradiation as well as during rapid variations of surface temperature.

Second, because of its greater thermal inertia, the stone base maintains a surface temperature higher than that of the bronze alloy and keeps the lower part of the horse warmer during the night, while the hindquarters cool down through radiant emission toward the sky (Fig. 6).

In general the bronze surface responds quickly, because of its scant thermal inertia, to the temperature variations of the surrounding air. Exceptions may include the legs, which are filled with a lead-tin alloy (*metallone*) and the belly of the horse, because of its thermal exchange with the stone base. The thermovision images of the legs are certainly influenced by the greater thermal capacity of the volumes filled with lead-tin alloy, which show up as lighter (i.e., hotter), while the dark areas correspond to "empty" spaces (Accardo et al. 1983).

From the structural point of view, one may conclude that the low level of energy released by the structure corresponds to incidents of temporary (elastic) deformation, particularly involving that section of the left-front leg of the horse already subject to the mechanical stresses of the monument's weight.

Finally, in regard to the electrochemical aspects, climate certainly has a decisive influence on the kinetics of the bronze's corrosion. Given the rapid adjustment of the metal surface to the temperature of the surrounding air, the events of precipitation and capillary condensation are the primary elements that accelerate electrochemical corrosion.
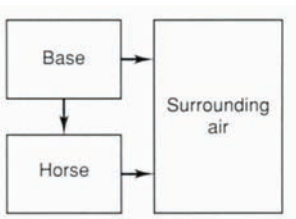
CLIMATE AND POLLUTION

In recent years damage functions have been developed to calculate the electrochemical corrosion of a metal object over the course of a year, taking into account the amount of time the surface remains wet and the integrated fluxes of deposition of the more destructive airborne pollutants. For the Roman climate, the time of wetness (*tw*) of a metallic surface exposed outdoors is given as:

$$tw = tw1 + tw2$$

where *tw*1 equals the time of wetness of the surface caused by rainfall and *tw*2 equals the time of capillary condensation (Marabelli et al. 1988). Capillary condensation is linked to the shape and diameter of capillary pores in the patina and starts at a relative-humidity value well below 100% (corresponding to traditional surface condensation).

In order to measure the threshold value of relative humidity corresponding to the beginning of capillary condensation, the ICR Chemistry Laboratory developed a prototype consisting of an automated apparatus programmed by computer and capable of measuring surface conductivity and volume conductivity of patinas, which is variable in terms of relative humidity (Marabelli et al. 1988). This instrument comprises a measurement cell of conductivity, which clings to the metal surface and within which a particular hygrometric progression is produced in a predetermined way.

In the case of the Marcus Aurelius, by increasing the relative humidity (RH), it was possible to document, after some 160 experiments, that the surface conductivity increases rapidly above approximately 80% RH (Marabelli et al. 1988). Figure 7 shows a typical experimental curve corresponding to the surface electrical conductivity function, f(RH). The resulting theoretical function is:

$$y = 0.8 \cdot \exp\left(-\,[80-x]\,/\,3\right)$$

where *y* equals the conductivity in microsiemens and *x* equals RH.

FIGURE 7. *Surface conductivity dependent on relative humidity.*

MARABELLI
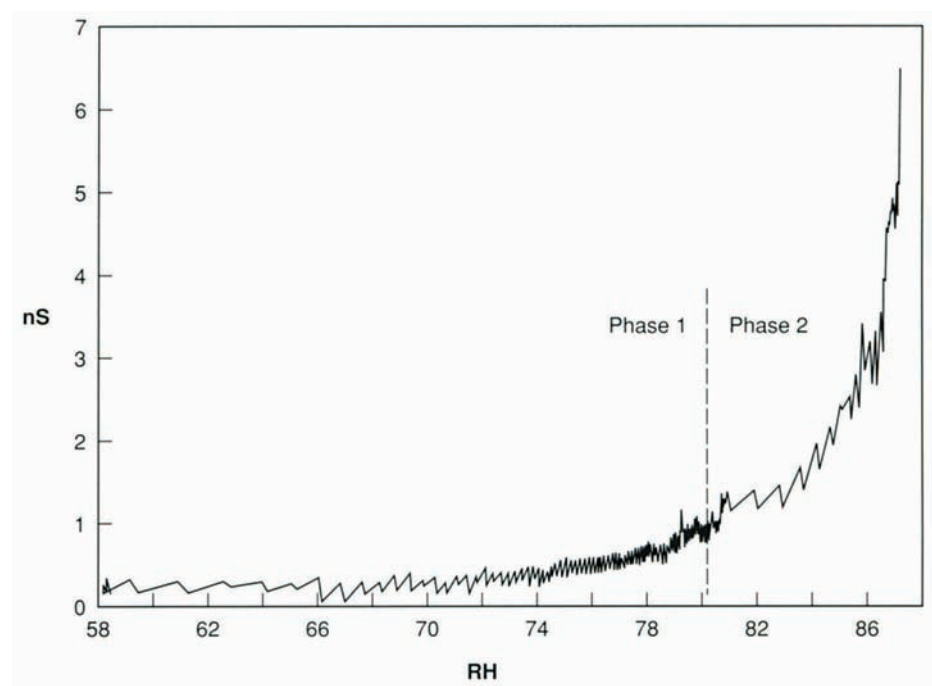
Knowing the daily distribution frequency of relative humidity over the course of a year, it was possible to determine that $tw2$ equals approximately 22.8 days, while $tw1$ can be roughly deduced from the monthly averages of pluviometric data for the historical center of Rome over a 10-year period. The total tw equals approximately 0.22 per year. This finding was used to calculate the corrosion velocity of the monument exposed outdoors by using a damage function developed by Benarie and Lipfert and slightly modified for this specific case (Marabelli 1992). The velocity of electrochemical corrosion, Vc, expressed in g/m² per year, equals:

$$Vc = tw \cdot 0.38 \cdot a \, (fSO_2 + 1.1 \cdot fCl^-)$$

where tw equals the total annual time of wetness; a equals the dilution factor of the pollutants, taking into account the elevated position of the plaza; and fSO_2 and fCl^- equal the integrated fluxes of deposition expressed in mg/m² per day.

As a result, it was possible to determine the velocity value of the electrochemical corrosion of the alloy at roughly 0.2 microns per year (Marabelli 1992). It would seem possible to extrapolate from these data encouraging indications for the conservation of the Marcus Aurelius outdoors. However, it must be remembered that the chemicophysical corrosion of the patina, caused by airborne acidic pollutants as well as rainfall, still causes a constant erosion of the surface with loss of gilding.

To better understand the conditions of the formation and transformation of corrosion products in relation to the climate and other environmental parameters in the broad sense, a series of samples of the patina differentiated by color, consistency, and orientation to sunlight and rainfall was taken and examined using X-ray diffraction.

Patinas and Types of Corrosion

The surface of the Marcus Aurelius reveals extensive sulfation, with the formation not only of brochantite but also antlerite and chalcanthite, a soluble copper sulfate. Since brochantite is stable between 3.5 and 6.5 pH, and antlerite is stable between 2.8 and 3.5 pH, the presence of the chalcanthite indicates that the pH level on the surface of the monument must have fallen below 2.8, probably as a result of microcondensation (Graedel 1987).

The partial dissolution of the patina evidently makes the already precarious mechanical adhesion of the gold even more unstable, to the point that even the application of a fixative may cause damage to the gilding. Furthermore, the gilding always appears so fragmentary and riddled with holes that water easily infiltrates the underlying patina (Fig. 8). The areas protected from the driving rain and from water runoff appear darker due to the accumulation of carbon substances and other components of the atmospheric particulate (gypsum, feldspars).

Conversely, the horizontal surfaces facing upward and those corresponding to the geodetic lines of rainwater appear lighter because of the absence of carbon particles. The alternation of darker (cathodic) stripes and lighter (anodic) stripes on the flanks of the horse form a typical zebra pattern (Fig. 9). Spots and whitish stains along with gray patinas covering the gold are rich in anglesite, present along with

brochantite in almost all the samples. A few areas of the monument bear traces of a brownish surface coating, the composition of which has not yet been defined.

Finally, atacamite, a basic copper chloride, is present below the brownish-black patina deposits, indicating an electrochemical attack on the alloy in the presence of a chloride ion. This ion accelerates the corrosion and, in certain cases, promotes pitting. Its presence can be attributed either to the airborne chloride deposits (marine particulate, emissions from the combustion of plastics containing chlorine), or to the attack of the surface by chemical compounds containing chlorine.

Process and Condition of the Gilding

Not all of the tests have been completed for this important and complex monument. Study of the gilding process in particular is still in progress. The first phase of testing involves metallographic analysis of samples taken from the horse and from the mantle of the horseman to obtain information on the thickness of the gold leaf, the stages of application, and the extent of the corrosion process.

Figure 10 shows the metallographic section of one sample: two pieces of gold leaf rest on corrosion products that penetrate to a maximum depth of 0.3 mm; the pieces are completely detached from the metal and separated from each other by the same oxidation products. The thickness of the gold leaf varies from 3 to 9 microns. This measurement is consistent with the values cited by Oddy et al. (1979).

Three other characteristics of the gilding of the monument should be noted: (1) residual gilding is present almost exclusively on the Roman sections and repairs; (2) the surface of the horseman shows minute scoring in definite directions, suggesting that the alloy was textured in this way to anchor the gold leaf more effectively (see the term *concisuris* in Pliny 1961, book XXXIV, chapter 19); and (3) in two areas of the horse's hindquarters, which are covered by the horseman, a series of roughly square gold leaves with sides varying from 5 to 9 cm are visible. A similar square pattern is present on the *Horses of San Marco* (Galliazzo 1981) and on some bronze statues cited by Oddy et al. (1979). In Pliny's treatise two methods of gilding

FIGURE 8. *Damaged gold surface.*

FIGURE 9. *Typical alternation of light and dark areas of surface corrosion.*
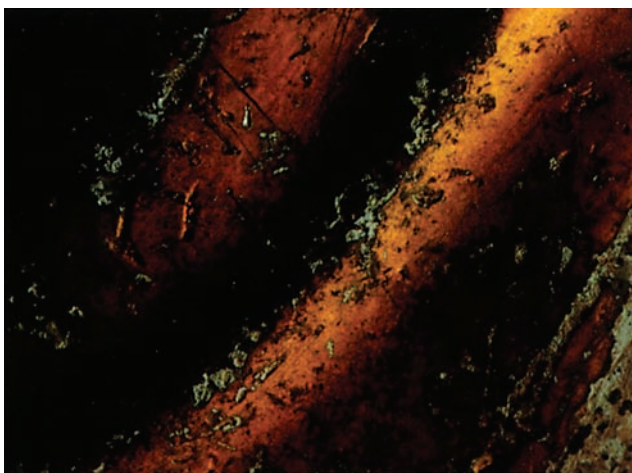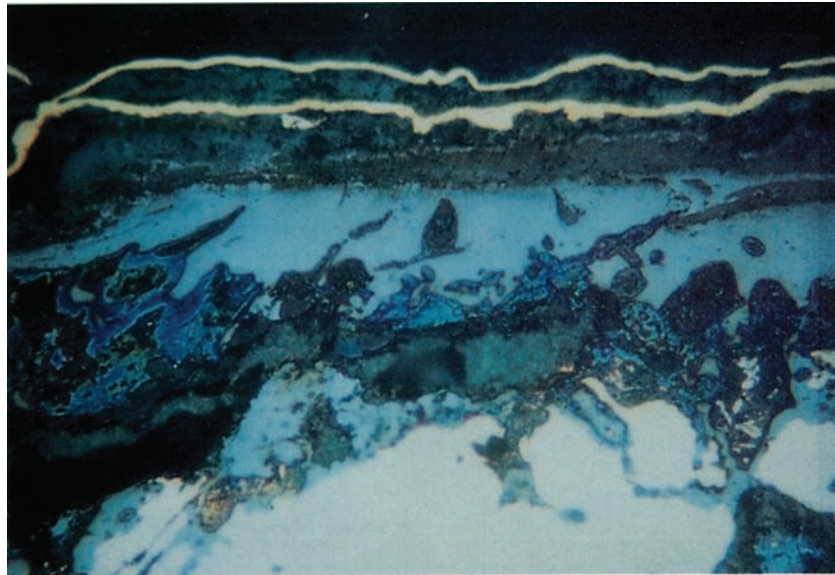
FIGURE 10. *Metallographic section of an alloy specimen from the horse.*

are cited directly (book XXXIII, chapter 20), and a third indirectly (book XXXIV, chapter 19), concerning a bronze statue of Alexander the Great, which the Emperor Nero later had gilded. Basically the methods involve gilding with cold mercury, gilding with proteic glue, and gilding with gold foil or gold leaf (*à l'hache*).

Oddy's hypothesis that fire (mercury) gilding began at the end of the second or beginning of the third century C.E. seems well founded (Oddy 1982). Both Oddy (1982) and Craddock et al. (1987–88) have published lists of bronzes that contain large quantities of tin and lead and were not gilded with mercury. On the other hand, lead bronzes (including the Marcus Aurelius) cannot be gilded with mercury, either by the cold process or the hot process. Therefore, discarding the hypothesis of gilding with proteic adhesive for the Capitoline monument, which was intended to be placed outdoors, only the *à l'hache* technique seems probable. However, the use of this process should be checked against both the analysis of alloy microsamples and the current foundry experiments.

Observations and Conclusions

During the restoration, several reagents and processes for cleaning the surface were perfected in collaboration with the restorer Paola Fiorentino. The practical experimentation was rather long and laborious, since the objective was essentially to remove the corrosion products on top of the gold without dissolving or detaching those underneath.

ICR and the Selenia Company, working in collaboration, carried out a test of eleven surface coatings for the conservation of bronzes outdoors (Marabelli and Napolitano 1991). At the end of the study, it was possible to establish that the best formula was provided by Incralac or Paraloid B72 as primer and Reswax WH (a mixture of a polyethylene wax and two microcrystalline waxes) as a protective finish.

Despite the studies completed thus far, a product capable of ensuring protection without extensive maintenance for a period of at least twenty to thirty years has not been developed. On the other hand, given the precarious adhesion of the gold,

massive fixative treatments or cyclical surface cleaning are inadvisable for the Marcus Aurelius if it is relocated outdoors. At the present time, therefore, the best and most rational solution for the conservation of the two statues would be a climate-controlled museum environment that provides filtration of the atmospheric pollutants. This does not exclude the future possibility of returning the monument to its original position outdoors, if protection and maintenance operations could be assured with little or no damage to the patina and residual gold.

References

ACCARDO, G., D. AMODIO, P. CAPPA, A. BENNICI, G. SANTUCCI, AND M. TORRE
1989   Structural analysis of the equestrian monument to Marcus Aurelius in Rome. In *Structural Repair and Maintenance of Historical Buildings,* 581–92. C. A. Brebbia, ed. Southampton, U.K.: Computational Mechanics Institute.

ACCARDO, G., A. BENNICI, M. TORRE, D. AMODIO, P. CAPPA, AND G. SANTUCCI
1989   An experimental study of the strain fields on the statue of Marcus Aurelius. In *Proceedings of the 1989 SEM Spring Conference on Experimental Mechanics*, 534–37. Bethel, Conn.: Society for Experimental Mechanics.

ACCARDO, G., C. CANEVA, AND S. MASSA
1983   Stress monitoring by temperature mapping and acoustic emission analysis: A case study of Marcus Aurelius. *Studies in Conservation* 28:67–74.

ACCARDO, G., F. CAPOGROSSI, G. SANTUCCI, AND M. TORRE
1984   Determinazione del carico. In *Marco Aurelio*: *Mostra di Cantiere*, 60. Rome: Arti Grafiche Pedanesi.

ACCARDO, G., F. DE SANTIS, F. GORI, G. GUATTARI, AND J. M. WEBSTER
1985   The use of speckle interferometry in the study of large works of art. In *Proceedings of the 1st International Conference on Non-destructive Testing in Conservation of Works of Art* 4(1):1–12. Rome: Istituto Centrale per il Restauro (ICR) and Associazione Italiana Prove non Distruttive (AIPnD).

CALEY, E. R.
1970   Chemical composition of Greek and Roman statuary bronzes. In *Art and Technology: A Symposium on Classical Bronzes,* 37–49. Cambridge: MIT Press.

CANELLA, G., M. MARABELLI, A. MARANO, AND M. MICHELI
1985   Esame ultrasonoro della statua equestre del Marco Aurelio. In *Proceedings of the 1st International Conference on Non-destructive Testing in Conservation of Works of Art* 1(8):1–12. Rome: Istituto Centrale per il Restauro (ICR) and Associazione Italiana Prove non Distruttive (AIPnD).

CRADDOCK, P. T., B. PICHLER, AND J. RIEDERER
1987–88   Legierungszusammensetzung in naturwissenschaftliche Untersuchungen an der Bronzestatue Der Jüngling vom Magdalensberg. *Weiner Berichte über Naturwissenschaft in der Kunst* 4(5):262–95.

DE LACHENAL, L.

1989   Il monumento nel Medioevo fino al suo trasferimento in Campidoglio. In *Marco Aurelio*: *storia di un monumento e del suo restauro*, 129–55. Milan: RAS.

FERRETTI, M., R. CESAREO, M. MARABELLI, AND G. GUIDA

1989   The analysis of bronze alloys from the equestrian statue of Marco Aurelio by means of a thin sample XRF technique. *Nuclear Instruments and Methods in Physics Research* B 36:194–99.

FIORENTINO, P.

1989   La doratura: Note sulle tecniche di esecuzione e osservazioni sulla superficie del monumento. In *Marco Aurelio*: *Storia di un monumento e del suo restauro*, 263–77. Milan: RAS.

FITTSCHEN, K.

1989   Il ritratto del Marco Aurelio: considerazioni, critiche dopo il restauro. In *Marco Aurelio*: *Storia di un monumento e del suo restauro*, 75–78. Milan: RAS.

GALLIAZZO, V.

1981   *I cavalli di S. Marco*. Treviso: Canova.

GRAEDEL, T. E.

1987   Copper patinas formed in the atmosphere III. *Corrosion Science* 27(7)[special issue]:741–69.

LECHTMAN, H., AND A. STEINBERG

1970   Bronze joining: A study in ancient technology. In *Art and Technology: A Symposium on Classical Bronzes,* 5–35. Cambridge: MIT Press.

MARABELLI, M.

1979   *Scheda di analisi* 684. Rome: ICR.

1992   The environment and the future of outdoor bronze sculpture: Some criteria of evaluation. In *Proceedings of "Dialogue 89."* Baltimore: National Association of Corrosion Engineers (NACE).

MARABELLI, M., A. MARANO, S. MASSA, AND G. VINCENZI

1988   La condensazione capillare di vapore acqueo in patine di bronzi esposti all'aperto. In *Preprints of the 2d International Conference on Non-destructive testing, Microanalytical Methods and Environment Evaluation for Study and Conservation of Works of Art* 2(25):1–20. Rome: ICR and AIPnD.

MARABELLI, M., AND G. NAPOLITANO

1991   Nuovi sistemi protettivi applicabili su opere o manufatti in bronzo esposti all'aperto. *Materiali e Strutture* 1(2):51–58.

MEDORI, M.

1983   Utilizzazione del piano di impedenza nelle ispezioni Eddy Current. In *Preprints: Conferenza nazionale Prove non Distruttive,* 1–25. Brescia: AIPnD.

MICHELI, M.

1989   Le tecniche di esecuzione e gli interventi di riparazione. In *Marco Aurelio*: *Storia di un monumento e del suo restauro*, 253–62. Milan: RAS.

ODDY, W. A.

1982   Gold in antiquity: aspects of gilding and of assaying. *The Journal of the Royal Society of Arts* (October):1–14.

ODDY, W. A., L. BORRELLI VLAD, AND N. D. MEEKS

1979   The gilding of bronze statues in the Greek and Roman World. In *The Horses of San Marco, Venice,* 182–87. G. Perocco, ed. Milan and New York: Olivetti.

PICON, M., S. BOUCHER, AND J. CONDAMIN

1966   Recherches techniques sur des bronzes de Gaule Romaine I. *Gallia* XXIV (1):189–215.

PICON, M., J. CONDAMIN, AND S. BOUCHER

1967   Recherches techniques sur des bronzes de Gaule Romaine II. *Gallia* XXV (1):153–68.

1969   Recherches techniques sur des bronzes de Gaule Romaine III. *Gallia* XXVI (2):245–78.

PLINIUS DER ÄLTERE

1985   *Über Kupfer und Kupferlegierungen, herausg: Projektgruppe Plinius 1984.* Essen: Verlag Gluckauf.

PLINY THE ELDER

1961   *Natural History*. Reprint. London: Heinemann.

STEINBERG, A.

1973   Joining methods on large bronze statues: Some experiments in ancient technology. In *Application of Science in Examination of Works of Art: proceedings of the seminar: June 15–19, 1970,* 103–37. Boston: Museum of Fine Arts.

TORELLI, M.

1989   Statua Equestris Inaurata Caesaris: mos e ius nella statua di Marco Aurelio. In *Marco Aurelio*: *storia di un monumento e del suo restauro,* 83–102. Milan: RAS.

B I O G R A P H Y

Maurizio Marabelli, chemist, is head of the Chemistry Laboratory at the Istituto Centrale del Restauro (ICR) in Rome, where he teaches chemistry at the ICR School of Restoration. He also teaches chemistry of restoration at the Faculty of Conservation of Cultural Property, University of Tuscia, Viterbo. Dr. Marabelli is the author of more than ninety papers in the fields of nondestructive technology, conservation of metals and mural paintings, and air-pollution control.

Restoration of the Monument of Marcus Aurelius: Facts and Comments

PAOLA FIORENTINO

Although the history and conservation of the gilt-bronze equestrian monument of Marcus Aurelius is already well known, it is appropriate to begin this discussion with a reminder that this monument is the only equestrian statue to have survived intact from ancient times (Fig. 1). The monument was already being discussed in the Middle Ages, when it stood in front of the cathedral of Rome as the image of Constantine, the first Christian emperor, symbolizing Rome's continuity of power and prestige from the pagan to the Christian world (*Marco Aurelio: Storia di un monumento e del suo restauro* 1989).

EARLY RESTORATIONS

FIGURE 1. *The monument of Marcus Aurelius prior to 1981.*

Marcus Aurelius has always existed as a monument from the time it was first manufactured (around 176 C.E.). It was never buried or excavated; rather, it has gone through a series of relocations in the open environment. The pedestal on which it rests has often been altered; in fact, it has been completely replaced several times throughout history. The monument has gained and lost decorative and sculptural elements, such as the figure of a barbarian upon which the horse's raised hoof once rested. Some of these changes have been recorded, from multiple restorations in the twelfth century to the most recent restoration efforts in 1912, during which some 2,189 repairs were counted (Apolloni 1912). The monument was last moved during World War II.

Past restorations focused on the importance of the visual presence and appearance of the two bronzes (the horse and the rider). To maintain the association of the rider and the horse, repairs were limited to those areas where damage had been visually disruptive. Efforts also focused on those threats that caused immediate concern for the survival of the monument. Little attention was paid to the materials of the bronze, the previous repairs, and the interaction of the monument with the environment. Structural repairs were often roughly made or, at best, served only to reinforce

older repairs that were in a state of collapse. New supports were added, however, such as the *metallone* (lead-tin alloy) casting in the horse's three load-bearing legs.

Other interventions more specific to the surface of the castings can still be recognized today. These include several regildings that took place up to the fifteenth century and the more recent applications of protective coatings with resinous films, which have certainly not helped the preservation of the bronze.

The entire monument is particularly predisposed to corrosion because of its extensively heterogeneous nature. This heterogeneity is due in large part to past structural and surface repairs, such as regilding, and the high lead content of the bronze alloy used for the original castings.

Current Condition of the Monument

Urban pollution has affected Roman monuments for more than a century and has further modified and accelerated the electrochemical corrosion process occurring on the Marcus Aurelius monument. The result has been a reduction in the thickness of the casting, with chemical attacks on the patina, causing a partial removal of the gilt layer. The monument also has many cracks and thin faults passing through the metal. These are particularly severe in the horse, which, as the bearing structure, undergoes load strain.

The extent of this damage, much more of which was revealed during the recent restoration, was partially hidden by a deposit of airborne particulate that, cemented with the alloy-alteration products, had grown 5–6 cm thick in the recesses less exposed to rain leaching (Fig. 2). Such concretions considerably altered the outline of the sculpture. In those areas with the most exposure to rain and the greatest loss of gilding, powdery patinas or the typical geodetic lines of the rain-washed patterns (anodic areas) have formed. The corrosion is clearly more extensive in these areas.

The Restoration Plan

Observed alterations and causes of degradation were investigated and experiments for deciding what restoration methods to use were undertaken. Seven chemical reagents for cleaning the surfaces were tested, of which trisodium EDTA, ammonium

FIGURE 2. *Trappings of the horse, detail showing particulate deposits.*

tartrate, and a cationic resin in acid form (RH) were found most suitable. The expediency of placing the monument in a controlled environment rather than depending on coatings or treatments—which might or might not inhibit corrosion and would surely require frequent maintenance—was also considered.

The restoration of a monument requires a detailed knowledge of its structure and the chemical and physical deterioration mechanisms it has undergone or is likely to undergo given its environment and the various stresses to which it is exposed. Restoration also requires a full identification and characterization of the materials originally used to manufacture the monument and any alteration compounds produced since its manufacture.

Considering this, the Marcus Aurelius can be seen as a unicum, or one-of-a-kind object. It may seem logical to compare it to the horses of St. Mark's Cathedral in Venice. Like the Marcus Aurelius, St. Mark's horses are gilt-bronze castings that have come down to us from antiquity and were continuously exhibited in the open (though, unlike the Marcus Aurelius, they were exposed to a marine as well as industrial atmosphere) until fifteen years ago. However, there are some important and striking differences between the two monuments. The St. Mark's horses are better preserved than the Marcus Aurelius and have undergone fewer repairs during their history. Of greater influence, however, was the fact that the horses were made of copper mixed with only about 2% secondary components. Ultimately then, the St. Mark's monument cannot serve as a specific reference model for the restoration of the Marcus Aurelius (Fiorentino and Marabelli 1977).

The team of experts that studied the Marcus Aurelius monument for two years was aware of the seriousness of the damage but based its research on the premise that the monument would remain in the Piazza del Campidoglio to which it is historically linked. Surveys were carried out to determine fusion, repair, and gilding techniques, following current practices. The studies pinpointed the causes and mechanisms of degradation. Climatic conditions around the monument and their effects were also studied. Calculations were made for the preparation of an internal consolidation structure which, as far as possible, would support the rider and relieve the load on the horse. The structure of Michelangelo's marble base and the dynamics of the corrosion process in relation to the microclimate conditions were examined.[1] Finally, research was done on reliable protective surface coatings for the preservation of gilt bronze. Specifically, new methods of evaluation were often applied to determine the suitability of coatings when applied to a bronze in a specific state of preservation and the ultimate effectiveness of these coatings in the open air (Marabelli and Napolitano 1991).

Restoration Methods

In 1981, following an initial series of examinations in situ, the Marcus Aurelius monument was transferred to a laboratory of the Istituto Centrale per il Restauro in Rome. There the first research workshop-laboratory was established that was solely dedicated to restoring the monument.[2] In these facilities, a series of evaluations was undertaken to clarify both the monument's structural integrity as well as the

corrosion processes it had undergone. The study of the monument's corrosion history involved a full characterization of the corrosion products present on the surface of the sculpture (Marabelli herein). Tests to identify the alloy-alteration products were required, involving some sixty samples taken from the external and internal surfaces of the sculpture. These samples were chosen according to specific characteristics such as color—dark green, light green, gray, whitish, yellowish, light blue, black, earthy—as well as their physical characteristics, such as smooth and compact or powdery and voluminous.

Brochantite was by far the most common mineral identified for the light- and dark-green samples. Anglesite was predominant for the gray samples. In some samples atacamite predominated, while in others cassiterite was present. In the blue samples, taken mainly from the areas where rainwater gathered, chalcanthite was clearly present. Gypsum and feldspar composed most of the particulate deposits. The extremely widespread black alterations—probably formed of amorphous sulfides, carbon particles, and oxidized organic material—did not provide clear diffraction patterns, and their identification is inferred.

Finally, the presence of gypsum and copper oxalate was found in many samples of the yellowish corrosion products, while in the internal walls of the castings, at points where there was the greatest accumulation of particulate on the outer areas, cupric chloride in a typical pitting formation was found. These tests revealed the extensive surface sulfation caused by urban pollution, and the obvious accumulation of airborne particulate that retained humidity in some areas, encouraging cyclic corrosion involving cupric chloride.

The monument presented many different corrosion patterns, alternating even within quite small areas and requiring a special, if not unusual, set of treatment interventions for the monument's conservation. Using a method already tested on the St. Mark's horses (Fiorentino and Marabelli 1977:233–46), researchers identified and isolated twelve sample areas of 9×6 cm each (Fig. 3). These twelve areas were used to evaluate the efficacy and suitability of washing with demineralized water. The purpose of the washing was to extract the harmful soluble salts contained in the corrosion patinas, as well as to remove any residue from chemical cleaning agents. The use of demineralized water avoided any damage to the gilding and the more stable corrosion patinas.

The twelve areas chosen had the following characteristics:

- relatively compact and sufficiently visible gilding
- gilding clearly covered with black alterations
- alteration both exposed and not exposed to rain
- zones with geodetic lines
- alterations where rainwater converged
- alterations in the insides of castings

Washing was carried out with standard methods, using 100 ml fractions of demineralized water and applying brushes for five minutes. The extraction of total soluble salts was calculated for each fraction of water by conductivity measurements
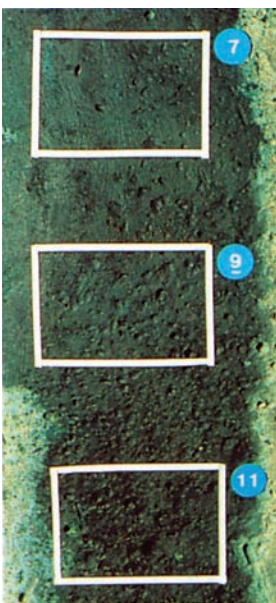

FIGURE 3. *Three sample areas chosen for the cleaning tests.*

of the runoff. The washing was repeated until a reasonable water-conductivity value was achieved; in other words, not exceeding 20 mS cm^{-1}.[3]

The maximum number of washings for the external surface was 14 fractions (1,400 ml total) on a partially gilded area with powdery alterations, and the minimum was 5 fractions (500 ml total) on a gilded area with black alterations. Up to 18 (1,800 ml total) fractions of deionized water were needed for the internal surface.

Some assumptions can be made from these tests: Any minute detachment of patina particles that occurred due to the mechanical action of the brush could be considered acceptable, and no gold particles were noted in the solutions collected. In addition, the proportion of soluble salts removed from the external surface was lower than that found inside the monument, where the salts had accumulated—obviously because the interior was less exposed to rainwater—and also where, given the greater surface adherence, it was possible to carry out longer treatments under safer conditions. Finally, the black alterations were found to be the least soluble and less likely to be removed. The water collected was then used to identify the ions released, with particular reference to sulfate, chloride, copper, and lead ions (*Marco Aurelio, mostra di cantiere* 1984:83–84).

Subsequently, sixty smaller sample areas were chosen (24 × 36 mm each, the size of photographic film) in which the eight different corrosion patinas characterized by X-ray diffraction were represented as homogeneously as possible. The purpose was to compare seven reagents for their efficacy in removing the deposits and alterations that concealed the gilding. The reagents were chosen for their relative inability to react with the underlying bronze alloy and gold gilding layer. Each type of alteration was represented by several samples taken from the statues of both the horse and the rider, providing a series of similar samples for the experiment.

The reagents used for the cleaning tests were as follows:

1. deionized water
2. aqueous solution of 2% Tween-20
3. EDTA trisodium solution 12%
4. Rochelle salt in saturated solution
5. ammonium tartrate in saturated solution
6. mixed-bed ion-exchange resin (Rm)
7. cationic ion-exchange resin in acid form (RH)[4]

These treatments also followed standard procedures, which included applying the reagents in a gel form, using 3.0 g of carboxymethyl-cellulose as a suspending medium per 100 ml of solution.

For the resin tests, 7.0 g of dry resin in 17 ml of water were used. The gels were applied for fifteen minutes each and repeated three times on each area, so the action of the reagent could be checked each time the gel was removed. The applications were followed by washing with demineralized water and soft brushing as previously described. The results of the treatments and subsequent washing are summarized in Tables 1 and 2.

Series	Type of Alteration	Sample No.	Water	Tween-20	EDTA	Rochelle	Amm. tartrate	Rm	RH
1	Dark green	10	IE	IE	SF	IS	IS	IS	IE
2	Uniform black	8	IE	IE	SF	IS	IS	IS	IE
3	Uniform black with underlying gold	8	IE	IE	IS	IE	IS	IE	ST
4	Nonuniform black with underlying gold	8	IE	IE	IS	IE	IS	IS	ST
5	Gray with underlying gold	8	IE	IE	SF	IE	SF	IS	IE
6	Whitish-gray with underlying gold	8	IE	IE	SF	IS	IS	IS	IE
7	Powdery light green	2	ST	—	—	—	—	—	—
8	Thick layer of gypsum deposits	8	IS	IS	IS	—	—	—	—

IE = ineffective

IS = insufficient

SF = sufficient

ST = satisfactory

TABLE 2. *Washing of areas treated with reagents, showing conductivity values (micro Siemens/cm).*[*]

Series	Type of alteration	No. wash	Water	No. wash	Tween-20	No. wash	EDTA	No. wash	Rochelle	No. wash	Amm. tartrate	No. wash	Rm	No. wash	RH
1	Dark green	5	112–17.5	2	10–3.8	4	318–18	3	340–15.5	3	354–13.3	2	9–4	3	19–4
2	Uniform black	5	68–20	2	8.4–5.2	3	440–16	3	331–17	4	465–10.5	2	10–5	3	13–4
3	Uniform black with underlying gold	4	46–18	2	7.2–4.5	3	260–6	2	275–11.5	4	357–6	2	6–4	3	135–9
4	Nonuniform black with underlying gold	2	7.5–5.2	2	16–10	5	333–6	3	351–18.5	3	349–15	2	6–4	3	40–4
5	Gray with underlying gold	2	20–12	2	13.5–6	5	333–9.5	3	343–13.5	3	343–13.5	2	5.5–4.5	3	54–4.5
6	Whitish-gray with underlying gold	3	29–10	2	10–6	3	331–13.5	3	333–16.5	4	385–2.0	2	6.5–4	3	31–5
7	Powdery light green	4	42–15	2	—		—		—		—		—		—
8	Thick layer of gypsum deposits	9	118–23	4	200–20	13	480–19		—		—		—		—

[*]The results of the areas where the highest conductivity values have been obtained, followed by the lowest values, are shown for each type of alteration and for each reagent, preceded by the total number of washings.
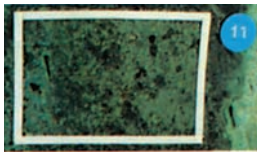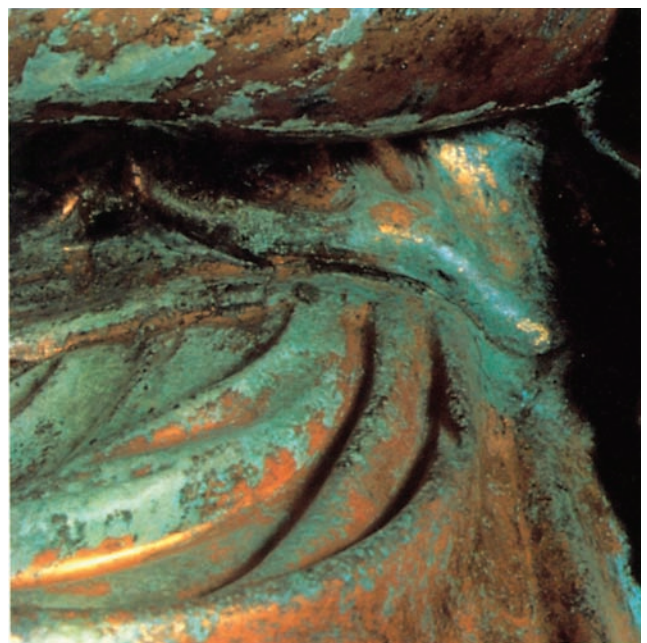
FIGURE 4. *An area of the monument after treatment with EDTA, showing the effectiveness of the reagent compared to the untreated region outside it.*

FIGURE 5. *Detail of the rider, left side, showing folds of the tunic before cleaning, below left.*

FIGURE 6. *Same area as in Figure 5, after cleaning, below right.*

Series No. 7 was treated only with water since the result was satisfactory. Series No. 8 was treated only with the first three reagents, since they were more specific for the deposits present there, which were essentially composed of gypsum and oxidation products of the alloy.

On visual inspection for series Nos. 3 and 7, the effectiveness of the reagents appeared quite satisfactory (Figs. 4–6). Therefore, some larger areas (about 30 × 30 cm) were chosen to check the various treatments on a working level; that is, areas considered representative for treatment of the monument. The test included all the above-mentioned alteration products and was used to assess both the possibility of repeating the various treatments and prolonging the washing, as well as the efficacy of subsequent drying by ventilation. A cleaning methodology was worked out on the basis of the different requirements of the surfaces of the two bronzes. Using the reagents found to be suitable (water, EDTA, ammonium tartrate, RH) it was possible to treat the whole surface except for the areas with thick and tenacious accumulations of particulate. Mechanical means—such as chisels, dentists' drills, or Cavitron—had to be adopted for these areas to reduce the layers. The various reagents were applied after the surfaces were freed of encrustation.

The treatment procedures, conducted with extreme caution, enabled all the existing gilding to be saved, and also revealed subtle and previously hidden aspects of the sculptural form, which in many cases had been concealed by thick encrustation. Inside the castings, various details of the fusion or assembly techniques were revealed. This provided new information regarding the fabrication techniques and repair methods used both in ancient times and at the times of the various restorations and repairs. Obviously, the restoration of such a degraded and mistreated monument involved other, less exacting operations, such as a more thorough electrochemical cleaning of the internal areas with pitting,[5] or retouching the patina of the Renaissance repairs which, being of a different and better-preserved alloy, were darker and did not match that of the restored monument.

Observations and Conclusions

The cleaning treatments used in this restoration of the statue of Marcus Aurelius have made the monument more aesthetically pleasing and, at the same time, have revealed some unresolved conservation problems. The surface of the monument remains porous and cracked, and the gold is not stable. The micro- and large fissures, previously concealed by encrustation, now allow rainwater to enter and spread to a greater extent and absorb water (rain and condensation). Closing them with repairs would once again require a brutal grafting on already fragile and nonhomogeneous castings. As an alternative, synthetic materials might be applied. Such materials would have to be proven suitable for the project, stable with regard to the main chemicophysical points of view, and resistant outdoors. These substances, if used as sealants, would result in a virtual plastification of the monument, which is contrary to any conservation principle. For these reasons, fractures, holes, and gaps have not been repaired.

For the most part, the surfaces have been freed of polluting salts by cleaning and washing, and are thus in a more balanced and stable state. But despite the treatments, cupric chloride is still present inside the crystalline structure of the alloy, and a corrosion-inhibition treatment would probably be more harmful than not because of the volumetric and chemicophysical modifications to the patinas, with negative consequences on the gilding. In any case, if the bronze were to be exposed in the open again, such a stabilization treatment could only be effective for a brief period.

The possibility still exists of finding a coating that, by remaining unaltered for a reasonable time, would postpone maintenance for as long as possible, even if this alone would not be enough to defend the monument from rain infiltration and the consequences of mechanical and thermal stress. But such maintenance of the Marcus Aurelius would also mean the replacement of the coating, and removing the coating would damage the corrosion patina permeated by the resin. In addition, for correct maintenance, it would be necessary to separate the two bronzes, but the maintenance would then be extremely difficult.

FIGURE 7. *Microscopic view of the first (older) oxidized coating, which is partially detached.*

In addition to these concerns, one must keep in mind that it was precisely the damage caused by the old coatings that prompted the team restoring the Marcus Aurelius to reflect on whether it was advisable to continue to use these substances. Traces of two different materials remain: the older coating, perhaps dating back to the early years of this century, was recognized in samples of hardened and oxidized material under the microscope (Fig. 7). Because the material was fractured and partially detached, it had formed blackish stains (cathodic areas), which were higher than the surrounding anodic areas, marked by powdery alterations. It was only possible to remove the remains of this by-product with careful, lengthy, and mechanical action, since solvents had no effect on it.[6]

It was clearly evident that the more recent coating, perhaps applied in the last twenty to thirty years, had shrunk and was tearing off the corrosion patina (Fig. 8). Mechanical means were also used to remove this patina, since solvents only restored a little elasticity. A new synthetic resin, selected from those currently in use and recently studied, applied on a cracked surface exposed to climatic variations would

soon behave like the previous resins, and could also lead to worse damage for the remaining gilding, which is now entirely exposed. At the most, a gentle consolidation of the corrosion patinas was necessary to prevent their continuous crumbling. A film of Paraloid B72 (concentration of 3% in trichloroethane) was applied as a fixative and not as a surface coating for the bronze alloy.

As the surveys and restoration gradually progressed, the decision was finally reached not to repair the lesions of the castings as well as not to protect the surface. This decision may at first seem defeatist. But there are various fundamental aims in the conservation of a work of art, such as respect for the historical value and the elimination or partial inhibition of the causes of degradation. A careful evaluation of the risk factors is always necessary.

For the Marcus Aurelius monument, the causes of decay have only been partially removed (Fig. 9). Continuing to work against the preservation of the monument is the environment of the Piazza del Campidoglio, which has not been improved and could rapidly reactivate the alteration processes if the equestrian statue were to be returned to the same location. The conservation of this monument mainly entails preventing, insofar as possible, any further work on or handling of the castings. Thus, the solution of conserving it in an air-conditioned environment, protected from dust, rainwater leaching, mechanical and thermal stress, as well as the avoidance of any introduction of a new support system between the rider and the horse, should not be considered a hasty measure but the most important conservation action carried out on the monument.

Even ignoring the mechanical causes of the deterioration, the extent of water-vapor absorption inside the surface and the speed with which the patina would continue to be corroded and leached if the monument were to be placed outside once again (Marabelli et al. 1988), tally with what can be directly observed on its surface.

FIGURE 9. *The monument of Marcus Aurelius after restoration.*

In 1912 Apolloni, who was restoring the monument at that time, carefully recorded the presence of ancient graffiti on its surface in the form of letters, crosses, symbols, and various figures left by pilgrims who visited Rome in the Middle Ages (Apolloni 1912). Of all those graffiti, only one remains: a barely perceptible star on the horse's raised hoof (Fig. 10). This causes one to contemplate the remarkable survival of this monument thus far and the loss for future generations if it were to be erected again in the open air and this link to the past were thereby destroyed.

Notes

1. For the study of the structure of the monument, see Accardo, Amodio et al. 1989; Accardo, Bennici, et al. 1989; Accardo, Caneva et al. 1983; Accardo et al. 1985; Accardo and Santucci 1988. For corrosion, see Marabelli et al. 1988.

2. The restoration was begun in 1987 and took 18 months to complete. Four restorers and the students of ICR's school of restoration participated under the author's technical management.

3. Demineralized water was used with conductivity values of 1.5 μS cm^{-1}. The conductivity values fell within the 175–4.5 μS cm^{-1} range for external surfaces and 700–4.0 μS cm^{-1} for internal surfaces.

4. The following reagents were used:
   - Tween 20-Merck (poliossietilensorbitanmonolaurato)
   - A 0.5 M (pH 6.5) solution of trisodium EDTA, obtained from 37.2 g bisodium EDTA + 43.4 g tetrasodium EDTA, in 1,000 ml of water
   - Cationic Bio-Rad Ag50W–X8 resin in acid form, 100–200 mesh, pH 5; mixed-bed resin made up of the above resin + Bio-Rad Ag1–X8 resin in OH^{-} form, 100–200 mesh, proportion 1:1.6 washed up to pH = 5.5

   For a similar use of the Rm resin see Fiorentino et al. 1982.

5. A localized treatment was carried out with repeated applications of 1 g of agar-agar and 6 g of glycerine in 80 ml of water + aluminium foil at 60–80 °C. Retouching was done with watercolors.

6. Alcohol, acetone, toluene, benzene, and xylene were used for this purpose.

References

ACCARDO, G., D. AMODIO, P. CAPPA, A. BENNICI, G. SANTUCCI, AND M. TORRE
1989   Structural analysis of the equestrian monument to Marcus Aurelius in Rome. In *Structural Repair and Maintenance of Historical Buildings,* 581–91. C. A. Brebbia, ed. Southampton, U.K.: Computational Mechanics Institute.

ACCARDO, G., A. BENNICI, M. TORRE, D. AMODIO, P. CAPPA, AND G. SANTUCCI
1989   An experimental study of the strain fields on the statue of Marcus Aurelius. In *Proceedings of the 1989 SEM Spring Conference on Experimental Mechanics,* 534–37. Bethel, Conn.: Society for Experimental Mechanics.

ACCARDO, G., C. CANEVA, AND S. MASSA

1983   Stress monitoring by temperature mapping and acoustic emission analysis: A case study of Marcus Aurelius. *Studies in Conservation* 28:67–74.

ACCARDO, G., P. DE SANTIS, F. GORI, G. GUATTARI, AND J. M. WEBSTER

1985   The use of speckle interferometry in the study of large works of art. In *Proceedings of the 1st International Conference on Non-destructive Testing in Conservation of Works of Art* 4(1):1–12. Rome: Istituto Centrale per il Restauro (ICR) and Associazione Italiana Prove non Distruttive (AIPnD).

ACCARDO, G., AND G. SANTUCCI

1988   Metodo di calcolo agli elementi finiti e misure estensimetriche per l'analisi strutturale dei manufatti storico-artistici. In *2d International Conference on Non-destructive Testing: Microanalytical Methods and Environment Evaluation for Study and Conservation of Works of Art* 1(3):1–18. Rome: ICR and AIPnD.

APOLLONI, A.

1912   *Vicende e restauri della statua equestre del Marco Aurelio: Atti e Memorie*. Rome: Accademia di San Luca.

FIORENTINO, P., AND M. MARABELLI

1977   *I cavalli di San Marco*. Venice: Procuratoria di San Marco.

FIORENTINO, P., M. MARABELLI, M. MATTEINI, AND A. MOLES

1982   The condition of the Door of Paradise by L. Ghiberti: Tests and proposals for cleaning. *Studies in Conservation* 27:145–53.

MARABELLI, M., A. MARANO, S. MASSA, AND G. VINCENZI

1988   La condensazione capillare di vapore acqueo in patine di bronzi esposti all'aperto. In *Preprints of the 2d International Conference on Non-destructive Testing: Microanalytical Methods and Environment Evaluation for Study and Conservation of Works of Art* 2(25):1–20. Rome: ICR and AIPnD.

MARABELLI, M., AND G. NAPOLITANO

1991   Nuovi sistemi applicabili su opere o manufatti in bronzo esposti all'aperto. *Materiali e strutture* 1(2):51–58.

MARCO AURELIO, MOSTRA DI CANTIERE.

1984   Rome: Arti Grafiche Pedanesi.

MARCO AURELIO: STORIA DI UN MONUMENTO E DEL SUO RESTAURO.

1989   Cinisello Balsamo (Milan): RAS.

BIOGRAPHY

Paola Fiorentino is chief restorer at the Istituto Centrale del Restauro (ICR) in Rome. She received her degrees at the Arts Academy of Rome and at the ICR School of Restoration, where she has taught metal-restoration techniques since 1966. She has worked for the ICR since 1961, specializing in metal preservation and the restoration of important monuments.

Bronze Objects from Lake Sites: From Patina to "Biography"

FRANÇOIS SCHWEIZER

Over the last decades, archaeologists have made extensive use of scientific methods to investigate, analyze, and interpret excavated artifacts. Apart from dating techniques, botanical, zoological, and sedimentological studies have contributed to a better understanding of the cultural and ecological development of ancient populations. As far as metal artifacts are concerned, research has been centered mainly on the examination of metal alloys and the history of technologies.

Considering all these investigations, it is surprising that little attention has been paid thus far to the composition and structure of corrosion layers on metals as an opportunity for archaeometric research. The aim of this contribution is to show that there is a close link between the composition of patinas and the environments in which they are formed. If one understands the relationship and interaction between soil types and the formation and stability fields of corrosion products on metals, one may be able to tell under what sort of environmental conditions these materials have grown. This information should provide investigators with the possibility of writing the *biography* of ancient metal artifacts.

This paper was written for the use of archaeologists; however, the results of the author's investigations on the composition and structure of corrosion layers of ancient bronzes from lake settlements are also included.

Few studies have been published on the effect of the soil type on the composition of patinas (Geilmann 1956; Tylecote 1979; Robbiola et al. 1988; Robbiola 1990).

ARCHAEOLOGICAL CONTEXT

The lake of Neuchâtel in the western part of Switzerland contains many important lake settlements that have been excavated over recent decades by the archaeological unit of the Canton of Neuchâtel under the directorship of Michel Egloff. The site of

Hauterive-Champréveyres was long occupied during the late Bronze Age, as dated by dendrochronology from 1050 to 870 B.C.E. (Benkert and Egger 1986). During the recent excavation, more than 5,900 bronze objects (needles, pins, bracelets, etc.) were found in the different occupation layers (Rychner 1991). The archaeologist in charge of the metal artifacts, Annemarie Rychner-Faraggi, was struck by their different appearances. She distinguishes two main groups of patina on bronze objects:

1. *Lake* patina—a smooth, dense, brown-yellow patina (approximately 70%)
2. *Land* patina—a thick, green-blue patina containing quartz grains

A few objects contained both patina types.

The great number of bronzes with land patina is very unusual for a lake settlement. Therefore, the question was raised as to whether this settlement was originally on dry land or on damp or wet ground. In approximately 750 B.C.E., the water level of the lake of Neuchâtel rose. From that time until their recent excavation, all the objects had remained underwater.

In collaboration with Rychner-Faraggi, five questions were formulated:

1. Are the different patinas due to different bronze-alloy compositions?
2. What is the composition and stratigraphy of each—the green-blue land and the brown-yellow lake—patina?
3. Under what sorts of environmental conditions (on dry land, in wet soil, in the water) were the patinas formed?
4. Are they primary corrosion products or were they formed later by chemical reactions with the soil?
5. Is it possible to retrace the *history* or the *corrosion biography* of an individual bronze object after its use?

ORIGIN AND TYPE OF BRONZE MATERIAL ANALYZED

To determine the origin and type of bronze material on the objects, five small bronze objects were initially studied: four pins and a fishing hook. Later, four more bronzes were added (Table 1).[1]

The first series of objects was analyzed using the five questions outlined above as a central focus. The second series contained objects that were used for metallographic examinations and for the investigation of corrosion mechanisms.

The site of Hauterive-Champréveyres contains five different archaeological layers (Rychner 1991):

Layer 1: Yellow, sandy layer of recent origin, probably formed by washing out the lower (older) layers, and containing artifacts from these layers. Its pH is 7.55.

Layer 2: Lake sediment of sand and clay.

Layer 3: Layer containing different strata of organic material due to human activities. Its pH varies between 7.1 and 7.7.

TABLE 1. *Data from analysis of several bronze objects.*

Lab MAH Genève	Inv. No. Neuchâtel	Object	Patina type	Archaeological layer
1st series				
85-27	17'773	pin	lake	1
85-28	3'389	pin	lake and land	3
85-29	3'967	fishing hook	lake	1
85-194	3'071	pin	lake and land	1
86-77	18'603	pin	lake and land	1
2nd series				
87-194	18'152	pin-needle	lake	3
87-195	3'031	pin-needle	land	1
87-196	6'567	metal piece	lake	3
87-197	6'246	metal piece	lake and land	1

Layer 4: Sandy stratum.

Layer 5: Layer rich in organic remains. This stratum is related to human activities during the Bronze Age and is on top of a neolithic lake sediment.

Table 1 indicates that the bronze objects examined are from layers 1 and 3.

Experimental Method

Different techniques were used to characterize the bronzes and their corrosion products, as follows:

To determine the chemical composition of the bronze alloys, first X-ray fluorescence analysis was used on the uncleaned surface to establish the alloy type.[2] Inductively coupled plasma (ICP)-atomic-emission-spectrometry[3] was employed for major and trace elements. A tungsten drill was used to sample between 30 and 50 mg of bronze from the uncorroded metal core.

To analyze the metallographic structure of the bronze alloys, sections across the samples were removed with a jeweler's saw, embedded in a polyester resin, ground on carborundum paper up to grade 1000, and polished with diamond pastes of 6μ, 3μ, 1μ, and 0.25μ. After observation, the samples were etched with alcoholic $FeCl_3$ solution.

For composition analysis of the corrosion product by X-ray diffraction, some grains were removed with a steel blade, mounted on a glass needle, and exposed in a Gandolfi camera (114.5 mmø) for 12–16 hours to Fe kα radiation, 30 kV, 20 mA, with no filter. Some samples were also examined[4] with the Debye-Scherrer camera using Fe radiation for 8 hours. Quantitative analysis on polished cross sections of the corrosion layers of the lake patina were undertaken with an electron microprobe.[5] The distribution of different elements in the corrosion layers (element mapping) was examined with the electron microanalyzer.[6]

A N A L Y T I C A L   R E S U L T S

The X-ray fluorescence analysis on the surface revealed that all objects are copper-tin bronzes containing a number of minor elements such as arsenic, nickel, iron, and antimony. The results of the ICP spectrometry are listed in Table 2.

The bronzes are classical, copper-tin alloys with minor constituents that were certainly not added intentionally. There is no systematic difference between bronzes with a lake patina (87-194 and 87-196) and those with a land patina (87-195 and 87-197).

The four objects analyzed showed a similar microstructure: a network of fairly regular twinned grains. Close to the surface, some grains contain slip lines. There was probably a series of working and annealing regimes after the casting process. In a final phase, they were again slightly cold-worked.

The corrosion products of the land patina are, essentially, basic copper carbonates and basic copper sulfates, as indicated below:

malachite $CuCO_3Cu(OH)_2$	ASTM 10-399
antlerite $CuSO_4(OH)_4$	ASTM 7-407
posnjakite $Cu_4SO_4(OH)_6 \cdot H_2O$	ASTM 20-364

Whereas malachite and antlerite are quite common corrosion products, with the latter especially prevalent in polluted urban areas, to the author's knowledge this is the first time that the presence of posnjakite—$Cu_4SO_4(OH)_6 \cdot H_2O$—on archaeological bronzes has been reported. Posnjakite is a light-blue mineral closely related to antlerite and brochantite. It was described first by Komkov and Nefedov (1967). Geologically, it is associated with auricalcite and other secondary minerals near oxidized chalcopyrite. The X-ray diffraction pattern is presented in Table 3.

The identification of the corrosion products of the lake patina proved to be more difficult than expected. In the author's preliminary publication (Schweizer 1988), the presence of an unusual mineral, sinnerite ($Cu_6As_4S_9$) which has an X-ray diffraction pattern close to chalcopyrite ($CuFeS_2$) was reported. Stephan Graeser of the Natural History Museum in Basel, who analyzed one of the samples, presumed the presence of colusite [CU_3 (As, Su, V, Fe) S_4] ASTM 9–10.

The difficulty of interpreting X-ray diffraction patterns of complex copper sulfides is well illustrated in Table 4, in which the specimen is listed together with reference minerals and American Society for Testing and Materials (ASTM) patterns. It was only by quantitative analysis of the chemical composition of the corrosion layer (as will be discussed herein) that the presence of chalcopyrite could be ascertained. The difficulties of interpreting X-ray diffraction patterns of archaeological corrosion products are fully discussed by Fabrizi and Scott (1987).

TABLE 2. *Results of the ICP spectrometry.*

Lab MAH No.	Cu	Sn	Pb	As	Sb	Ag	Ni	Co	Zn	Fe
87-194	89.22	9.57	0.34	0.19	0.26	0.15	0.05	0.06	0.05	0.09
87-195	91.29	5.65	0.51	0.55	1.00	0.22	0.69	0.06	0.01	0.02
87-196	87.52	8.02	1.46	0.60	0.81	0.21	1.04	0.25	0.03	0.05
87-197	89.85	8.02	0.34	0.34	0.60	0.18	0.55	0.10	0.01	0.02

TABLE 3. *X-ray diffraction lines of posnjakite Cu₄SO₄ (OH)₆ · H₂O found on a bronze needle (Lab MAH 87-27, inv. 17773) from the site of Champréveyres. Gandolfi camera 114.5 mmø, 30 kV, 20 mA, 11 hours, Fe unfiltered radiation.*

TABLE 3. *X-ray diffraction lines of posnjakite $Cu_4SO_4(OH)_6 \cdot H_2O$ found on a bronze needle (Lab MAH 87-27, inv. 17773) from the site of Champréveyres. Gandolfi camera 114.5 mmø, 30 kV, 20 mA, 11 hours, Fe unfiltered radiation.*

Sample 87-27/001	Film No. 303	Reference	ASTM 20-364
d (A)	I	d (A)	I
7.67	40		
6.95	100	6.94	100
5.25	30	5.25	8
		5.15	4
4.84	10	4.85	6
4.65	5	4.77	4
3.80	15	3.74	2
3.46	50	3.47	30
		4 weak lines	
2.70	50	2.70	25
2.61	30	2.614	16
		2.576	2
2.41	50	2.422	25
2.33	25	2.334	12
2.25	5	2.260	8
2.01	40	2.018	12
1.95	25	1.952	6
1.86	15	1.870	4
		1.734	2
1.66	15	1.662	4
1.61	15	1.616	2
1.58	15	1.585	4
1.54	45	1.541	10

On one sample (85-197), chalcocite (Cu_2S) and djurleite ($CU_{1.93}S$) were also found.

A small section of needle 87-194 was examined by different techniques to get a better understanding of the formation mechanism of the chalcopyrite lake patina. The copper-tin alloy was attacked locally, resulting in a fingerlike structure. The thickness of the corrosion layer was found by metallographic examination to vary between 100 and 150 μm. The layer is separated into three zones. The first zone, close to the metal, shows evidence of pseudomorphic replacement of metal grains by corrosion products (Fig. 1a). The second zone, clearly visible in dark-field illumination (Fig. 1b) is very regular and free of any inclusions or holes. The third layer is quite porous. The number and size of the pores increase toward the surface.

After etching with alcoholic $FeCl_3$ solution, one can clearly see the crystalline appearance of the structure of the corrosion layer on top of the corroded α-phase grains (Fig. 1c). The corrosion proceeds into the metal through the grains like a root.

To gain a better understanding of the formation of the corrosion layer, the element and its distribution were analyzed.[7] Analysis showed the area represented in Figures 2a–d to be the same as that in Figure 1a. The results may be summarized as

SCHWEIZER

TABLE 4. *X-ray diffraction lines of corrosion products from bronzes from the site lake of Hauterive-Champréveyres, Switzerland, and of the minerals Sinnerite ($Cu_6As_4S_9$) and Chalcopyrite ($CuFeS_2$).*

Sample/ reference mineral	Corrosion on bronze LabMAH 85-28		Corrosion on bronze LabMAH 85-28		Sinnerite $Cu_6As_4S_9$ Lengeubach, Binn		Sinnerite $Cu_6As_4S_9$ ASTM 25-264		Chalcopyrite $CuFeS_2$ Westphalia		Chalcopyrite $CuFeS_2$ ASTM 35-732	
Notes (below):	a		b		c		d		e		f	
	d(Å)	I	d(Å)	I	d(Å)	I	d(Å)	I	d(Å)	I	d(Å)	I
			5.0525	10b								
											4.715	1
					4.2581	<10						
			4.1349	10b								
	3.34	60	3.3578		3.3627	40	3.34	20	3.33	30		
	3.02	100	3.0586	100	3.0288	100	3.02	100	3.03	100	3.038	100
					2.6897	<10						
	2.62	20	2.6598	10	2.6305	70	2.611	40	2.64	10	2.644	5
											2.606	2
					2.5333	40	2.538	40				
					2.4812	40						
											2.308	<1
					2.1787	40						
					2.2460	40	2.237	10b				
					2.1787	40	2.177	5b				
							2.149	5b				
					2.1266	40						
							2.109	5				
					2.0586	40	2.054	10	2.04	20		
							1.915	5b				
	1.85	80	1.8705	90	1.8598	90	1.852	80	1.86	90	1.8697	22
											1.8570	37
	1.75	30	1.7651	50	1.7466	20			1.75	10		
							1.667	5				
							1.640	5				
							1.614	5				
	1.59	60	1.6030	80	1.5849	80	1.581	70	1.59	40	1.5927	27
											1.5753	14
							1.556	20				
					1.5222	30						
							1.514	5			1.5192	1
	1.32	20	1.3265	10	1.3211	30	1.329	5			1.3219	3
					1.3132	30	1.312	20				
							1.297	5			1.3027	<1
							1.288	5				
	1.21	30	1.2067	10	1.2067	40	1.205	30	1.212	10	1.2125	3
									1.204	10	1.2052	5
											1.1998	3
					1.1769	30	1.172	5				
	1.08	40	1.077	10	1.0743	40	1.072	20	1.079	10	1.0770	5
									1.070	10		
							1.060	5				
											1.0452	<1
									1.019	20	1.0173	4
					1.0118	40	1.010	10b			1.0128	5

[a] Corrosion product from bronze needle (Lab MAH, Inv. 3389). Gandolfi camera 114.5 mm, Fe radiation unfiltered, 30 kV, 14 mA, 15 hours. Film Lab MAH No. 302.
[b] Same sample as noted above X-rayed by S. Graeser, Natural History Museum, Basel. Fe radiation, 8 hours. Film Lab MAH, No. G 451p.
[c] Sinnerite sample from the Lengenbach mine near Binn in the Valais, Switzerland. X-rayed by S. Graeser, National History Museum, Basel. Fe radiation, 8 hours. Film Lab MAH No. G 452p.

[d] Ref. Makovisky and Skinner, *Am. Mineral*. 57:824–34 (1972), synthetic crystal.
[e] Sample from Victoria Mine, Westphalia, obtained from J. Deferne, Natural History Museum, Geneva. XRD: Gandolfi camera 114.5 mmø, Fe radiation unfiltered, 30 kV, 14 mA, 17 hours. Film Lab MAH No. 427.
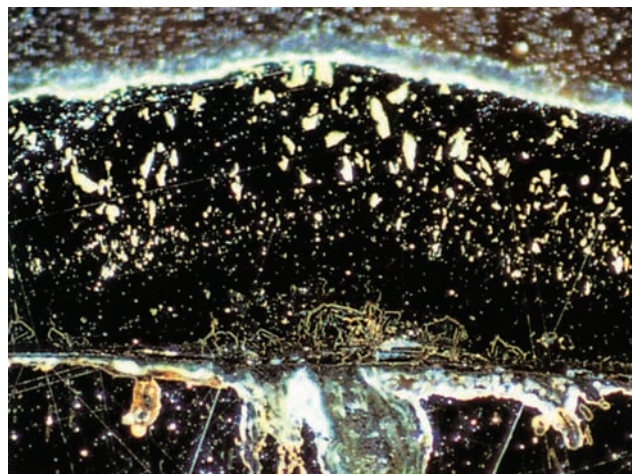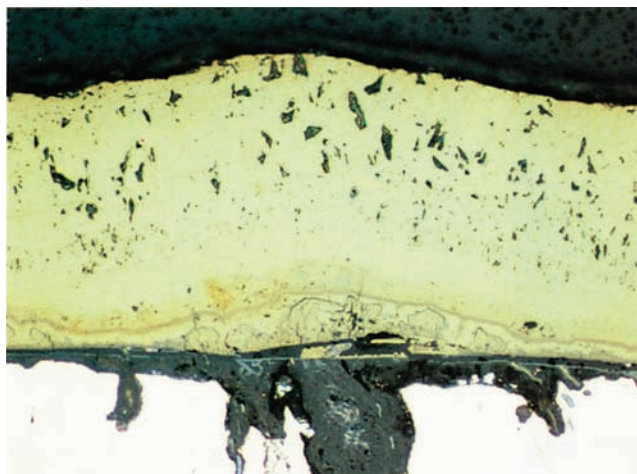[f] Ref. Nat. Bur. Stand. (U.S.) Monogr. 21 (1984). Sample from Merkur Mines, Germany.

FIGURE 1a–c. *Cross section of a chalcopyrite lake patina on a bronze needle, showing (a) above left, unetched, bright field with layered structure on top of the metal; (b) above right, unetched, dark field with different zones in the corrosion layer; and (c) right, region etched with alcoholic FeCl$_3$. Note grainlike area of the corrosion layer on top of the corrosion pit and its rootlike bottom in the latter image. Lab MAH 87-194.*

follows. The bronze alloy corrodes by selectively eliminating copper, which is redeposited as chalcopyrite on the surface (Fig. 2b). There is an enrichment in the tin content due to the preferential corrosion of copper in the alloy (Fig. 2c). The corrosion layer does not contain any tin. Sulfur and iron are distributed in exactly the same manner (Fig. 2d). They have diffused slightly into the corroded areas of the bronze and are evenly distributed in the corrosion layer. An element scan shows that the corrosion layer contains only copper, iron, and sulfur. No other elements can be detected.

To analyze the chemical composition of the lake patina, a small sample of bronze needle 87-194 was studied with the electron microprobe.[8] The results are listed in
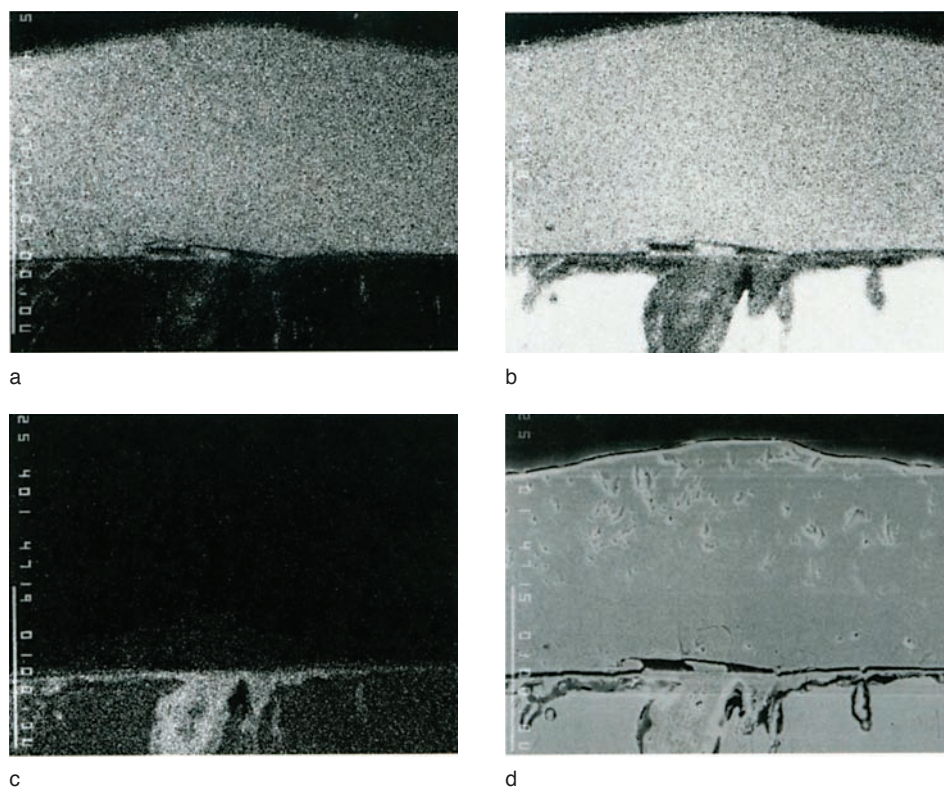
Table 5. The first column gives the composition of the bronze. Some differences in the analyses by atomic-emission spectrometry are probably due to inhomogeneities in the alloy (Table 2). At the interface bronze-corrosion layer, the tin content increases and traces of sulfur are present. The iron values are still very low. Optically, two layers may be distinguished in the corrosion crust. Their compositions are listed in columns 3 and 4 of Table 2. One may observe that there is no significant difference between them. Both layers have a composition consistent with that of chalcopyrite. The corrosion layer contains no tin and only very little arsenic and zinc.

Most publications on microbial corrosion of metals under anaerobic conditions concern the corrosion of ferrous metals (Panter 1980). A short review of literature

TABLE 5. *Electron-*
microprobe analyses of the
corrosion layer of a bronze
needle from the lake site of
Hauterive-Champréveyres[a]
(Lab MAH 87-194).

	Bronze	Bronze int. crust	Int. crust[b]	Ext. crust[c]	Chalcopyrite $CuFeS_2$
Fe %	0.17	0.77	30.69	30.25	30.43
S %	nd[d]	0.03	33.14	33.76	34.94
Pb %	nd	nd	nd	nd	_____
As %	1.70	1.59	0.66	0.14	_____
Zn %	0.13	0.13	0.02	0.01	_____
Cu %	92.40	88.34	34.52	35.44	34.62
Sn %	5.58	9.10	nd	nd	_____
	99.98	99.96	99.03	99.60	99.99

[a] Analyses by R. Oberhänsli, Mineralogical-petrographical Institute of the University of Berne, Switzerland.
[b] Mean values of 3 measurements.
[c] Mean values of 5 measurements.
[d] nd=not detected.

on microbial corrosion of nonferrous metals has been published by McDougall (1966). For archaeological copper-tin alloys, Tylecote published a short note in his excellent paper on the effect of soil conditions on the long-term corrosion of buried bronze alloys (1979:352).

More recently, Duncan and Ganiaris (1987) reported an interesting investigation on bronze and lead alloys found on London waterfront sites. For the formation of the gold- and black-colored sulfides, they postulate two possibilities: (1) precipitation reactions with copper and ions in the soil, and (2) direct action of hydrogen sulfide on the metal-oxide surface.

Based on the foregoing, and in the absence of electrochemical investigations, the formation of the chalcopyrite corrosion layers may be described as follows:

1. Sulfate-reducing bacteria produce hydrogen sulfide in the organically rich soil close to the metal artifacts. It is unlikely that they grow on the bronze alloy, as they normally cannot resist more than 2,000 ppm of copper (McDougall 1966:11).
2. Copper is dissolved preferentially in the α-copper-tin grains, leaving a tin-enriched phase.
3. Copper ions from the metal, iron ions from the surrounding soil, and sulfur ions combine and precipitate as chalcopyrite.
4. The chalcopyrite forms a fairly uniform protective layer on the copper alloy.
5. The growth rate of the chalcopyrite layer must slow down after some time due to increased diffusion times of the copper ions through the corrosion layer.

It is also important to consider the relationship of the different patinas and their composition and appearance on the bronze objects. As Table 6 shows, one may find different types of patinas on the same object. Their different composition is not related to the chemical composition of the alloys nor to the methods of manufacture.

It is obvious that the different compositions of the corrosion products are related to the environmental conditions in which they were formed. The presence of land-type and lake-type patinas on the same object (Figs. 3, 4) still leaves the question of which one was formed first. Is it even possible that both were formed simultaneously?

Even after all the corrosion products have been identified, it is still not possible to answer this question nor those posed here initially. In order to write the *biography* of

FIGURE 3. *Bronze pin with lake and land patina. Lab MAH 86-77.*

FIGURE 4. *Small bronze shaft with lake and land patina. Lab MAH 86-77.*

	Lab MAH No.	Object	Patina	Composition
TABLE 6. *Appearance and composition of patinas on the bronze objects.*	85-194	needle	brown, shiny green, granular white, granular	chalcopyrite $CuFeS_2$ malachite $CuCO_3 \cdot Cu(OH)_2$ calcite $CaCO_3$
	85-27	needle	blue, granular green, granular	posnjakite $Cu_4SO_4(OH)_6 \cdot H_2O$ malachite $CuCO_3 \cdot Cu(OH)_2$
	85-77	needle	brown, shiny blue-green, granular	chalcopyrite $CuFeS_2$ antlerite $Cu_3(SO_4)(OH)_4$
	85-29	fishing hook	brown, shiny	chalcopyrite $CuFeS_2$
	85-28	needle	brown, shiny	chalcopyrite $CuFeS_2$
	87-194	pin-needle	brown, shiny	chalcopyrite $CuFeS_2$
	87-195	pin-needle	green-blue granular	malachite $CuCO_3 \cdot Cu(OH)_2$
	87-196	metal piece	brown, shiny	chalcopyrite $CuFeS_2$
	87-197	metal piece	green-blue granular and brown, shiny	posnjakite $Cu_4SO_4(OH)_6 \cdot H_2O$ chalcocite Cu_2S djurleite $Cu_{1.93}S$

the bronze objects, the environmental factors affecting corrosion-mineral formation and their fields of stability must first be considered.

Environmental Considerations

When a new copper or bronze object is deposited in the soil, its corrosion behavior will depend on different factors:

- composition of the alloy
- acidity of the soil (pH)
- oxidation and reduction potential of the environment—dry (sandy) and oxygen-rich soils or wet, anaerobic soils rich in organic materials
- cations and anions present in the soil

To take a simple case first, the corrosion products that can be formed in the presence of copper, water, and carbon dioxide are tenorite, CuO; cuprite, Cu_2O; malachite, $CuCO_3 \cdot Cu(OH)_2$; and azurite, $2CuCO_3 \cdot Cu(OH)_2$. Which products will actually form depends on the pH of the environment and its oxidation-reduction potential (Eh). Every aqueous system can therefore be characterized by four areas (Pourbaix 1977): oxidizing and acidic, oxidizing and alkaline, reducing and acidic, and reducing and alkaline (Fig. 5).

The fields of stability of the minerals constituting the corrosion products are published (Pourbaix 1977) and are illustrated in a simplified diagram in Figure 6. One can see that alkaline and reducing conditions favor the formation of tenorite (CuO), whereas azurite is stable in an oxidizing and slightly acidic environment. The region between the two oblique lines represents the range of stability of water. Fields of stability for some copper sulfides are shown in Figure 7.

FIGURE 5. *Potential versus pH diagram showing acid, alkaline, reducing, and oxidizing areas in aqueous solutions.*
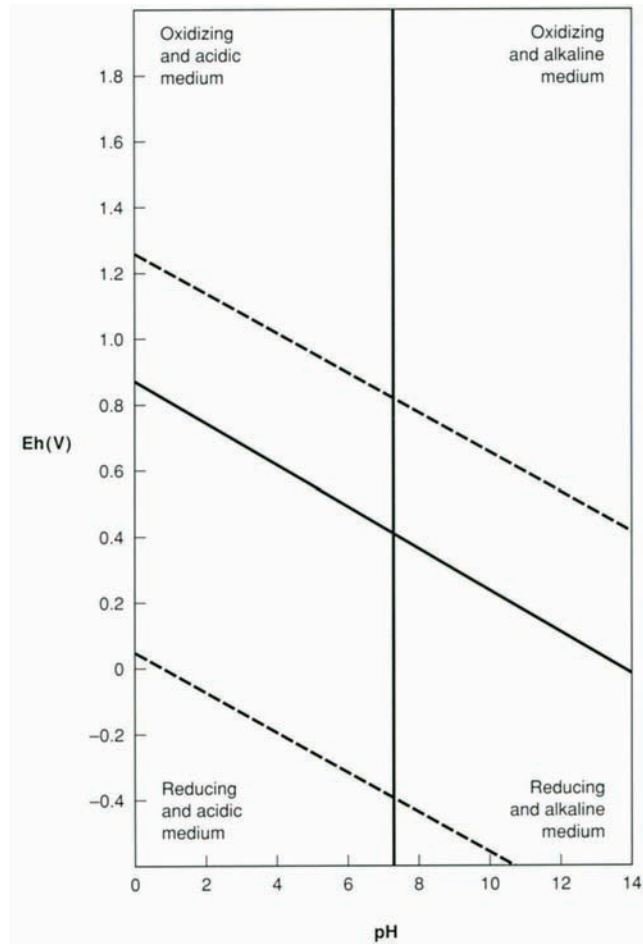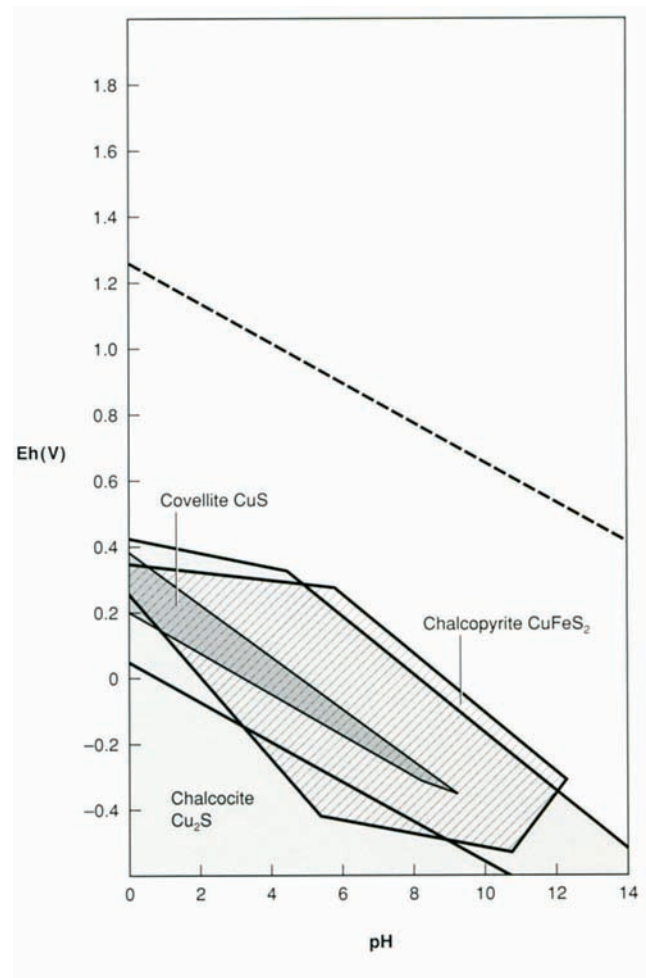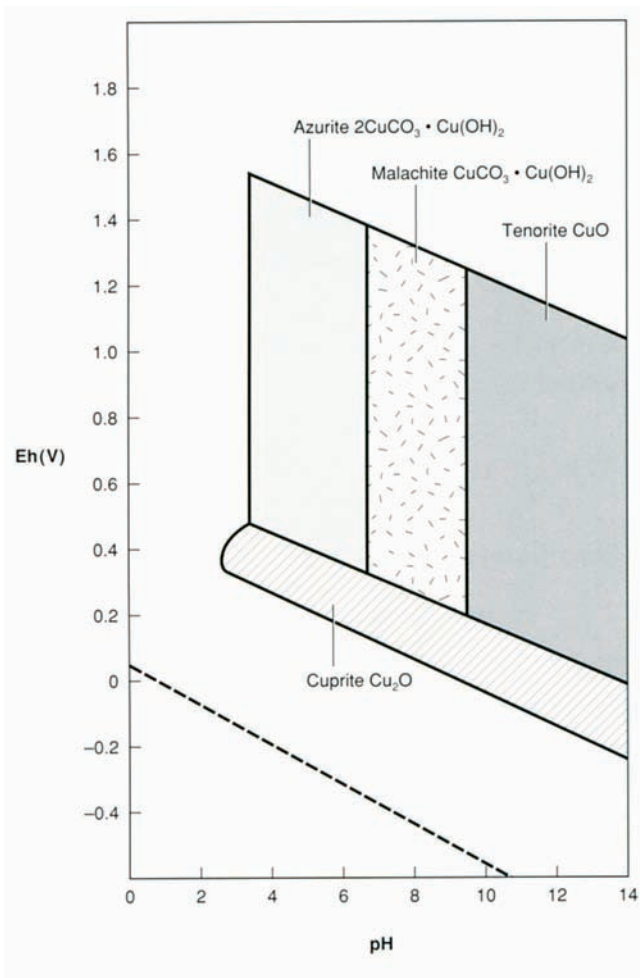
FIGURE 6. *Simplified pH-Eh diagrams for the ternary system Cu-CO$_2$-H$_2$O (after Pourbaix 1977).*

FIGURE 7. *Simplified pH-Eh diagrams for the ternary system Cu-S-H$_2$O (after Pourbaix 1977).*

As the patinas of the bronze objects were formed in the soil, a relation between the fields of stabilities (pH-Eh diagrams) of the corrosion products and different types of soil must now be established. This should indicate the sorts of environmental conditions in which the bronzes acquired their patina.

Soil Types

The formation of soils over long periods of time is a very complex process and is influenced by many factors: composition of the original rocks, degree of erosion, sedimentation, clay content, organic substances, bacteriological activity, type and concentration of soluble salts, and water content. All these factors lead to different soil types.

The earth sciences have tried to characterize soils by measurable parameters. Apart from the chemical, mineralogical, and biological composition, the acidity (pH) and the redox potential (Eh) have proven to be of great interest. A large number of pH-Eh diagrams of different soils have been published (Garrels and Christ 1965; Baas Becking et al. 1960). Figure 8 shows the position in the pH-Eh diagrams of some natural environments.

Basically there are three main regions:

- well-aerated soils in contact with the atmosphere
- transitional environments
- soils isolated from the atmosphere

Clearly, it is possible to characterize the formation areas and fields of stability of copper corrosion products as well as soil types by using pH-Eh diagrams. It is therefore logical to combine these two diagrams.

The information in Figures 6 and 7 is combined in Figure 9. This new diagram may be compared with Figure 8 showing the pH-Eh diagram of soil types. One can see clearly that the fields of stability for copper sulfides correspond to pH-Eh regions of soils, which are isolated from the atmosphere. Malachite and azurite, however, are formed in well-aerated soils.

With these considerations in mind, the formation of the patinas on the different bronze objects may now be considered.

FORMATION "BIOGRAPHIES"

The objects are subdivided into three groups according to their patina composition in Table 6:

- objects with lake patinas only
- objects with lake and land patinas
- objects with land patinas only

Four objects (85-29, 85-28, 87-194, and 87-196) have a patina of chalcopyrite, or lake patina, only (Figs. 10a, b). This copper sulfide must be the primary corrosion product and the objects must have been deposited soon after their use in an anaerobic, damp, and humus-rich soil. The chalcopyrite could not have been formed later
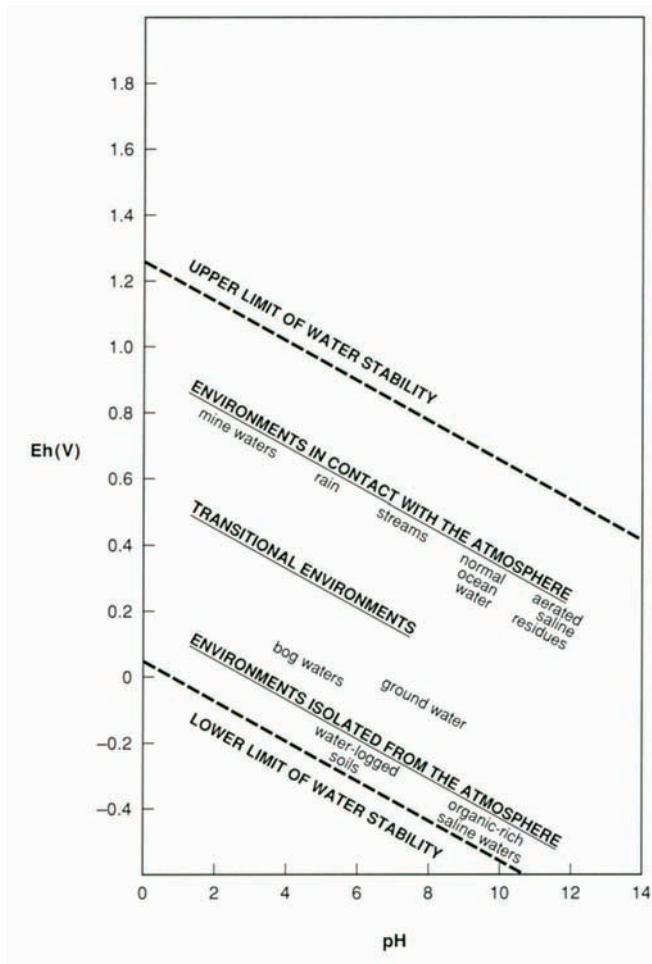
FIGURE 8. *Approximate position of some natural environments as characterized by pH and Eh, above left (after Garrels and Christ 1965).*
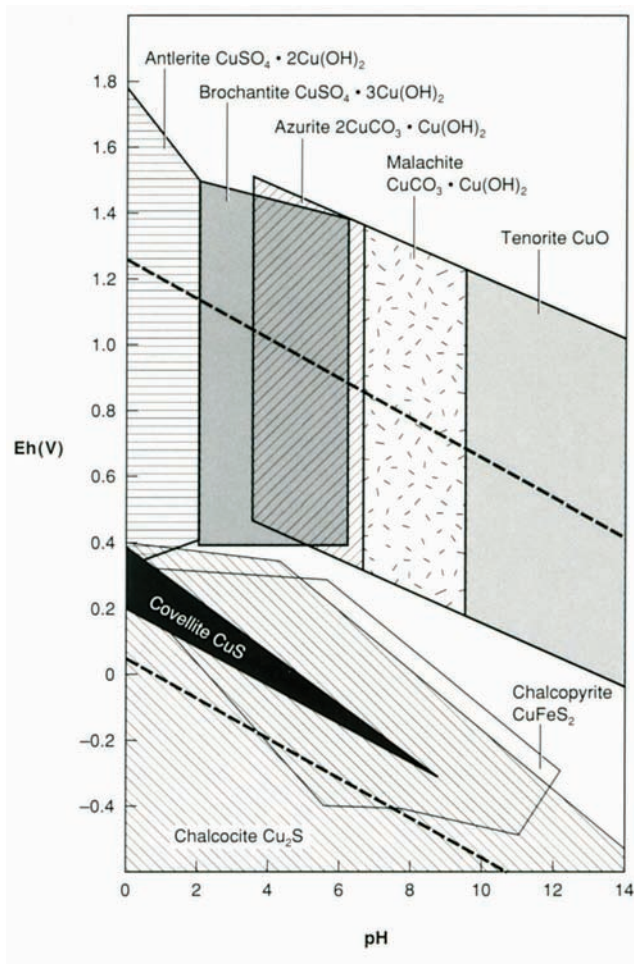
FIGURE 9. *Fields of stability of the corrosion products identified on the bronze objects, above right (after Pourbaix 1977 and Garrels and Christ 1965).*

FIGURE 10a, b. *Chalcopyrite corrosion layer on a pin-needle showing (a) the apparent good condition of the underlying bronze metal, and (b) detail of chalcopyrite corrosion layer typical for a lake patina. Lab MAH 87-196.*

from basic copper carbonates or sulfates. The latter corrosion layers have a granular microstructure, whereas the chalcopyrite layers are smooth and adhere closely to the surface of the metal.

Three objects show both lake and land patinas. They contain corrosion products in which formation conditions and fields of stability correspond to different environmental soil types. On needle 85-194, chalcopyrite and malachite were found; on needle 85-77 (Fig. 3), chalcopyrite and antlerite; and on the metal piece 87-197 (Fig. 4), chalcocite, djurleite, and posnjakite (see Table 6).
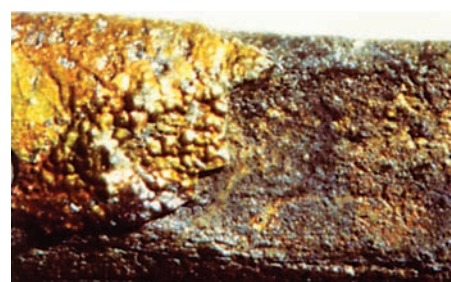
Three hypotheses may therefore be formulated:

1. All corrosion products were formed simultaneously. This possibility can be excluded as the fields of stability for the copper sulfides and the basic copper carbonates and sulfates are too different (Fig. 9).

a

b

2. Malachite, antlerite, or posnjakite was formed and subsequently reduced to copper sulfides. This possibility seems unlikely. First, the transformation of basic copper carbonates and sulfates into copper sulfides requires the presence of sulfate-reducing bacteria and a humus-rich anaerobic environment. This condition is certainly not fulfilled in layer 1, which is sandy. Second, one would expect to see granular sulfide layers in the metal cross sections and not compact ones, which adhere closely to the metal.

3. Copper sulfides were formed under anaerobic conditions and subsequently oxidized to basic copper carbonates and sulfates. This type of transformation is well known, and many minerals are formed in the earth from copper sulfides in the so-called oxidation zone. The mechanism of this transformation has been studied by Sato (1960) and Garrels (1954). The formation of malachite and azurite from copper-sulfide minerals was investigated in the 1930s (Schwartz 1934). Posnjakite does occur near oxidized chalcopyrite deposits (Komkov and Nefedov 1967). The formation of these minerals is activated in well-aerated soils and by partial dehydration.

One may conclude that the formation of the first corrosion products (copper sulfides) took place under anaerobic conditions. The formation of malachite, antlerite, and posnjakite is secondary.

Two objects with land patinas, a needle (85-27) and a pin-needle (87-197), contain no copper sulfides. Needle 85-27 has a corrosion layer of malachite and posnjakite, pin-needle 87-197 only of malachite.

As explained previously, posnjakite is a mineral formed by oxidation of copper sulfides. It is, therefore, probably a secondary corrosion product. Malachite can also be formed directly or by oxidation of copper sulfides. When looking at the cross section, structures observed under the malachite crystals appear to resemble copper-sulfide layers. It is therefore very likely that these two objects were first exposed to anaerobic conditions (wet and humus-rich soil) before they were oxidized.

Summary

The five archaeological questions posed earlier in this paper may now be addressed:

Question 1: Are the different patinas due to different bronze-alloy compositions?

Answer: The compositions of the bronze alloys are very similar and have no influence on the formation of a land or lake patina.

Question 2: What is the composition and stratigraphy of each—the green-blue land and the brown-yellow lake—patina?

Answer: The green-blue land patina contains basic copper carbonates (malachite and azurite) and basic copper sulfates (posnjakite and antlerite). It has a granular structure with quartz-grain inclusions. The brown-yellow, smooth and shiny lake patina is composed of copper sulfides. The presence of chalcopyrite is predominant

with some djurleite. The patina adheres closely to the metal surface. It is quite uniform and measures 100–150 μ.

Questions 3, 4: Under what sorts of environmental conditions were the patinas formed? Are they primary corrosion products or were they formed later by chemical reactions with the soil?

Answer: The lake patina was formed under anaerobic conditions in a soil rich with organic matter and in the presence of sulfate-reducing bacteria. It is a primary corrosion product. The land patina was formed in aerated soil in contact with the air. It is composed of secondary corrosion products, which were formed by oxidation from the primary sulfite layers.

Question 5: Is it possible to retrace the *history* or the *corrosion biography* of an individual bronze object after its use?

Answer: After their use by lake-dwelling settlers, the bronze objects studied must first have fallen into damp, waterlogged soil or sunk to the bottom of the lake close to shore. They must have remained there for quite a long time in close contact with organic remains and sulfate-reducing bacteria. Under these conditions, the chalcopyrite corrosion layers were formed. After the water level of the lake receded, parts of the objects must have been exposed to oxidizing conditions. The copper sulfides were transformed into basic copper carbonates and basic copper sulfates.

The inverse process seems extremely unlikely. The transformation of granular and porous copper carbonates and sulfates to sulfides would not have resulted in a smooth and dense layer, which adheres closely to the metal. A simultaneous formation of both patina types seems also unlikely. The formation conditions and fields of stability are too different.

After the lake water level rose, around 750 B.C.E., the objects with the land patina must have remained underwater in the washed-out upper layers.

Acknowledgments

Notes

1. The samples in the left-hand column of Table 1 are from the Laboratoire de recherche, Musée d'art et d'histoire (Lab MAH), Genève, and all the photographs in this chapter are reproduced by courtesy of the same.

2. Energy-dispersive X-ray fluorescence spectrometer used was a Kevex tube 40 kV, 0.3 mA, 0.8 mm Ø collimator, Seforad Si (Li) detector with a Tracor Northern 5400 multichannel analyzer.

3. This analysis was carried out by the Swiss Federal Laboratories for Materials Testing and Research, Dübendorf.

4. This was done by S. Graeser of the Natural History Museum, Basel.

5. This was done by R. Oberhänsli of the Mineralogical-petrographical Institute, University of Berne.

6. See note 3 above.

7. This was done by P. O. Boll of the Swiss Federal Laboratories for Materials Testing and Research, Dübendorf.

8. This was carried out at the Mineralogical-petrographical Institute of the University of Berne by R. Oberhänsli.

R E F E R E N C E S

BAAS BECKING, L. G. M., I. R. KAPLAN, AND D. MOORE
1960   Limits of the natural environment in terms of pH and oxidation-reduction potentials. *Journal of Geology* 68(3):243–84.

BENKERT, A., AND H. EGGER
1986   Dendrochronologie d'un site du bronze final Hauterive-Champréveyres (Suisse). *Bulletin de la Société Préhistorique Française* 83(11–12):486–502.

CHRISTEN, B. H.
1981   The mineralogy of bronze corrosion. BSC diss., Institute of Archaeology, London University.

DUNCAN, S. J., AND H. GANIARIS
1987   Some sulphide corrosion products on copper alloys and lead alloys from London waterfront sites. In *Recent Advances in the Conservation and Analysis of Artifacts,* 109–18. J. Black, comp. London: Summer School Press.

FABRIZI, M., AND D. A. SCOTT
1987   Unusual copper corrosion products and problems of identity. In *Recent Advances in the Conservation and Analysis of Artifacts,* 131–33. J. Black, comp. London: Summer School Press.

GARRELS, R. M.
1954   Mineral species as functions of pH and oxidation reduction potentials, with special reference to the zone of oxidation and secondary enrichment of sulphide or deposits. *Geochemica and Cosmochimica Acta* 5:153–68.

GARRELS, R. M., AND C. L. CHRIST
1965   *Solutions, Minerals and Equilibria.* A Harper International Student Reprint. New York: Harper and Row.

GEILMANN, W.

1956   Verwitterung von Bronzen im Sandböden Angew. *Chemie* 68:201–12.

KOMKOV, A. I., AND E. I. NEFEDOV

1967   Posnjakite, a new mineral. *Zap. Vses. Mineralog. 0bschch.* 96:58–62 (in Russian).
Summary in *American Mineralogist* 52:1582–83, 1972.

MCDOUGALL, J.

1966   Microbial corrosion of metals. *Anti-corrosion Methods & Materials* 1(8):9–13.

PANTER, I. F.

1980   The role of sulphate-reducing bacteria in the corrosion of iron from anaerobic
environments. BSC diss., Institute of Archaeology, London University.

POURBAIX, M.

1977   Electrochemical corrosion and reduction. In *Corrosion and Metal Artifacts: A Dialogue
Between Conservators and Archaeologists and Corrosion Scientists.* B. F. Brown, H. C. Burnett,
W. T. Chase, M. Goodway, J. Kruger, M. Pourbaix, eds. NBS Special Publication 479:1–16.
Washington, D.C.: U.S. Department of Commerce, National Bureau of Standards.

ROBBIOLA, L.

1990   Caractérisation de l'altération de bronzes archéologiques enfouies à partir d'un corpus
d'objets de l'âge de bronze: Mécanismes de corrosion. Ph.D. diss., University of Paris 6.

ROBBIOLA, L., I. QUEIXALOS, L. P. HURTEL, M. PERNOT, AND C. VOLFOVSKY

1988   Etude de la corrosion des bronzes du Fort-Harrouard: Altération externe et mécanisme
d'altération stratifiée. *Studies in Conservation* 33:205–15.

RYCHNER, A.-M.

1991   Hauterive-Champréveyres: Métal et parure au bronze final. Typescript.

SATO, M.

1960   Oxidation of sulphide ore bodies II: Oxidation mechanisms of sulphide minerals at
25 °C. *Economic Geology* 55:1203–31.

SCHWARTZ, G. M.

1934   Paragenesis of oxidized ores of copper. *Economic Geology* 29:55–75.

SCHWEIZER, F.

1988   Die Patina von Bronzen aus Seeufersiedlungen: Eine Biographie? *Arbeitsblätter für
Restauratoren,* 221–34.

TYLECOTE, R. F.

1979   The effect of soil conditions on the long-term corrosion of buried tin-bronzes and
copper. *Journal of Archaeological Science* 6:345–68.

Biography

François Schweizer received his doctorate in chemical engineering in 1965 in Zürich. Since 1974, he has been head of the laboratory and keeper of conservation at the Musée d'art et d'histoire in Geneva. From 1983 to 1989, he directed the National Research Programme 16, Methods for the Preservation of Cultural Properties, of the Swiss National Science Foundation. His main subject of interest is the ancient technology and conservation of metals, ceramics, and stained glass. Schweizer is a fellow and a member of the Council of the International Institute of Conservation and a member of the Swiss Commission of Ancient Monuments, the ICOM Committee of Conservation, and the Technical Committee of the Corpus Vitrearum.

The Royal Art of Benin: Surfaces, Past and Present

JANET L. SCHRENK

An understanding of the surfaces of ethnographic metal objects pre- and post-collection is important for conservation and curatorial considerations. Historical references to the appearance of copper-alloy objects of Benin Kingdom (Nigeria) prior to 1897 are scarce. However, there is some evidence for clean surfaces on the objects and the application of blood to objects used on altars. Since the removal of these objects from Africa in 1897, they have been subjected to a variety of coatings and other surface treatments. These treatments have left the surfaces discolored, corroded, and saturated with oils and waxes, and thus not generally representative of the original West African aesthetic.

The Benin collection in the National Museum of African Art at the Smithsonian Institution provides an interesting array of surfaces that vary according to the object's collection history. Analysis of samples of coatings and corrosion from these objects reveals a variety of corrosion products, modern pigments, oils, and waxes. A frequently observed problem is the presence of turquoise, fatty-acid metallic salts due to the breakdown of the oils and subsequent attack of the metal surface.

BACKGROUND AND HISTORY

Copper-based alloys were cast throughout West Africa. The most impressive of these were cast in Nigeria, particularly in the kingdom of Benin. The metal casters in Benin City produced an amazing array of copper-alloy plaques, commemorative heads, hip masks, vessels, and other objects between the fourteenth and nineteenth centuries for the exclusive use of the *oba* (king) of Benin.

In 1897 the British launched a so-called punitive expedition against the kingdom of Benin. Oba Ovaramwen was exiled, and the British removed more than 4,000 copper-alloy objects from the royal palace. Some of these objects went to expedition participants, and others were sold at government auction to dealers, private collectors,

and museums. Due to the circumstances of their collection[1] and their exquisite crafts-manship, these Benin objects were highly prized as curios. Today they are dispersed throughout the world's museums and private collections.[2] The National Museum of African Art has twenty-two of these objects, upon which this study is based.

The impetus for this research was the observation of a direct correlation between the surface appearance of these twenty-two objects and their past collection history.[3] For example, objects previously in the private collection of the Pitt-Rivers family[4] have a dark, saturated surface that is different from that of other copper-alloy objects owned by the National Museum of African Art, such as the waxy, dark-green corrosion characterizing objects from the J. P. Howe collection. This research was initiated to learn more about the surface condition of the National Museum of African Art objects—including identification of coatings, corrosion, and "investment"—and the resulting interactions of these materials with the metal surface. This information will help facilitate conservation treatments and identification of past surface treatments.

ALLOY COMPOSITION

The Benin copper-alloy objects are predominantly brass, although a few bronze objects exist. Objects in the National Museum of African Art collection were examined by X-ray fluorescence spectroscopy and found to have compositions that range from 64 to 94% copper, 0 to 7% tin, 1 to 17% lead, and 0.6 to 26% zinc.[5] Small quantities of arsenic, silver, antimony, and nickel were also detected. Iron contents of 0.4–5% are probably due, at least in part, to surface dirt.

Objects are occasionally ornamented with copper sheet, iron and copper nails, and cast bronze. An example is the pendant hip mask (NMAFA 85-19-5) in the National Museum of African Art collection (Fig. 1). Although the surface is heavily obscured by treatments that occurred prior to entering the museum's collection, X-ray fluorescence reveals that the decorative strip down the nose is in excess of 98% copper. The pupils of the eyes were fashioned from iron, presumably iron nails. Finally, every other mudfish around the neck is cast in bronze (Table 1). Because each of these alloys would have a higher melting point than the brass base, which only contains 71% copper,[6] these adornments could be laid into the wax form and cast into place through the lost-wax casting process. This is clearly evident in close examination of the "rivets" that hold the bronze mudfish in place.

TABLE 1. *Elemental analysis of pendent hip mask (NMAFA-85-19-5).*

Item	%Cu	%Zn	%Pb	%Sn	%Fe	Other
Brass base	71	26	1	trace	1	—
Mudfish	93	1	2	2.5	1	trace As, Ag
Copper strip (nose)	98.5	0.4	0.6	trace	0.9	trace As, Ag
Eyes (pupils)	—	—	—	—	~100	trace Ca, As, Pb

SURFACE CONDITION BEFORE 1897

The variation in materials suggests that importance was placed on surface color and appearance in these objects prior to their entering Western collections. Throughout much of West Africa, the color red was highly prized and carried much significance. Today in Benin, copper's red color and shiny surface are seen as beautiful as well as frightening (Ben-Amos 1980:15). Throughout Benin history, the red stone and coral beads have been highly prized and an important part of the *oba's* regalia (Freyer 1987:57; Read and Dalton 1899:22). In 1862 Burton observed that the doors of the Ogboni secret society house were decorated in yellow, red, and black (Read and Dalton 1899:9). If completely cleaned, the pendant mask would have all three of these colors. The copper nose inlay and the bronze mudfish would appear red compared to the yellow brass, and the iron pupils would appear dark, almost black. It

seems reasonable to believe that these differences were an important part of the Benin aesthetic.

Very little has been written concerning the original appearance of these objects. The earliest mention of the plaques occurs in 1668 by Dapper, a Dutch author who compiled accounts by visitors to Benin City (Roth [1903] 1968:160). He writes that within the palace there were

> beautiful and long square galleries about as long as the Exchange at Amsterdam, but
> one larger than another resting on wooden pillars, from top to bottom covered with
> cast copper on which are engraved pictures of their war exploits and battles, and are
> kept very clean.

The phrase "kept very clean" conjures an image of a shiny, polished surface, without the red-clay "investment" material that is so strongly associated with Benin art. Later accounts merely confirm the continued presence of plaques hanging on pillars in the palace.[7]

Commemorative heads and other objects were placed on sheltered altars outdoors in the palace courtyard.[8] Some accounts report the application of blood from sacrifices to the altars, including the ivory tusks and the commemorative heads. While virtually all the accounts prior to the punitive expedition mention animal and/or human sacrifice, observations of blood on these objects seem to date from the period of the expedition.[9] It is possible that some exaggeration may have occurred to fuel the sensationalism surrounding the works of art and the punitive expedition.

Even if the objects were coated with sacrificial blood, according to Benin studies expert R. E. Bradbury, "Traditionally the cleaning and refurbishing of shrines was an institutionalized art of ritual performance" (Dark 1973:31). Also according to Bradbury, "Much of the loot removed from Benin in 1897 was in a good state of preservation, showing that care had been taken of it. In fact, there were people in the palace whose job it was to look after its treasures" (Dark 1973:29). Routine cleaning might be expected to remove not only blood but also dirt and any residual investment material.

Many of the Benin copper-alloy objects have a red-clay soil in the crevices, unless scrubbed completely clean. It is unclear whether this is an intentional addition by members of the Benin Kingdom to enhance the surface details, or material left over from the casting process, or merely accumulated dirt. This red clay serves to highlight the intricate details of the design and *could* represent a change in aesthetics from the time of Dapper's description of "very clean" surfaces.

The red soil-like appearance extends beyond the crevices of objects in some collections. H. O. Forbes, director of the Liverpool Museums, wrote in 1897 concerning two new acquisitions (1897:57):

> Both of the tusk holders [commemorative heads] like some of the other pieces
> in the collection, are of so rich a terra-cotta color, that, they might easily pass,
> on superficial inspection for clay. Whether this color results from a fine coat-

ing of laterite, from the clay molds in which they were cast—which would of course be removed from the chiseled portions—or is a patina artificially produced or naturally arising from long exposure to the air, is not yet determined. If these (and other) figures be of antiquity, which there is some evidence to show that they are, it appears rather surprising to find, after so long an exposure to the air and weather, any clay adhering to them; and practically no oxidation of the metal.

Surfaces that fit this description and on first glance appear almost paintlike may be found in museum collections such as those in Vienna's Museum für Volkerkunde.[10]

Other objects are heavily corroded. In 1897 Commander Bacon wrote: "The [King's] storehouses contained chiefly rubbish. . . . But buried in the dirt of ages, in one house, were several hundred unique bronze plaques, suggestive of almost Egyptian design, but really superb castings." The objects were probably not buried but had accumulated dirt while in the building. This may have been the house and burial chamber of an *oba,* and the objects closely associated with his reign (Read and Dalton 1899:9). This could account for the observation of heavily corroded surfaces on some objects, generally in large museum collections established immediately after the punitive expedition and thus less likely to have been heavily cleaned.[11]

It is likely that at least some of the objects had a cuprite layer on their outer surface at the time they were removed from Nigeria. Cuprite is the corrosion product that one would expect to form first on a copper surface. Ancient objects typically have a cuprite layer adjacent to the remaining core metal. Cuprite has been identified on a number of these objects. In addition, the objects that have copper fatty-acid salts on their surface (discussed later) contain flakes of cuprite within those extruding crystals. Small areas of other copper corrosion products, such as malachite and copper chlorides, have also been identified on a few of the objects from the National Museum of African Art collection.

Surface Modifications Since 1897

Dealers clearly believe the red material "belongs" in the crevices of these objects. For example, many areas on the pendant hip mask are obscured by a combination of cadmium sulfide, hematite, and calcium sulfate pigments.[12] Since cadmium pigments were not available until after the punitive expedition—they were first produced in Germany in 1925 (Wehle 1975:89)—this cannot be an indigenous addition. A textile impression on the pigments at the proper right edge of the right eye may have been intended to mimic the roughness of the clay material observed on other objects.

Many inappropriate surfaces, such as those found on the pendant mask, exist on the Benin objects. These often include the presence of modern pigments. For example, one of the plaques (NMAFA 85-19-19) in the collection has major portions of its surface obscured by the pigment Prussian blue.[13]

Other objects have chemically or electrochemically stripped surfaces, such as the collection's unique figure of a mudfish (NMAFA 85-19-8) (Fig. 2). Not only is the surface badly etched, but a flat-black waxy coating completely obscures the surface (Fig. 3). The surface details include inlaid sheet-copper decorations. An arsenic-rich green pigment, emerald green, has been applied to all of the crevices.[14] One has to wonder whose aesthetic this was designed to please.
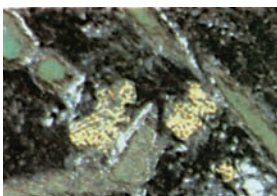
APPLICATION OF "PROTECTIVE" COATINGS

The above examples are deliberate post-punitive-expedition modifications of the appearance of the Benin objects. The application of oils to these objects may have been intended to enhance their appearance or may have been intended to protect their surfaces. In either case the application of oils to metal objects is consistent with European housekeeping practices in the earlier part of this century. Unfortunately, the application of oils has resulted in saturated, discolored, and corroded surfaces. In general, as these objects appear today they cannot represent the original West African aesthetic.

For example, reports indicate that the Benin objects in the private collection of the Pitt-Rivers family were coated with neat's-foot oil, an oil typically used on leather, possibly because of plans to exhibit these pieces outdoors (Fagg, pers. comm. 1989).While the examination of the composition of fatty acids in the coating is inconclusive at this time, the objects previously in the Pitt-Rivers collection have surfaces that are dark and saturated. The tarry black coating is frequently pooled in the crevices, and in some cases dark, disfiguring drips of the oily coating material can be seen (Fig. 4). A goal of this ongoing research is the identification of the oils used on the various collections of Benin objects based on the ratio of fatty acids present.

Despite the oily appearance, it is often presumed that these surfaces are stable. As a consequence, the choice may be made not to treat the object. Unfortunately, these coatings often mask the severe corrosion occurring underneath. It is disconcerting to realize, as in the example of the Pitt-Rivers objects, that the dark, tarry
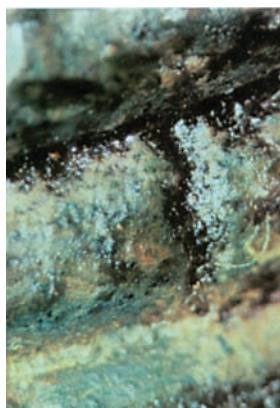
appearance is due to a coating that is now amber-colored over extensive turquoise corrosion. As discussed in the following section, this turquoise corrosion is a result of the breakdown of the oils and subsequent reaction with the metal surfaces.

These coatings contain part of the history of the object. But the presence of these coatings and other surface modifications influences one's perspective of the Benin aesthetic. These materials also may obscure inlays, details of surface finishing, and other features. The removal of coatings without recording what is present may result in the loss of important information necessary to the understanding of that object, its appearance, and possibly its authentication. The choice of whether to remove a coating will also affect the long-term stability of the object.
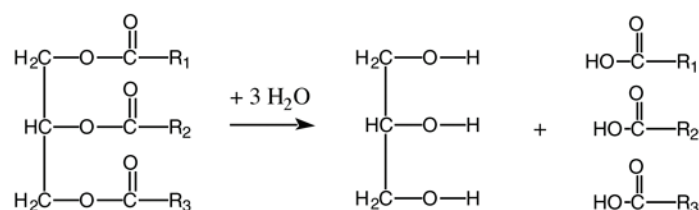
Fatty-acid Metallic Salts

The most widespread problem identified on the Benin objects in the National Museum of African Art is the presence of the fatty-acid salts of copper and, occasionally, zinc and lead. These salts have been found on at least thirteen of the twenty-two objects, representing a minimum of four different European collections. This corrosion originates with the breakdown of the oils, followed by attack of the metal surface, as illustrated in Table 2. All oils and fats have three ester linkages, which may be hydrolyzed (addition of water across the bond) to give free fatty acids (Reaction 1). This process occurs slowly but may be either acid or base catalyzed. The result is a free fatty-acid molecule available to attack the metal surface. If the metal is oxidized, then fatty-acid salt will be formed (Reaction 2). The reaction of free fatty acids with copper is an extremely efficient process.[15] This efficiency strongly suggests that the slow step is hydrolysis of ester linkages in the oil to produce the free fatty acids.

On undisturbed surfaces, this corrosion may extrude from the metal surface as if forced through a press (Fig. 5), or it may be a fuzzy blue-gray material, almost

FIGURE 4. *Detail from the neck rings on a plaque of men with leopard-skin bags, showing the extremely saturated surface with thick accumulation of aged oil in the crevices. In the lower crevice where the pooled oil was removed, there is waxy turquoise corrosion. Edo Peoples, Benin Kingdom, Nigeria, mid-sixteenth to seventeenth century, cast-copper alloy. H:47 cm. NMAFA 85-19-13.*

TABLE 2. *Analysis of the corrosion of Benin objects, caused by the hydrolysis of fats and oils (Reaction 1) which leads to fatty-acid attack on copper (Reaction 2).*

Reaction 1: The hydrolysis of fats and oils

$$H_2C-O-\overset{\overset{\displaystyle O}{\|}}{C}-R_1$$
$$HC-O-\overset{\overset{\displaystyle O}{\|}}{C}-R_2 \quad +\ 3\ H_2O \longrightarrow$$
$$H_2C-O-\overset{\overset{\displaystyle O}{\|}}{C}-R_3$$

$$H_2C-O-H$$
$$HC-O-H \quad + \quad$$
$$H_2C-O-H$$

$$HO-\overset{\overset{\displaystyle O}{\|}}{C}-R_1$$
$$HO-\overset{\overset{\displaystyle O}{\|}}{C}-R_2$$
$$HO-\overset{\overset{\displaystyle O}{\|}}{C}-R_3$$

R_1, R_2, R_3 are long hydrocarbon chains, typically containing 12, 14, 16, 18, or 20 carbons

Reaction 2: Fatty-acid attack on copper

$$Cu\ +\ 2\ HO-\overset{\overset{\displaystyle O}{\|}}{C}-R \xrightarrow{O_2,\ H_2O} Cu\left(O-\overset{\overset{\displaystyle O}{\|}}{C}-R\right)_2$$
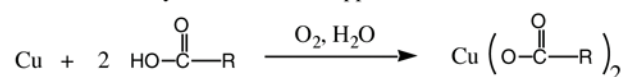
FIGURE 5. *Detail, near right, from Benin relief sculpture, area between the tassels over the central figure's wrapper, showing the extruding turquoise crystals. Edo Peoples, Benin Kingdom, Nigeria, probably seventeenth century, cast-copper alloy. H:46 cm. NMAFA 82-5-3.*
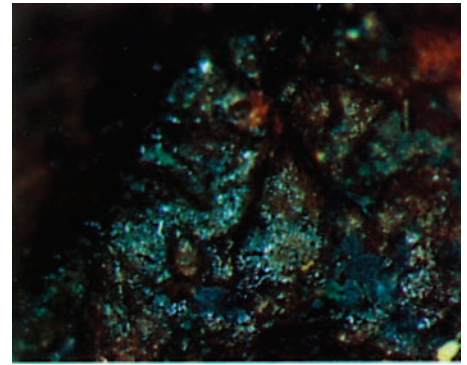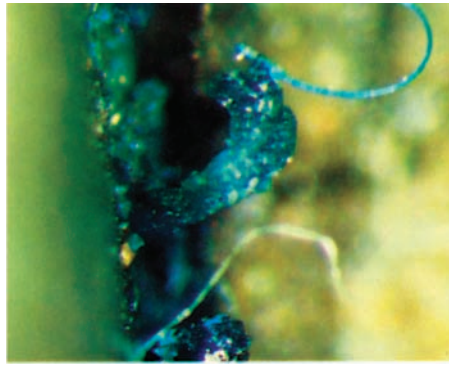
FIGURE 6. *Detail, far right above, from Edo musketeer figure, area between the figure's legs, showing the "fuzzy" blue-gray corrosion. Edo Peoples, Benin Kingdom, Nigeria, nineteenth century, cast-copper alloy, iron rods. H:51.4 cm. NMAFA 85-19-15.*
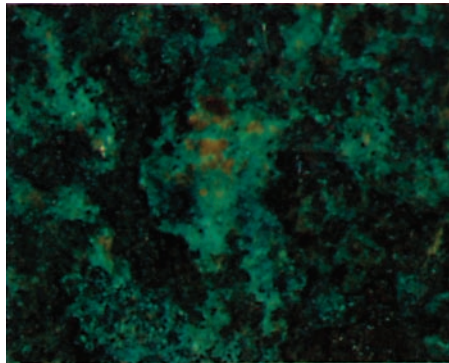
FIGURE 7. *Detail, above right, from the reverse of plaque of multiple figures, showing waxy blue-green corrosion. Edo Peoples, Benin Kingdom, Nigeria, mid-sixteenth to seventeenth century, cast-copper alloy. H:48.9 cm. NMAFA 85-19-18.*

FIGURE 8. *Scanning electron micrograph of a corrosion sample of a figure of an* oba, *taken from under the figure's proper left arm, showing a combination of the waxy and fuzzy forms of the fatty-acid metallic salts. Edo Peoples, Benin Kingdom, Nigeria, nineteenth century, cast-copper alloy. H:41 cm. NMAFA 85-19-12.*
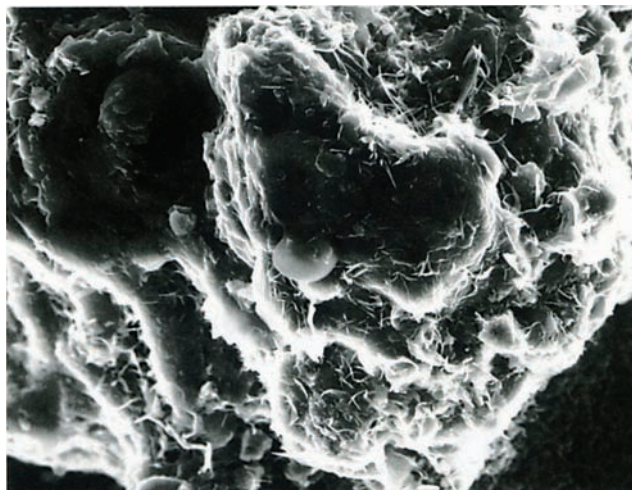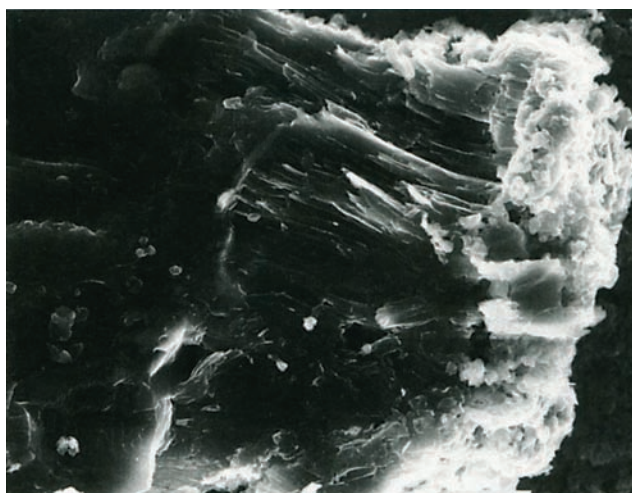
moldlike in appearance (Fig. 6). When disturbed or on other surfaces it appears to be very soft and waxy (Fig. 7). Scanning electron micrographs illustrating these morphologies have been previously published (Schrenk 1991:807–8).

Scanning electron micrographs illustrate combinations of these morphologies. Figure 8 shows the smooth, waxy form in combination with the almost hairlike surface of the fuzzy blue-gray. Figure 9 illustrates the extrusion of a turquoise crystal out of a more waxy base. Dirt particles, at the right-hand edge of the photograph, have been pushed away from the metal surface. What is controlling the morphology is unclear, though it may be the particular combinations of fatty acids or metal ions present.

A combination of analytical techniques has been used in the identification of the fatty-acid salts of copper and other metals. These include Fourier transform infrared

(FTIR) spectroscopy, X-ray diffraction (XRD), gas-liquid chromatography (GLC), and scanning electron microscopy with energy-dispersive analysis (SEM-EDS). Details and representative spectra have been published previously (Schrenk 1991).

FTIR spectroscopy is a good diagnostic tool because of the carbonyl stretching band that occurs in the region between 1500 and 1800 cm^{-1}. In a fat, oil, or wax this band occurs around 1730–1740 cm^{-1}. The free fatty acids may be found at about 1700 cm^{-1}. In sharp contrast, the band for the copper fatty acid salt is shifted to 1588 cm^{-1}, while in the zinc salt it appears at 1538 cm^{-1}, and in the lead salt at 1514 cm^{-1}.[16]

The beautiful morphologies probably occur due to the long periods of time in which the crystals have formed. In contrast, samples obtained from a chemical supply house are very waxy and produce much poorer XRD patterns. The typical XRD pattern for these corrosion products consists of one or more d spacings between 10 and 15 Å. A quick scan of the powder diffraction files shows relatively few copper complexes with such large d spacings.

Confirmation of the metals present was obtained by SEM-EDS. Typical spectra for the copper fatty-acid salts have two characteristic features: (1) sharp peaks for copper (and any other metals present), and (2) a large, broad band at lower energies indicative of organic scattering. In some cases aluminum and silicon appear due to the presence of clay materials on the object's surface.

GLC confirms the presence of fatty acids in both the coatings and the corrosion products. Typically the most prominent peaks correspond to palmitic, oleic, and stearic fatty acids. It is hoped that continued research in this area will lead to identification of the particular oils and waxes used on the objects.

Conclusion

The twenty-two objects in the National Museum of African Art show a wide variety of surface conditions predominantly due to their past collection history. Many of these surfaces clearly misrepresent the West African aesthetic, especially those containing modern pigments and oils and those that have been electrochemically or chemically stripped. Perhaps most alarming is the identification of metallic fatty-acid

Schrenk

salts on at least half of the collection. The identification of cuprite on several objects, as well as in the extruding turquoise corrosion of some metallic fatty-acid salts, suggests that at least some of the objects had cuprite on their surface when they left Nigeria. Understanding the appearance of the objects prior to the punitive expedition of 1897 is critical to the proper understanding and interpretation of the Benin aesthetic.

Ongoing work will continue to address the issues related to the surface appearance and condition of the royal art of Benin Kingdom, both past and present. Particular issues being addressed are the identity of the coating materials, examination of the metallic fatty-acid corrosion products, the origin of the red-clay material characteristic of these objects, and historical documents that provide clues to the appearance of the objects prior to leaving Africa.

Acknowledgments

Notes

1. The London newspapers sensationalized the events leading up to and including the punitive expedition which resulted from the British government's desire to end the practice of human sacrifice. Few could believe "savage" people could produce such beautifully crafted works of art.

2. An attempt to catalogue these objects and their location is available (Dark 1982).

3. This observation was first made by Bryna Freyer, curator, and Stephen Mellor, chief conservator, at the National Museum of African Art.

4. The private collection of General Pitt-Rivers should not be confused with the collection of the Pitt-Rivers Museum in Oxford, England, which he established prior to collecting Benin art.

5. Unpublished data obtained by X-ray fluorescence examination of 20–40 areas (approximately one-quarter inch in diameter) over the surface of the object. Quantification was completed using software developed by W. Thomas Chase and the Freer and Sackler museums.

6. The melting points of pure copper and pure iron are 1035 °C and 1538 °C, respectively. Based on binary-phase diagrams, a copper-tin alloy (bronze) containing 93% copper would have a melting point of about 1050 °C, while a copper-zinc alloy (brass) containing 71% copper would have a melting point of about 950 °C. While the alloys are more complex than this indicates, it is reasonable to expect a lower melting point for the brass (Askelund 1985:250, 552).

7. For example, based on the 1630 accounts of Peter de Marcez, Ogilby writes: "But all [s]upported on Pillars of Wood, cover'd from the top to the bottom with melted Copper, whereon are Ingraven their Warlike Deeds and Battels, and are kept with exceeding Curi[os]ity" (Ogilby 1670:470). In 1820 Lt. King "noticed that the flat ceilings were traversed by beams covered with metal and ornamented with various figures" (Read and Dalton 1899:8).

8. For example, an 1891 photograph of a palace altar is published in Roth ([1903]1968:79). A 1970 photograph by Eliot Elisofon of a palace altar is published in Freyer (1987:19).

9. According to Roth, "Neither Dapper nor the officials say that the blood of the human victims was sprinkled on the ivories and metal work on the altars, but Landolphe noticed it, and Dr. Allman, who was on the punitive expedition, informs me he found blood and human entrails on the altars, and my brother likewise medical officer to the expedition, tells me the same. The native officials, no doubt, have some diffidence in giving the whole truth on this matter" (Roth [1903]1968:72). According to Sir R. Moor, a punitive expedition participant, "Their blood was smeared over the altar and allowed to run down the steps in front . . . brass and ivory [figures] were not painted, but covered with blood, human or otherwise" (Forbes 1897:56).

10. Excellent color photographs of objects in Vienna's Museum für Volkerkunde have been published (Duchateau 1990).

11. The author has observed such surfaces on objects at the Museum of Mankind (British Museum) in London and the Field Museum in Chicago.

12. Identification of cadmium and relatively large quantities of iron by X-ray fluorescence, along with a list of red pigments (Wehle 1975), facilitated the interpretation of the XRD pattern of the mixture of pigments.

13. Prussian blue was identified based on FTIR spectroscopy, in particular the distinctive $C\equiv N$ stretching frequency at about 2090 cm^{-1}. This was confirmed by XRD and SEM-EDS.

14. X-ray fluorescence revealed the presence of arsenic, and a list of green pigments (Wehle 1975) facilitated the interpretation of the XRD pattern.

15. This efficiency was demonstrated by the application of a mixture of stearic, palmitic, and oleic acids on a sheet of polished copper. The reaction was followed by FTIR. Within four days there was a 50% conversion of the free fatty acids to the copper fatty-acid salts (Schrenk 1991:811).

16. Values are based on commercial samples of stearic acid, copper stearate, zinc stearate, and lead stearate.

References

ASKELUND, D. R.
1985   *The Science and Engineering of Materials*, alternate ed. Boston: PWS Engineering.

BACON, R. HUGH
1897   *Benin: The City of Blood*. London: Edward Arnold.

BEN-AMOS, P.
1980   *The Art of Benin*. New York: Thames and Hudson.

DARK, P. J. C.

1973   *An Introduction to Benin Art and Technology*. Oxford: Clarendon Press.

1982   *An Illustrated Catalogue of Benin Art*. Boston: G. K. Hall.

DUCHATEAU, A.

1990   *Benin Tresor Royal, Collection du Museum für Volkerkunde, Vienna.* Paris: Editions Dapper.

FORBES, H. O.

1897   On a collection of cast-metal work, of high artistic value, from Benin, lately acquired by the Mayer Museum. *Bulletin of the Liverpool Museums* 1:49–70.

FREYER, B.

1987   *Royal Benin Art in the Collection of the National Museum of African Art*. Washington, D.C.: Smithsonian Institution Press.

OGILBY, J.

1670   *Collection of African Travels*. Based on accounts written about 1630 by Peter de Marcez. London.

READ, C. H., AND O. M. DALTON

1899   *Antiquities from the City of Benin and Other Parts of West Africa in the British Museum*. London: British Museum.

ROTH, H. L.

[1903] 1968   *Great Benin: Its Customs, Art and Horrors.* Reprint. New York: Barnes and Noble.

SCHRENK, J. L.

1991   Corrosion and past "protective" treatments of the Benin "bronzes" in the National Museum of African Art. In *Material Issues in Art and Archaeology II; Materials Research Society Symposium Proceedings,* vol. 185:805–12. P. Vandiver, J. Druzik, and G. Wheeler, eds. Pittsburgh: Materials Research Society.

WEHLE, K.

1975   *The Materials and Techniques of Painting*. New York: Van Nostrand.

B I O G R A P H Y

Janet L. Schrenk received her doctorate in inorganic chemistry from the University of Minnesota. In 1985 she joined the faculty of the University of Delaware/Winterthur Museum Art Conservation Program. In 1988 she joined the Research and Testing Laboratory of the National Archives and Records Administration. The following year she received the Smithsonian Institution's Conservation Analytical Laboratory Post-doctoral Research Fellowship in Conservation Science to pursue research on the Benin collection of the National Museum of African Art. Since 1990 she has served on the faculty of The University of the South in Sewanee, Tennessee.

Considerations in the Cleaning of Ancient Chinese Bronze Vessels

JANE BASSETT AND W. T. CHASE

Cast as symbols of power and wealth, Chinese bronze vessels in antiquity were collected, given in tribute, used in ceremony, and buried—both in sacrifice and with the dead. Few, if any, of the vessels known today survived the ensuing centuries without being buried. Within the last thousand years, vessels unearthed throughout China have been collected and distributed and are greatly prized and valued. Throughout these centuries of use, burial, rediscovery, restoration, and redistribution, great changes have occurred in their bronze surfaces.

The cleaning of any archaeological bronze surface is an irreversible process, demanding careful consideration before treatment is undertaken. In the case of Chinese bronze vessels, this decision is complicated by the potential wealth of information provided by an artifact's surface. The aesthetic and ethical implications of the cleaning of ancient Chinese bronze vessels should, therefore, be considered in light of the complexity of the surfaces which are presented.

As with the cleaning of all bronzes—especially when the surface no longer exists in its original form—the point at which cleaning begins and ends is arbitrary and is often left to the discretion of the individual conservator. Although some conservators may intuitively sense many implications of the cleaning of ancient Chinese vessels, the factors that should guide their judgment are not clearly articulated in the literature and are often conflicting.

EVALUATING STABILITY

The primary objective in any cleaning treatment should be long-term stabilization. The first step must be to determine through examination whether or not the bronze is strong enough to allow cleaning, as highly mineralized bronzes may not be able to withstand even the gentlest of cleaning actions. Careful visual examination, including X-radiography and ultraviolet-light examination, will indicate cracks, repairs,

and degree of mineralization, which will help in making this decision. A miniaturized metal detector, made by attaching a small (2–3 mm diameter) coil to an inexpensive metal detector can enable the conservator to detect totally mineralized bronzes.

A variety of safe cleaning methods is available today. All rely on careful removal, under low magnification, of soils and corrosion products using mechanical rather than chemical means. Due to the porosity of the corrosion products as well as that of the corroded bronze itself, absorption of cleaning agents such as dilute acids and complexing agents cannot be controlled. Therefore, only the gentlest of mechanical methods should be considered appropriate for the cleaning of bronze surfaces.

Numerous examples exist of Chinese bronze vessels damaged in the past due to acid cleaning. Perhaps the most extreme damage was caused by stripping procedures carried out to remove chlorides. In the 1940s, the Shang Dynasty *ding* (Fig. 1) was electrolytically cleaned in order to remove chloride salts. With the exception of a few small patches of cuprite, all surface accretions and corrosion products were removed from the exposed bronze surface, leaving a deeply fissured and pitted vessel that is a dull mustard-yellow color. Today such stripping methods are considered inappropriate, yet pieces such as this *ding* remain as examples of the importance of balancing

FIGURE 1. *Shang Dynasty* ding, *bronze, shown after electrolytic stripping. H:18.6 cm, D:17.9 cm. Honolulu Academy of the Arts, Honolulu; gift of Mrs. T. A. Cooke, 1939; no. 4776.*

scientific advances with other considerations. If we look at metallographic sections such as those of the Michigan mirror (see Chase herein) or those of the Kelley bronze (Gettens 1969:128–29), it becomes clear that electrolytic cleaning down to sound metal will, in the case of a heavily corroded bronze, leave a very rough and fissured appearance. Any evidence of the original surface (such as a cuprite marker layer) will be removed. Deep penetration of corrosion, as at pits or fissures, will also be removed, leaving these features clearly visible. A more careful consideration of the actual condition of this deeply corroded vessel might have prevented this damage.

Numerous examples of more subtle damage due to chemical cleaning may be found. The original surface on Chinese bronzes is often replaced by a smooth and even tin oxide corrosion layer. Acid cleaning agents can attack the corrosion below the tin oxide, causing pitting and damage to the tin oxide layer. Patchy, broken tin oxide layers may be seen on a *ding* in the Arthur M. Sackler Gallery (S1987.50), especially on the bottom of the body where acid has etched below the surface (Delbanco 1983:73; Bagley 1987). A well-known set of four *fang-ding* vessels also shows the same appearance. Etching is most notable on one leg of the *fang-ding* (FGA50.7) that belongs to the Freer Gallery of Art (Pope et al. 1965:191). One of the counterpart vessels from the same set in the National Palace Museum, Taiwan, has been treated more vigorously and shows patches of redeposited copper in many places.

Even cleaning treatments that are more conservative may effect the stability of bronze surfaces. The mechanical removal of slowly formed, compact corrosion layers, for example, may allow active corrosion to occur in areas that previously had achieved some degree of stability. Although this phenomenon may be a lesser problem with Chinese bronzes than with those from Southeast Asia and other areas, the problem should not be overlooked. One advantage of removing soil from an archaeological bronze is that a potential source of moisture and salts is eliminated.

Determining Objectives

After considering the possible effects of cleaning on the stability of the bronze surface, the next step is to determine what information can be gained by removing obscuring soils and corrosion products. One of the primary advantages of cleaning is that it may allow access to surface details, enabling the study of the vessel as a technological record. A growing interest is developing among art historians and collectors in the production processes of Chinese bronze vessels. The numbers of vessels being excavated in China at present underline the importance of bronze production in Shang and Zhou societies. Communication, trade, and labor systems can be better understood through research into the processes of mining and smelting ores and the casting of bronze vessels. The Chinese system of casting using clay molds is extremely complex and has many variables. Although radiography will reveal many of the casting details hidden by surface accretions, cleaning may allow an even more detailed study of a piece. Casting flaws, ancient repairs, inlay, decorations, finishing marks, and inscriptions all bear subtle differences and clues to help conservators understand the individual piece and therefore the technology as a whole.

Yet the conservator must be aware that indiscriminate cleaning may obliterate the remnants of surface technologies. Traces of original, intentional surface patinas may remain only in the corrosion layers, and their removal may eliminate the only chance for analysis. Other surface-coloration techniques must be anticipated and preserved, including black-silica and carbon inlays, which are found most often on Shang Dynasty and early Western Zhou vessels, as illustrated in Figures 2 and 3 (Gettens 1969:197–204). The same precautions apply to more unusual surface-coloration techniques such as the painted decoration found on Han period burial vessels (Nelson 1980:127–54). Other surface-patination techniques will undoubtedly come to light in time, such as the unidentified red coloration on the Eastern Zhou silver-inlaid animal figure exhibited in the United States in 1988–89 in conjunction with the Son of Heaven exhibition (Thorp 1988:134).

Another important concern must be the potential loss of archaeological evidence through cleaning. The majority of bronzes in Western collections were unearthed without the benefit of scientific excavation. Any information that can be retrieved may help to determine an object's original burial location or circumstances and its ceremonial uses. Soils and corrosion products can provide information about burial location (Holmes and Harbottle 1991:165–84; Smith 1978:123–33) and environment. Surface accretions, such as carbonaceous material on the bottom of cooking vessels, may reveal information about usage, as illustrated on the *xian* steamer vessel illustrated in Figure 4. These accretions may also contain remnants of materials placed adjacent to the vessel in burial, such as wood (Keepax 1989:15–20), textiles (Jakes and Sibley 1984:402–22), and cinnabar, which was sometimes scattered in Shang Dynasty tombs (Thorp 1980:51–64). Accretions on the interior of ceremonial cooking vessels may also contain remnants of offerings such as food and wine.

FIGURE 2. *Shang Dynasty* ding, *bronze, middle Anyang period. H:18.4 cm, D:16.5 cm. Honolulu Academy of the Arts, Honolulu; acquired by exchange, 1973; no. 4150.1.*

FIGURE 3. *Detail, Shang Dynasty* ding *(Fig. 2). Note black inlay.*

FIGURE 4. *Shang Dynasty* xian *steamer vessel, bronze. Note black soot on bottom. Honolulu Academy of the Arts, Honolulu, purchase no. 5850.1.*

Since materials removed can never be put back, present and future analytical capabilities need to be anticipated before cleaning is carried out. Colors of corrosion products should be recorded both photographically and with color analysis such as Munsell scales. Photomacrographs can be used to record corrosion patterns. Written descriptions of the texture and hardness of the corrosion products should also be recorded. In addition to photographic and written documentation, samples removed during cleaning should be saved and carefully labeled, with location references noted on corresponding photographs. Samples should include soils and corrosion products removed from the interior as well as the exterior of the vessel. Whenever possible, a section should be left uncleaned in an inconspicuous area (Jedrzejewska 1976:101–14). Although mineralized remains of organic materials on the surface can be photographed, and impressions can be made and samples saved, the limits that their removal will place on future research must be considered.

The conservator must also weigh the effects of treatment on the vessel as a cultural artifact. The vessel was made to reflect the power and wealth of the owner and the owner's ancestors, and the presence of soils and corrosion products may be

considered to increase the strength and value of the artifact, as these attributes attest to the object's great age. From this viewpoint, the surface of the excavated bronze should not be violated, as the removal of corrosion products would deny the sanctity of its antiquity.

AESTHETIC CONSIDERATIONS

The effect of cleaning on the aesthetics of the vessel as a work of art is of considerable importance in designing treatment. However, aesthetic expectations for treatment may be based more on an interest in certain anticipated appearances than on a desire for increased technological or archaeological understanding of the piece. In considering the aesthetic repercussions of treatment, two factors should be recognized: (1) The majority of vessels now in Western collections have been treated previously, usually involving some degree of cleaning, which may limit current treatment options, and (2) aesthetic standards of appearance are subjective by their very nature and will change with time; therefore, one must be conservative in the application of these standards in treatment. The demands of making vessels aesthetically pleasing to the viewer must be tempered by the conservation principles of reversibility and minimum intervention.

The following examples demonstrate how varying aesthetic expectations may influence treatment. An example of the cleaning of bronzes adopted on a large scale can be found in the Chinese Imperial Palace collections. Imperial Palace bronzes, such as the Western Zhou *ding* illustrated in Figure 5, were treated by removing soil, polishing down corrosion products, and applying a shiny wax or varnish to the

FIGURE 5. *Western Zhou Fugeng Li* ding, *bronze. 1100–1000 B.C.E. H:21.2 cm, D:16.9 cm. Arthur M. Sackler Gallery, Washington, D.C., no. S1987.303.*

surface, probably for stabilization purposes (Lawton 1987–88:51–79). It may be assumed that this treatment, particularly in environments of extreme and uncontrolled humidity, did provide a degree of protection for the bronze surfaces. Whatever the initial purpose for the treatment, the sheer number of similarly treated objects in the imperial collections indicates that an aesthetic of darkened, polished, and shiny surfaces ensued, setting an aesthetic standard for a huge number of bronze vessels. These vessels can presently be found in large numbers in the National Palace Museum in Taiwan and in smaller numbers in museums in Beijing and throughout North America and Europe. This heavily cleaned, coated, and polished appearance became so accepted, in fact, that later archaistic reproductions were sought to duplicate this aesthetic.[1]

In Western collections today, viewers are more accustomed to the uneven, matte, and colorful appearance of natural burial accretions. A well-known example of this contrast in aesthetics can be illustrated with an early Zhou *hu* now in the collections of the Freer Gallery of Art (Gettens 1969:227). The black-and-white photograph of the *hu* (Fig. 6) was taken before the object entered the Freer collections. The photo shows a glossy, even-valued surface. In contrast, the present surface as illustrated in Figure 7 is a matte light-green color with areas of dark, highly contrasting corrosion products where the lid joins the vessel. It is thought that when the *hu* entered this country the vessel retained a shiny, dark patina indicative of Imperial Palace bronzes. In a New York dealer's workshop, this dark patina was altered to give an appearance more similar to the colorful corroded surfaces to which Western collectors had become accustomed. In keeping with the client's expectations, the dealer was able to create the anticipated surface appearance through chemical treatment.

FIGURE 6. *Early Western Zhou Dynasty* hu, *bronze, near right, eleventh to early tenth century* B.C.E. *Photographed before acquisition by the Freer Gallery of Art (Gettens 1969:226). H (with lid):24.5 cm, W:15.5 cm. Freer Gallery of Art, Washington, D.C., no. 59.14.*

FIGURE 7. *Same Western Zhou Dynasty* hu *as in Figure 6, photographed after acquisition by the Freer Gallery of Art. Note darker area of corrosion products where lid joins vessel.*

BASSETT AND CHASE

A less drastic approach to achieving an acceptable aesthetic appearance can be seen with the Zhou Dynasty *gui* (Fig. 8). When this vessel entered the collection of the Freer Gallery of Art, it retained its shiny, dark surface which can be seen on the left in this photograph of the vessel taken during treatment. The right side of the vessel illustrates the results of swab-cleaning with organic solvents. When completed, the treatment revealed the state of the original materials unobscured by the darkened, glossy coating. Although any potential for analysis of archaeological remains was removed when the surface was polished, samples of the removed waxlike coating were saved for later analysis. One day, evidence hidden in such surface coatings may enable conservators to trace vessels to certain collectors or locations.

Present aesthetic standards can be illustrated with Eastern Zhou inlaid pieces. Gold, silver, copper, and gemstones such as malachite and turquoise were incorporated into bronze surfaces beginning in the sixth century B.C.E. In Western collections today, these stone surfaces are often meticulously cleaned to reveal the full contour of the inlay. Similarly, gold and silver inlay are brought to a high luster by the removal of surface accretions and tarnish. Although cleaning silver inlay permits an appreciation of the intricacy of its patterns, an arbitrary value relationship is established which may have little to do with the artifact's original appearance. Although one may rightfully assume that the silver was polished to a high luster when the object was first made, the original coloration of the surrounding bronze cannot be known for certain. In the case of these pieces, intentional cleaning of one metal surface to a higher degree than the other was possible simply because of differences in the corrosion processes.

FIGURE 8. *Zhou Dynasty* gui, *bronze, shown during treatment with cleaned section on the right. Freer Gallery of Art, Washington, D.C., no. 68.29.*

In contrast to gold and silver inlay, copper is generally not taken to a high polish. For example, early cleaning tests on the copper inlay in the lid of an Eastern Zhou *fang-hu* at the Freer Gallery (FGA61.32) were considered unsuccessful; the polished copper was thought too bright in color and therefore inappropriate. Two points are of interest here: First, the public has come to accept polished silver surfaces on ancient pieces in Western museums, yet a polished copper inlay was, in this instance, unacceptable; one day a highly polished archaeological silver surface may be considered extreme. Second, in light of recent work on the patination of such inlaid pieces, it is fortunate that cleaning of the copper was not undertaken (see Chase herein).

In determining the appropriateness of cleaning, the final consideration must be whether an aesthetically acceptable cleaning is possible. In reaching this decision the conservator must work in close cooperation with the curator, as the definition of an acceptable aesthetic standard may vary considerably. The conservator must be able to evaluate each surface before cleaning is undertaken and be able to communicate what that surface will look like after treatment. Experience with similar surfaces will be a considerable advantage.

Certain corrosion products may be indicative of a well-preserved surface. The cuprite marker layer may retain original surface detail. Additionally, corrosion layers such as botryoidal malachite may indicate the presence of a well-preserved surface below. Less desirable aesthetic effects of cleaning may include surface blotchiness where different corrosion layers have been cut through, or the complete loss of relief details due to extensive, blistering corrosion. These conditions should be diagnosed accurately before cleaning is attempted; in some cases it is simply better to leave the bronze alone. During the process of mechanical cleaning, the initial area may clean very nicely, but then deep pitting of an area that does not clean well mechanically may be encountered. In this case, the surface will probably look better with the original patina left in place; aesthetic sensitivity is expected of the conservator who is wielding the chisel.

Contextual Issues

Once the pros and cons of cleaning are understood in general terms, each artifact must be examined to determine the appropriate course of treatment. To do this, the function of the individual artifact in today's surroundings needs to be defined. Although research may help clarify the ancient function and meaning of Chinese bronze vessels, these objects are now unearthed, out of context, removed in most instances from their place of origin. The continuum of their ceremonial use has been broken by generations of change within China. Whether in private collections, anthropology museums, or art galleries, conservators and curators must decide what role each individual piece fulfills in present-day context, asking such questions as, How does this vessel work within the goals of the collection in which it is housed? and How can it add to our knowledge of Chinese bronze vessels in general? Each vessel may be seen as an archaeological or technological record; it may

be viewed as a cultural artifact, valued for the build-up of wear and accretions of age, or simply appreciated as a unique work of art.

The process of determining an artifact's function should involve input from as many experts as possible, with the goal of increased knowledge for all. During such discussions the conservator's responsibility is to explain the various possible degrees of cleaning, the appearances that might result from each degree of cleaning, and the risks involved. The art historian or archaeologist has a similar responsibility to educate the conservator, sharing such knowledge as the rarity of the vessel type or decoration and its possible ceremonial or burial circumstances.

Conclusions

The keys to responsible treatment of ancient bronzes are as follows:

1. Communication with other specialists
2. Thorough documentation
3. Thorough examination to determine the extent of corrosion and previous treatments the piece may have undergone
4. Evaluation of the function of the vessel in today's context, including an understanding of the archaeological and technological information that may be lost in cleaning, as well as an appreciation of the aesthetic repercussions of treatment
5. Respect for the vessel and the people who made it

With these essential points in mind, the conservator can proceed with enlightened, successful, and conservative cleaning of ancient vessels.

Acknowledgments

Note

1. Examples include a *hu* (FGA09.254) and a *yu* (FGA09.260) in the Freer Gallery of Art study collections. For a survey of historic references to the forgery of Chinese bronze vessels, see Barnard 1968.

References

BAGLEY, R. W.
1987   Shang Ritual Bronzes in the Arthur M. Sackler Collections. *Ancient Chinese Bronzes in the Arthur M. Sackler Collections,* vol. 1. Washington, D.C. and Cambridge: Harvard University Press.

BARNARD, N.

1968   The incidence of forgery amongst archaic Chinese bronzes: Some preliminary notes. In *Monumenta Serica*, 91–168. H. Busch, ed. Los Angeles: Monumenta Serica Institute, University of California.

DELBANCO, D. H.

1983   *Art from Ritual: Ancient Chinese Bronzes from the Arthur M. Sackler Collections*, catalogue no. 24. Cambridge: Arthur M. Sackler Museum, Harvard University.

GETTENS, R. J.

1969   *The Freer Chinese Bronzes, Volume II: Technical Studies*. Oriental Studies, no. 7, Smithsonian Publication 4706. Washington, D.C.: Smithsonian Institution, Freer Gallery of Art.

HOLMES, L. L., AND G. HARBOTTLE

1991   Provenance study of cores from Chinese bronze vessels. *Archeomaterials* 5:165–84.

JAKES, K. A., AND L. R. SIBLEY

1984   Examination of the phenomenon of textile fabric pseudomorphism. In *Archaeological Chemistry*, J. B. Lambert ed., *Advances in Chemistry* 205:402–22. Washington, D.C.: American Chemical Society.

JEDRZEJEWSKA, H.

1976   A corroded Egyptian bronze: Cleaning and discoveries. *Studies in Conservation* 21:101–14.

KEEPAX, C. A.

1989   Corrosion "preserved wood": Advances since 1975. In *Evidence Preserved in Corrosion Products: New Fields in Artifact Studies*, 15–20. R. Janaway and B. Scott, comps. Leeds: The United Kingdom Institute for Conservation.

LAWTON, T.

1987–88   The Imperial legacy revisited: Bronze vessels from the Qing Palace collection. *Asian Art* 1:51–79.

NELSON, D. M.

1980   Bronze *Ming-Ch'i* vessels with painted decoration: A regional study in Han pictorialism. *Artibus Asiae,* 127–54.

POPE, J. A., R. J. GETTENS, J. CAHILL, AND N. BARNARD

1965   *The Freer Chinese Bronzes, Volume I: Catalogue*. Oriental Studies, no. 7, Smithsonian Publication 4706. Washington, D.C.: Smithsonian Institution, Freer Gallery of Art.

SMITH, A. W.

1978   Stable carbon and oxygen isotope ratios of malachite from the patinas of ancient bronze objects. *Archaeometry* 20:123–33.

THORP, R. L.

1980   Burial practices of Bronze Age China. In *The Great Bronze Age of China: An exhibition from the People's Republic of China*, comp. Wen Fong, 51–64. New York: The Metropolitan Museum of Art and Alfred A. Knopf.

1988   *Son of Heaven: Imperial Arts of China.* Seattle: Son of Heaven Press.

Biographies

Jane Bassett, associate conservator of sculpture and decorative arts at the J. Paul Getty Museum, received her bachelor of arts degree in art history from Stanford University and her master's degree in conservation from the Cooperstown Graduate Program in New York. From 1986 to 1991 she was objects conservator at the Pacific Regional Conservation Center at the Bishop Museum in Honolulu, Hawaii.

W. T. Chase is head conservator of the Department of Conservation and Scientific Research of the Arthur M. Sackler Gallery and the Freer Gallery of Art, Smithsonian Institution. He majored in conservation of art at Oberlin College and later studied at the Conservation Center of the Institute of Fine Arts at New York University. During his graduate studies, he took his student internship at the Freer Technical Laboratory under Rutherford J. Gettens. After completing his degree in 1966, he returned to the Freer, where he became head conservator in 1968. His primary research interest is technical study of ancient Chinese bronzes.

Tomography of Ancient Bronzes

STEPHEN D. BONADIES

The Cincinnati Art Museum has been fortunate to have had the technological resources of General Electric Aircraft Engines in Evendale, Ohio, close at hand. With General Electric's generous support and cooperation, the museum has been able to study a number of objects from its collection using industrial computed tomography (CT) to gain a better understanding of ancient methods of manufacture as well as the condition of these objects. Industrial CT is one tool in the repertoire of nondestructive evaluation techniques that is uniquely suited to the visual examination of the inner structures of an object. The images that result from an industrial CT examination are aesthetically appealing as well as intellectually tantalizing.

INDUSTRIAL COMPUTED TOMOGRAPHY

Industrial CT is an adaptation of computerized axial tomography (medical CAT-scanning) developed in the late 1960s and early 1970s (Dennis 1989). Since the 1970s, efforts have been directed toward the application of computed tomography in industry and research. The technique was first applied to the study of museum objects in the 1980s. Although medical scanners can provide high-quality images of ceramics, plastics, and aluminum as well as those of soft tissue and bone, these systems are limited in their ability to scan heavier metals, such as bronze and steel. Industrial CT systems, however, are capable of scanning large, dense objects, using higher-energy X-ray sources with higher-resolution detectors and imaging systems. Early applications of industrial CT included the inspection of large rocket motors, small precision castings, and other aircraft engine components.

The first CT studies of museum objects included those done by Miura (1980) and by Tout, Gilboy, and Clark (1980), involving wood and bronze sculptures, respectively. The latter study also noted the possible application to dendrochronology. While

many of the initial studies relied on medical CT systems, their limitations for penetrating dense materials as well as scanning large objects were quickly encountered. The first use of an industrial CT system is noted by Miura and Fujii (1987), who examined a small gilt bronze in this way. Although hollow, the bronze's composition and thickness required the use of a high-energy (420 kV) source.

One problem that has consistently plagued computed tomographic examinations is the low quality of visual reproduction. Avril and Bonadies (1991) overcame this difficulty by using a high-resolution imaging system and photographing the scanned image directly off the monitor. Continued improvements in image-processing software and the use of direct digital-to-photographic printers will eventually eliminate this problem.

FIGURE 1a, b. *Schematic illustrating (a), top, the CT process, and (b), bottom, the digital radiographic process.*

The CT process begins with a narrow, fan-shaped X-ray beam—the thickness of which defines the thickness of the cross-sectional slice to be measured—interrogating the object under study (Fig. 1a). The attenuation of the beam as it passes through the object is directly related to the density and thickness of the material as well as to the energy of the X-ray beam. The object is rotated slowly so data can be collected from many different angles. The data are transmitted through a data-acquisition system to a high-speed computer, which generates a two-dimensional image by the application of a filtered back-projection algorithm. Within a matter of seconds, the image appears on a high-resolution video screen (1024 by 1024 pixels). Subsequent enhancement may be achieved through addition of color, by sharpening and enlarging, and by varying the brightness and contrast. A hard copy of the image may be obtained with a laser printer or by photography, and the image data can be stored on magnetic tape or optical disk for later retrieval. While an object 1.83 m (6 ft) in diameter by 0.91 m (3 ft) in height can be accommodated, the maximum scanning width is 0.61 m (2 ft).

Industrial CT systems can also be used to quickly scan an entire object to produce a digital radiograph (Fig. 1b). The digital radiographic image is similar to that obtained with conventional film radiography. Digital radiographic images are used for radiographic inspection of objects as well as to mark areas where the slices should be taken. While the resolution of the typical digital radiographic image is not as great as with film radiography, higher resolution can be achieved by repeating the digital radiograph scan with a slight shift of the detector. A significant factor limiting image sharpness is the detector resolution, which in turn is determined by spacing of individual detecting elements. Details smaller than this spacing cannot be accurately defined.

The advantages of CT over conventional radiography are numerous. Whereas radiography compresses the structural information from a three-dimensional object into a two-dimensional image, CT is uniquely able to inspect the internal structure of an object without interference from protruding parts or highly decorated surfaces. CT is extremely sensitive to variations in object density as well as to differences in material composition. Minute density differences can be visualized and measured. Unlike conventional film radiography, in which magnification frequently occurs due to the distance between object and film, a CT scan allows precise dimensional measurements of up to 50.8 microns (.002 inches). Cheng and Mishara (1988) utilized
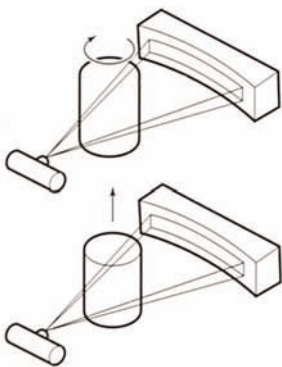
this capability to provide technical information on violin construction that included precise dimensions of the instrument's parts.

Perhaps the most exciting possibility presented by this technology is the ability to reconstruct an accurate three-dimensional image of an object. By taking hundreds of adjacent CT slices and then stacking them one on top of the other, a three-dimensional image can be created (General Electric's Digital Replica™ process) through computer-processing techniques. This computer model can then be "cut up" electronically to enable the study of previously inaccessible interior surfaces or the structures of enclosed hollow objects. Early medical uses of this technique were applied to the paleoanthropological study of fossil skulls (Conroy and Vannier 1984; Vannier et al. 1985).

The impetus for analyzing the museum's Chinese bronzes was the ongoing cataloging project of the permanent collections. In an attempt to gain as much technical information as possible, the museum decided to study these objects with X-radiography. The purpose of these analyses was to detect hidden damage and repairs in the vessels and to learn more about ancient casting techniques. Until fairly recently many museums studying ancient metal work have relied on conventional X-ray equipment (Bagley 1987). However, when museum staff approached officials at General Electric Aircraft Engines, they suggested that industrial CT be used instead. In addition to the Chinese bronzes, other objects examined with CT from the museum's collection included an Achaemenid silver rhyton, a Roman bronze bull, an Iranian portrait head, and an Egyptian mummy.

Ancient Chinese Bronze Ritual Vessels

The Chinese aristocracy of the Shang Dynasty (ca. 1550–1030 B.C.E.) commissioned sumptuous vessels cast in bronze for making ritual offerings of food and wine to their esteemed ancestors. The technical sophistication and extravagant consumption of raw materials required to produce these vessels attest to their importance as symbols of power for the ruling class. Enormous wealth was expended on the furnishing of tombs, in part because Chinese nobles believed that reverence for the needs of the ancestors in the afterlife would ensure the continued success of the clan on Earth. Indeed, such extravagance also served to legitimize the status of the ruling clans in Shang society.

The Cincinnati Art Museum's collection of Shang Dynasty Chinese ritual bronzes comprises superb examples dating from the thirteenth to eleventh centuries B.C.E. Most come from the area of the ancient Shang capital at Anyang (in modern Henan province) and represent the classic phase of Shang Dynasty bronze production.

Ancient Chinese Casting Techniques

During the Shang Dynasty the Chinese developed a multistage process for casting bronze in ceramic section molds. First, a model of the finished vessel was carefully

built up in fine clay, then allowed to dry. The outer mold sections were produced by pressing moist primary loess around the model; this outer layer was then cut away in sections, fired, and reassembled to receive the molten metal (Wood 1989). Depending on the shape of the vessel being produced, the mold assembly needed one or more cores, also of loess, in addition to the outer mold parts. Metal spaces, or chaplets, were carefully placed between inner cores and outer mold parts to maintain the proper distance for the desired wall thickness. Vessels were cast upside down so that the legs or base served as inlets for pouring the alloy of copper, tin, and lead.

The lost-wax method, the more common technique for casting bronze in the ancient world, was used in the ancient Near East as early as the fourth millennium B.C.E., but was not employed in China until the sixth century B.C.E. (Thorp 1988).

Results of the Examination of Selected Bronzes

Digital radiographic and CT images were generated at 420 kV for each bronze examined by industrial CT, except for the Roman bronze bull, which required an even higher energy source. Repairs otherwise difficult to detect become obvious in the digital radiographic image because of differences in material density. With color enhancement, these differences can be made even more apparent. A yellow line through the digital radiographic image marks the location of the subsequent CT slices to be taken in order to provide more information such as wall thickness, core construction, and porosity. Slices taken for this particular analysis were 508 μm (20 mils) each.

Two ceremonial wine beakers of the *gu* shape illustrate basic casting techniques. The vessels were cast in a four-part mold with two inner cores, one to form the circular base, the other to form the wine container. The foot core was supported during the pour with cross-shaped projections. Remnant voids (approximately 1.0 by 1.6 cm in one *gu*, 1.4 by 1.9 cm in the other; opening thickness 0.16 cm in each) from the spacers were cleverly employed in the decoration of the vessels, appearing as openwork crosses in the completed vessels. Centering the inner cores was crucial for producing a thin-walled, symmetrical vessel; misalignment of mold parts could result in casting failure. CT scans reveal how successfully Chinese artisans achieved a thin wall of uniform thickness under conditions that allowed little tolerance for error (Fig. 2).

Small tripod vessels with slender legs, such as the *jue*, were cast upside down in a single pour. The digital radiographs and CT images of the *jue* illustrate the porosity problems ancient artisans frequently encountered while working with molten metal and reveal concentrations of trapped air bubbles in the rounded bottom of the vessel. One of the fortuitous qualities of the primary loess used by the Chinese for section molds is its ability to absorb trapped gases that could otherwise pit the surface of a casting. Although the digital radiographic image reveals some porosity problems (Fig. 3), the CT scans specifically locate and reveal the extent of trapped air bubbles

FIGURE 2. *CT slice of Chinese Shang Dynasty* gu *wine beaker. Section taken through circular base shows uneven wall thickness due to misalignment of core with respect to mold.*

TOMOGRAPHY OF ANCIENT BRONZES

with respect to the vessel walls (Fig. 4). This dramatically illustrates how close the casting came to failure.

Study of the *jia*, another tripod wine-warming vessel, revealed the most startling condition problems of the bronzes analyzed. In the digital radiographic image (Fig. 5), numerous repairs—on the handle, in the core cast legs, and along the rim— appear in bright white due to the probable use of a lead-tin solder. Two of the legs have major repairs. One leg was reassembled using a modern screw, indicating that the object was probably repaired shortly before the museum purchased it in 1948.

FIGURE 3. *Digital radiograph of Chinese Shang Dynasty* jue *tripod vessel, near right, showing trapped air in knobs and at rounded bottom of vessel.*
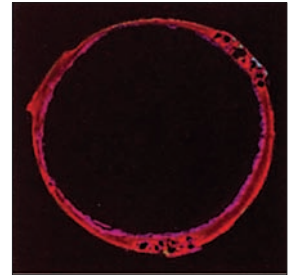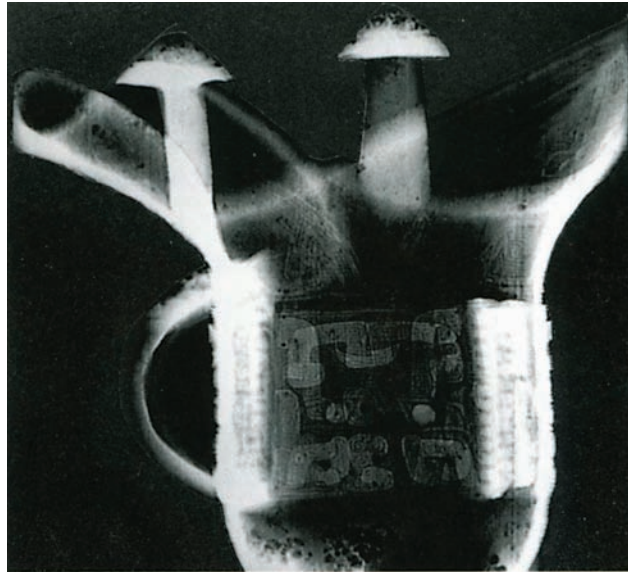
FIGURE 4. *CT slice of* jue, *far right, reveals extent of porosity, as well as variation in wall thickness.*
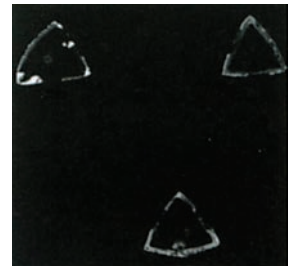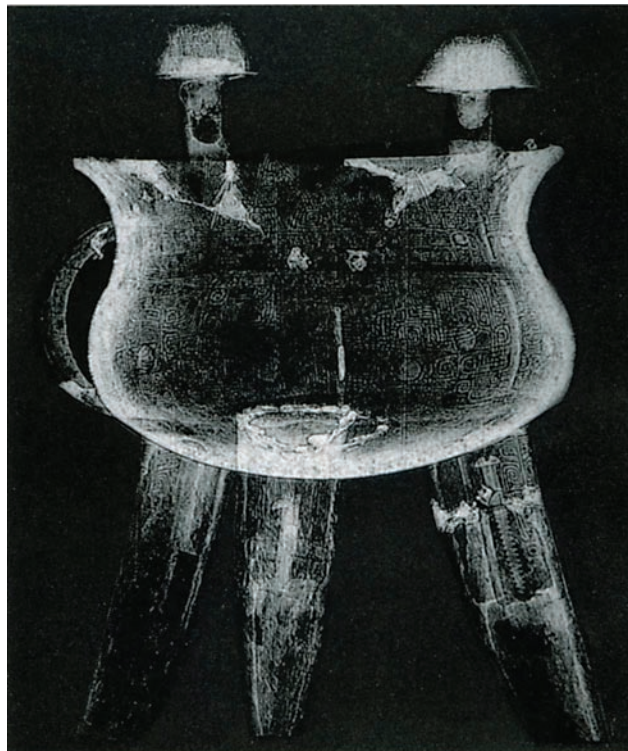

FIGURE 5. *Digital radiograph of Chinese Shang Dynasty* jia *wine-warming vessel, near right, showing core-cast legs, numerous repairs, and reassembly of legs.*

FIGURE 6. *CT slice taken through legs of the* jia, *far right, reveals location of screw and pin with respect to interior walls of the legs. Pin is in lower leg, whereas screw is in upper left leg.*

Another leg has a less obvious break and was reassembled using a metal pin. This repair appears older and may have been performed in antiquity, since no evidence of the break is visible on the surface; it is completely concealed by patination accumulated during its extended burial. CT scans taken through the legs show the exact location of the screw and pin with respect to the interior walls of the legs (Fig. 6). An additional CT scan, taken where the legs join the vessel body, clearly shows the reattachment of one leg.

A *guang*-type lidded wine vessel in the form of composite fantastic animals represents the most complex casting of the bronzes analyzed. Digital radiographic images reveal only one condition problem: a hairline fracture in the center of the lid. A close-up digital radiograph of the *guang* handle reveals that it was cast around a clay core. Four CT scans taken through the handle depict core shape and wall thickness in those locations as well as confirm the presence of tenons extending from the body for the handle's attachment (Fig. 7). Visual evidence of metal overflow onto the surface decoration of the body confirms that the handle was cast on as a separate unit (Bagley 1987).

To fully characterize the configuration of the clay core and determine the nature of the join between the handle and body of the *guang*, a three-dimensional model was constructed by taking CT slices horizontally through the entire vessel at 508 µm (20 mil) increments. The data were then processed to form a three-dimensional reconstruction of the *guang*. By electronically slicing the computer model in half lengthwise and rotating it on the screen, the interior of the handle was exposed, thus revealing the shape of the clay core inside.

Among the manipulations possible with three-dimensional replication (Fig. 8) is the ability to create a synthetic CT in any direction through the vessel using data accumulated in the previous scanning. This technique also proved useful in the analysis of the *guang*. Synthetic CTs were created vertically through the handle. The resulting images, when combined with horizontal CT and digital radiographic views,

FIGURE 7. *Digital radiograph of Chinese Shang Dynasty* guang *lidded wine vessel, below left, shows tenons extending from the body. Yellow lines indicate where subsequent CT scans will be taken.*

FIGURE 8. *Industrial CT workstation for examination and further manipulation of the three-dimensional reconstruction, below right.*
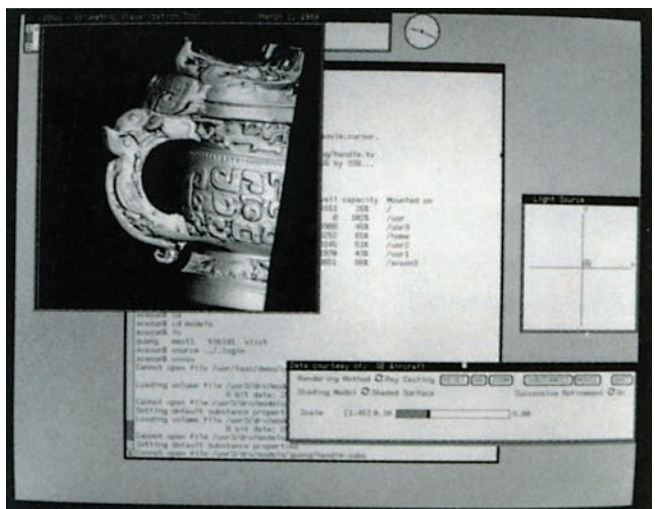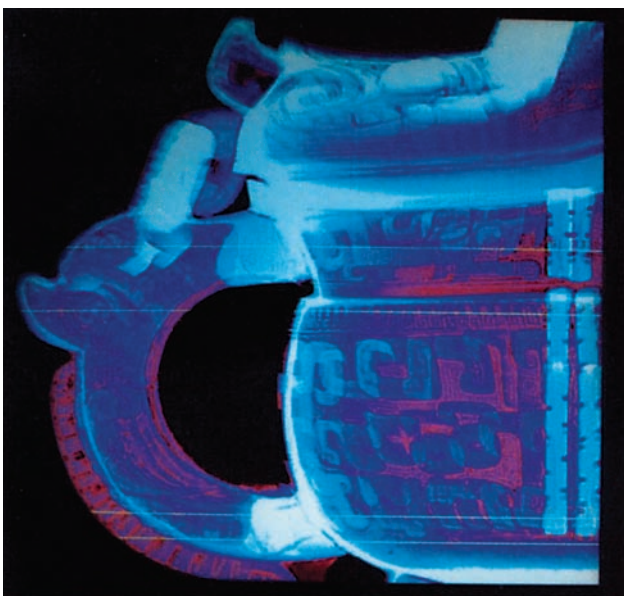
FIGURE 9. *CT slice of Roman bronze bull, first century B.C.E. to first century C.E., showing extent and specific depth of plaster restorations.*

FIGURE 10. *CT slice of Bronze Age Iranian portrait head, revealing bands of differing densities.*

provided a full characterization of the join and confirmed suspicions that the handle was indeed cast over tenons extending from the previously formed body.

A unique Roman bronze bull, dating from the first century B.C.E. to the early first century C.E., proved interesting to study for two reasons. First, it is the largest known example of a cast-bronze representation of an Apis bull; and second, the object had previously been studied with conventional film radiography a number of years ago. Thus, direct comparisons between film radiography and industrial computed tomography could be made.

As noted earlier, the 420 kV source was unable to penetrate the bull, resulting in electron scatter that effectively obliterated any details in the CT image. This was probably due to the thickness of the metal as well as to its composition (Cu 86%, Pb 4%, Sn 9%). Instead, a 2 million volt (2000 kV) source was successfully used to penetrate the object. Since there was still a slight problem with electron scatter in the CT, the image quality was not as fine as images made previously. Even though problems were encountered, however, useful information was obtained about the extent of surface restorations. While these restorations are obvious in the film radiograph, the CT slices additionally depicted their depth (Fig. 9).

An Iranian portrait head (Cu 96.67%, As 1.77%, Fe 0.76%, Ni 0.74%) from the second millennium B.C.E. is one of the very few examples extant from the Bronze Age. This piece and a cast portrait of similar style and date from the collection of The Metropolitan Museum of Art are the earliest known examples of Iranian portraiture in any medium. The two objects allegedly came from the same find.

As part of a comparative study, the museum's portrait head was scanned. The CT slices revealed both extensive porosity of the metal and obvious bands of differing metallic density and composition within the wall (Fig. 10). Once the companion piece from The Metropolitan Museum of Art is examined, investigators hope to shed light on the early development of bronze casting in Iran.

THE FUTURE OF INDUSTRIAL COMPUTED TOMOGRAPHY

An industrial CT workstation has been developed by General Electric Aircraft Engines that enables researchers to view and manipulate the three-dimensional reconstruction at a computer terminal. The model can be rotated, sliced, and viewed from any angle, and actual or synthetic CT images can be accessed individually to study details of an object. Examination of the reconstructed image allows one to view interior surfaces and to dissect joins. In the past such an inspection would only have been possible with the destruction of the object. Future developments will most likely be directed toward improving the speed at which the reconstruction is obtained by using a three-dimensional X-ray system.

Through the application of today's sophisticated nondestructive evaluation techniques, the combination of modern technology with art history advances the knowledge of ancient metallurgy, providing safe examination methods to aid in the preservation of many such works of art.

Acknowledgments

References

AVRIL, E., AND S. D. BONADIES

1991   Non-destructive analysis of ancient Chinese bronzes utilizing industrial computed tomography. *Materials Issues in Art and Archaeology*, vol. 185. Pittsburgh: Materials Research Society.

BAGLEY, R. W.

1987   Shang Ritual Bronzes in the Arthur M. Sackler Collections. *Ancient Chinese Bronzes in the Arthur M. Sackler Collections*, vol. 1. Washington D.C. and Cambridge: Harvard University Press.

CHENG, Y.-T., AND J. MISHARA

1988   A computerized axial tomographic study of museum objects. *Materials Issues in Art and Archaeology*, vol. 123. Pittsburgh: Materials Research Society.

CONROY, G. C., AND M. W. VANNIER

1984   Non-invasive three-dimensional computer imaging of matrix-filled fossil skulls by high-resolution computer tomography. *Science* 226(4673):456–58.

DENNIS, M. J.

1989   Non-destructive evaluation and quality control. *The Metals Handbook*, vol. 17, 9th ed. Metals Park: ASM International.

LEVEQUE, M. A.

1987   An approach to the conservation of Egyptian mummies; the mummy of Lady Nesmutaatneru. In *Recent Advances in the Conservation and Analysis of Artifacts, Jubilee Conservation Conference, London, 6–10 July 1987*. London: University of London.

MIURA, S.

1980   Investigation of a wooden sculpture of Buddha. *Science for Conservation* 19:9–14.

MIURA, S., AND M. FUJII

1987   Investigation of a gilt bronze statue by a high energy X-ray scanner. *Science for Conservation* 32:40–46.

REIMERS, P., AND J. RIEDERER

1984   Die Anwendung der Computertomographie zur Untersuchung kulturgeschichlicher Objekte. *Berliner Beiträge zur Archäometrie* 9:171–90.

RIEDERER, J.

1986   Neue Durchstrahlungstechniken zur Untersuchung von Kunstwerken im Rathgen-Forschungslabor. *Berliner Museen* 3:8–9.

1988   Ausgrabungen nach Röntgenbild. *Archäologie in Deutschland* 1:24–27.

TAGUCHI, E., I. NAGASAWA, S. YABUUCHI, AND M. TAGUCHI

1984   Investigation of a wooden sculpture using X-ray computed tomography. *Scientific Papers on Japanese Antiques and Art Crafts* 29:43–50.

THORP, R. L.

1988   *Son of Heaven: Imperial Arts of China*. Seattle: Son of Heaven Press.

TOUT, R. E., W. B. GILBOY, AND A. J. CLARK

1980   The use of computerized X-ray tomography for the non-destructive examination of archaeological objects. In *Proceedings of the 18th International Symposium on Archaeometry and Archaeological Prospection, Bonn, 14–17 March 1978*. Köln: Rheinland Verlag.

TYERS, I.

1985   Tree ring dating by X-ray. *The London Archaeologist* 5(4):87–88.

UNGER, A.

1988   Zerstörungsfreie Zustandanalyse an Kulturgut as Holzmittles Röntgen-Computertomographie. *Conservation-restoration of leather and wood; Training of restorers; Sixth International Restorer Seminar, 1987 Veszprém, Hungary*. István Éri and Gábriella Sárközy, eds. Budapest: National Center of Museums.

UNGER, A., AND J. PERLEBERG

1987   X-ray computer tomography (XCT) in wood conservation. In *ICOM Committee for Conservation: 8th Triennial Meeting, Sydney, Australia, 6–11 September 1987*. Marina del Rey, Calif: The Getty Conservation Institute.

VANDIVER, P., W. A. ELLINGSON, T. K. ROBINSON, J. J. LOBICK, AND F. H. SEGUIN

1988   Radiographic imaging technologies for archaeological ceramics. *Expedition* 29(3):55–63.

VANNIER, M. W., G. C. CONROY, J. L. MARSH, AND R. H. KNAPP

1985   Three-dimensional cranial surface reconstructions using high-resolution computed tomography. *American Journal of Physical Anthropology* 67(4):299–311.

WOOD, N.

1989   Ceramic puzzles from China's Bronze Age. *New Scientist* 18(2):50–53.

Biography

Stephen D. Bonadies, chief conservator at the Cincinnati Art Museum, received his initial conservation training at the Cooperstown Graduate Program in New York. He gained additional experience as part of a team of conservators sent to northeastern Italy under the auspices of the Friuli Italian Arts and Monuments Committee after a series of devastating earthquakes there in 1976. After receiving his master's degree in 1979, he became a Mellon Fellow at the Philadelphia Museum of Art. In 1980 Bonadies returned to the Art Conservation Program at Cooperstown to teach conservation science. He was appointed to the staff of the Cincinnati Art Museum in 1981.